UNITED STATE DEPARTMENT OF THE INTERIOR
GEOLOGICAL SURVEY

EVALUATION OF EARTHQUAKE-INDUCED GROUND FAILURE

BY

JOHN M. FERRITTO

A DRAFT TECHNICAL REPORT OF SUBCOMMITTEE 7,
"EVALUATION OF SITE HAZARDS,"
A PART OF THE INTERAGENCY COMMITTEE ON SEISMIC SAFETY IN CONSTRUCTION

SUBCOMITTEE CHAIRMAN - WALTER W. HAYS
U.S. GEOLOGICAL SURVEY
RETSON, VA 22092

OPEN FILE REPORT 82-880

Reston, Virginia

1982

FOREWORD

This draft technical report, "Evaluation of Earthquake-Induced Ground Failure," was developed within the Subcommittee for Evaluation of Site Hazards of the Interagency Committee on Seismic Safety in Construction (ICSSC). The membership of the Subcommittee during the preparation of this report was:

Manuel G. Bonilla	Geological Survey
Rutlage J. Brazee	Nuclear Regulatory Commission
Karl J. Dreher	Bureau of Reclamation
John M. Ferritto	Naval Civil Engineering Labortory
John T. Greeves	Nuclear Regulatory Commission
William H. Hakala	National Science Foundation
William F. Harley	Department of Housing and Urban Development
Walter W. Hays *	Geological Survey
Guan S. Hsiung	General Services Administration
Robert E. Jackson, Jr.	Nuclear Regulatory Commission
D. Earl Jones, Jr.	Department of Housing and Urban Development
William D. Kovacs	National Bureau of Standards
Ellis L. Krinitzsky	Army Corps of Engineers
James F. Lander	National Oceanic and Atmospheric Administration
Richard D. McConnell	Veterans Administration
David M. Patrick	Army Corps of Engineers
Leon Reiter	Nuclear Regulatory Commission
Lawrence Salomone	National Bureau of Standards
Case K. Tong	Naval Facilities Engineering Command
T. Leslie Youd	Geological Survey

* Chairman

The Subcommittee has recommended that this draft technical report be submitted to all concerned agencies with the request that they test its implementation through use in planning, design, contract administration, and quality control, either on a trial or real basis during 1983 and 1984. Following the trial implementation, the Subcommittee plans to review the draft report, revise it as necessary, and then recommend its adoption by the Interagency Committee as a manual of standard practice for evaluating earthquake-induced ground failure for Federal Buildings. Comment on this draft is welcomed. Comment should be forwarded to the author, John M. Ferritto, or to the Chairman:

Mr. John M. Ferritto
Senir Project Engineer
Naval Civil Engineering
Port Hueneme, California 93043

Dr. Walter W. Hays
Chairman, ICSSC Subcommittee 7
Evaluation of Site Hazards
U.S. Geological Survey
905 National Center
Reston, Virginia 22092

CONTENTS

ILLUSTRATIONS

Continued

ILLUSTRATIONS (Cont'd)

Continued

ILLUSTRATIONS (Cont'd)

Continued

ILLUSTRATIONS

TABLES

1.0 GENERAL

This technical report was written to provide guidance to geotechnical and structural engineers in evaluating the effects from seismically induced pore pressure buildup. The field of study is indeed dynamic in that much research is in progress and new data will improve our understanding of the problem.

This report will discuss procedures for estimating earthquake induced ground failure. Specifically, the following should be considered in the design of a facility against dynamic earthquake effects:

- Settlements and Ground Distortion
- Shear Failure in Bearing
- Slope Stability
  - Slides Land
  - Embankment Failure
  - Dam Analysis
- Liquefaction
  - Subsidence
  - Settlement
  - Flow Failure
  - Bearing Failure
- Ground Rupture

Ground rupture is discussed in a separate technical report.

The basic approach to a geotechnical analyses may be outlined as follows:

1. Identify modes of failure.

2. Identify type of structure and potential risks involved in postulated failure.

3. Identify and review available geotechnical data for site area.

4. Based on risks and available geotechnical data determine appropriate geotechnical field exploration program and the type of analysis to be performed.

5. Evaluate soil strength based on field or laboratory tests or other available data.

6. Compute earthquake loading using appropriate analytical techniques. Compare loading to strength either by deterministic or probabilistic means and evaluate safety.

2.0 SETTLEMENTS IN SANDS

Earthquakes have caused settlements of cohesionless soil deposits. Seed and Silver (1972) report that the San Fernando 1971 earthquake caused compaction of a 40-foot deep sandfill which resulted in settlements of 4 to 6 inches of a building constructed on spread footings. The settlement of sand during earthquakes is mainly caused by the horizontal shearing components of motion. The settlements discussed in this section are for sands which are dry or have no major increases in pore pressure. Liquefaction results in major settlements which will be treated in Section 5.

2.1 EVALUATION OF SETTLEMENTS IN DRY SANDS

A procedure has been developed by Seed and Silver (1972) correlating vertical strain to cyclic shear strain. An analysis is performed to determine the distribution of shear strain with depth. Such techniques are discussed in detail under Procedures for Analysis of Liquefaction of Soils. A soil element at a given depth may then be considered to undergo a given number of cycles of horizontal shear strain subject to a known effective overburden pressure. Figure 1 shows vertical strain as a function of a cyclic shear strain for 10 cycles of loading and several relatve densities. The vertical strain is a function of the magnitude of the earthquake which determines the level of cyclic shear strain. The duration of the shaking determines the number of cycles. As noted in Figure 1 the relative density of the insitu material is also a significant parameter. Test data indicates that overburden pressure does not have a significant effect on settlements since it both affects the compaction characteristics of the sand and the shear strains induced by any given base motion. Seed and Silver (1972) developed data presented in Figures 2 and 3. Such data may serve as the basis for estimating vertical strain for soil deposits; however, caution must be exercised since errors of up to 50% are possible.

Implementation of this procedure would consist of dividing the soil deposit into a series of layers, computing the time history of shear strain or at least the maximum strain levels, determining the equivalent number of uniform cycles of shear strain, either conducting a laboratory test applying the uniform shear strain and measure vertical strain or use data from literature to estimate the vertical strain, then determine total settlement using the thickness of the horizontal layer.

Youd and Craven (1972) note that the number of cycles of previous strain is a significant factor on the compaction behavior of sands. They show that variations of two orders of magnitude in settlement are possible.

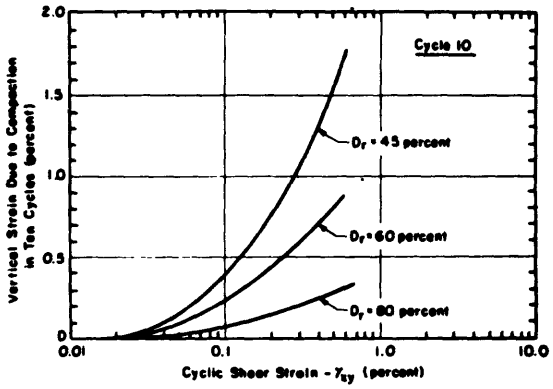

Figure 1. Effect of relative density and shear strain on settlement of sand (Seed and Silver, 1912).

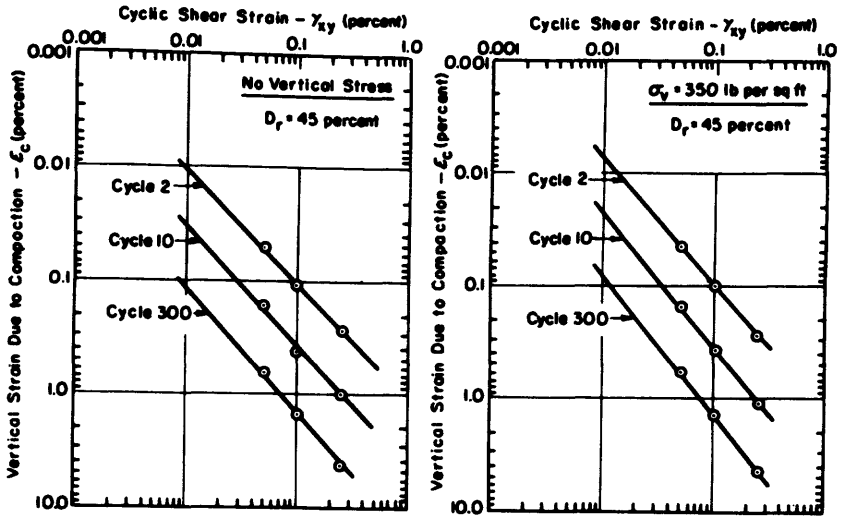

Figure 2. Vertical settlement-shear strain relationship for silica sand (D_r = 45%) (from Seed and Silver, 1972).

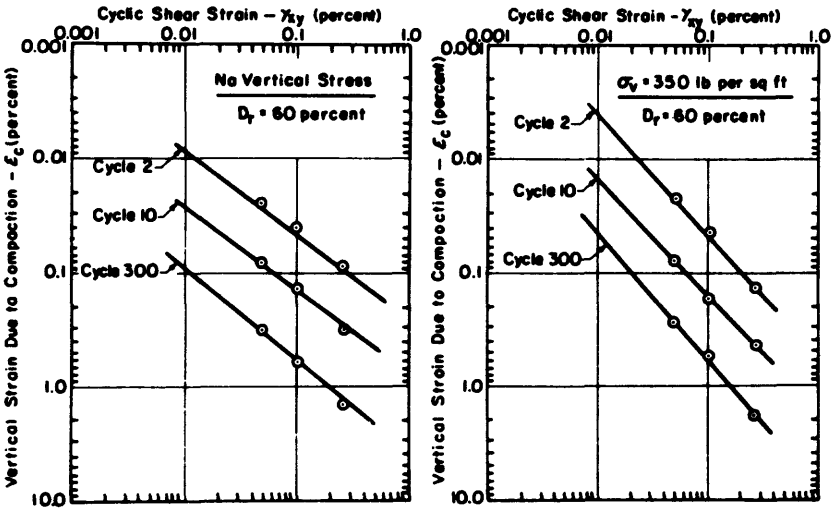

Figure 3. Vertical settlement-shear strain relationship for silica sand (D_r = 60%) (from Seed and Silver, 1972).

Pyke et al (1975) extended the method suggested by Seed and Silver (1972) to include multidirectional shaking. Pyke et al (1975) conducted an extensive experimental study of the settlement of sands under combined horizontal and vertical accelerations. They noted that the effect of two components of horizontal acceleration approximately doubled the vertical settlement. The effect of the vertical shaking would be about 25% of the settlements of the combined horizontal motions. Thus, the total estimate of maximum settlements will be obtained by multiplying the computed one directional shaking settlements by 2.5.

Martin et al (1974) performed a detailed study of volumetric strain increment as a function of volumetric strain. The volume strain increment may be expressed by

$$\Delta\varepsilon_{vd} = C_1(\gamma - C_2\,\varepsilon_{vd}) + \frac{C_3\,\varepsilon_{vd}^2}{(\gamma + C_4\,\varepsilon_{vd})}$$

where $\Delta\varepsilon_{vd}$ = volume strain increment (%)

γ = cyclic shear strain (%)

ε_{vd} = volumetric strain (%)

For Crystal Silica No. 20 sand having a D_{10} = 0.5 mm, a uniformity of 1.5 and a relative density of 45%:

$$C_1 = 0.80$$
$$C_2 = 0.79$$
$$C_3 = 0.45$$
$$C_4 = 0.73$$

Under dynamic loading the volume strain increment may be assumed to be all vertical strain. The equation may be related to other relative densities, D_R, by

$$(\Delta\varepsilon_{vd})_2 = R(\Delta\varepsilon_{vd})_1$$

where $R = 0.00031(100 - D_R)^2 + 0.062$ for $45 \leq D_R \leq 80$

Finn and Byrne use the above equation with a dynamic equivalent strain-dependent linear analysis to compute shear strain histories and volumetric strain histories. They note that the settlement of sand will be affected by the existence of a structure. They concluded that the structure increased total settlements and that free field level ground estimates of a sand provide lower bound estimates of settlement. They suggest use of surcharge loading to partially consider the structure.

Youd (1977) notes that for practical applications the incremental volume change, $\Delta\varepsilon_{vd}$, can only be obtained from undisturbed tests of the sand in question since these types of relationships are very dependent on the soil and the previous strain history.

Finn et al (1975) has noted that the response of saturated sands in the drained and undrained state are almost identical until the porewater pressures of the undrained sands are above 30% of the overburden pressure. Settlement of saturated sands would be delayed until dissipation of the excess porewater pressure.

2.2 EVALUATION OF SETTLEMENTS IN SATURATED SANDS

Lee and Albasia (1974), using cyclic triaxial tests, have investigated the settlements from volume change due to the dissipation of increased pore pressures. Their work is intended to represent general ground subsidence which might be expected from soil compaction and water drainage at stresses less than that required to induce complete liquefaction. Figure 4 shows a series of triaxial test results, considering the effects of confining pressure, relative density, and grain size on volumetric strain. Using Figure 5, the increase in pore pressure at any cycle less than N_L may be estimated. This increase in pore pressure can be used in conjunction with Figure 4 to estimate the volumetric strain from the rise in pore pressure and resulting drainage.

Figure 4a, b, and c are limited to conditions in which complete liquefaction does not occur. The volumetric strain and the thickness of the layer can be used to estimate the vertical settlement. This is intended for level areas without concentrated footing loads which may cause shear displacements. The volumetric settlements from pore pressures lower than those causing liquefaction are generally less than 1%. Lee and Albasia (1974) have also investigated cases when liquefaction occurs. Their data, Figure 4d, indicates that vertical settlements from drainage effects may be as much as 3% of the height of the affected soil layer. This does not consider the effects of soil bearing failures but only the "regional" subsidence.

2.3 REFERENCES

1. Lee, K. L. and Albasia, A. (1974) "Earthquake Induced Settlements in Saturated Sands, Journal of the Geotechnical Division, ASCE, No. GT4, Apr 1974.

2. Seed, H. B. and Silver, M. L. (1972) "Settlement of Dry Sands During Earthquakes," Soil Mechanics and Foundation Division, ASCE, No. SM4, Apr 1972.

3. Pyke, R., Seed, H. B. and Chan, C. K. (1975) "Settlement of Sands Under Multidirectional Shaking," Journal of Geotechnical Engineering Division ASCE GT4, 1975.

4. Martin, G. R., Finn, W. D. L. and Seed, H. B. (1974) "Fundamentals of Liquefaction Under Cyclic Loading," Journal of Geotechnical Engineering Division, ASCE, GT5, 1974.

5. Finn, W. D. L. and Byrne, P. M. (1976) "Estimating Settlements on Dry Sand During Earthquakes," Canadian Geotechnical Journal, Vol 13, Number 4, 1976.

6. Finn, W. D. L., Byrne, P. M. and Martin, G. R. (1975) "Seismic Response and Liquefaction of Sands," Soil Mechanics Series No. 24, University of British Columbia, Vancouver, B.C.

7. Youd, L. T. and Craven, T. N. (1972) "Discussion of Paper Settlements of Dry Sands During Earthquakes," Journal of Soil Mechanics and Foundation Division, Vol 98, ASCE, SM 12, Dec 1972.

8. Youd, L. T. (1977) "Discussion of Seismic Response and Liquefaction of Sands," Journal of Geotechnical Engineering Division, ASCE, GT7, Jul 1977.

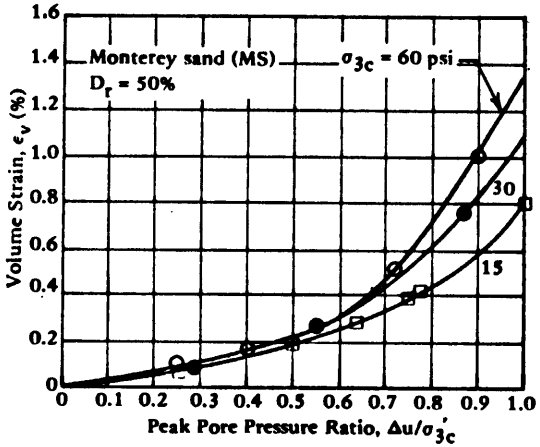

(a) Confining pressure on reconsolidation volumetric strain.

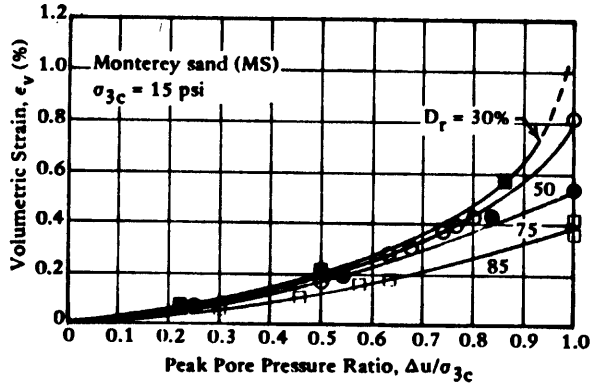

(b) Relative density on reconsolidation volumetric strain.

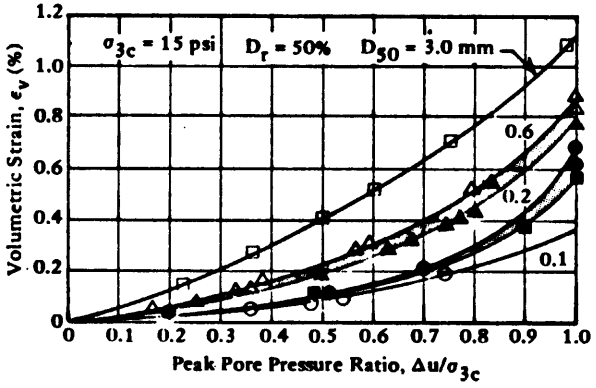

(c) Grain size on reconsolidation volumetric strain.

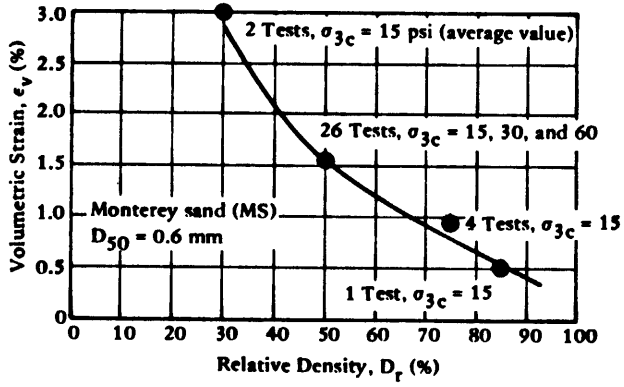

(d) Relative density on volumetric strain following complete liquefaction.

Figure 4. Effect of various factors on volumetric strain (from "Earthquake Induced Settlements in Saturated Sands," by K. L. Lee and A. Albasia, in Journal of the Geotechnical Division, ASCE, vol. 100, GT4, Apr 1974).

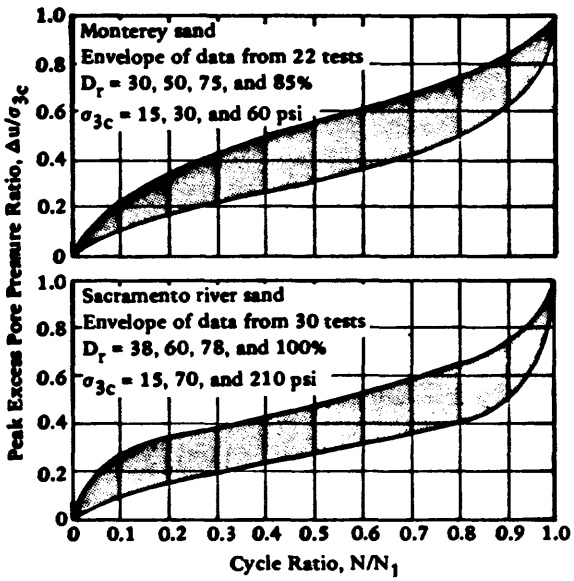

Figure 5. Compilation summary of pore pressure buildup data (from "Earthquake Induced Settlements in Saturated Sands," by K. L. Lee and A. Albasia, in Journal of the Geotechnical Division, ASCE, vol. 100, no. GT4, Apr 1974).

3.0 LANDSLIDES AND EMBANKMENT ANALYSIS

The sudden ground motion of earthquakes induce large inertial forces in land formations and embankments. These inertial forces alternate in direction many times during an earthquake. As a result of these forces slope failures, differential movements and cracking can occur. In the past embankments have been designed to withstand earthquakes by including the equivalent static inertial forces in the traditional stability analysis and checking that the factor of safety is sufficiently above unity. Static methods must be used only with caution since large errors are possible. True dynamic methods are recommended.

Evaluation of saturated cohesionless soils can only properly be made when pore pressures and the resulting reduced confining stresses are taken into account. Cohesive soils also exhibit complex behavior. The yield stress for these materials is substantially less than the strength. Thus, large deformations can occur under oscillating loads even though maximum applied stresses are less than the static strength of the soil.

3.1 PROCEDURES FOR EMBANKMENT STABILITY

A stress analysis is based on values of soil strength or resistance to deformation determined by laboratory tests approximating the in-situ soil conditions. The design process evaluates the forces acting on the embankment such as dead weight, water pressure, inertial pressure, surcharge load, etc. The inertial forces depend on the variation of acceleration within the soil mass. Seed (1966) illustrates use of the method of slices prior to an earthquake to determine the initial static stress state along the failure surface. This stress state as a function of location in the soil mass forms the basis for establishing the principal stress state in laboratory triaxial tests. The deformations resulting from cyclic loading give an indication of the deformation state which will occur in the soil mass from the same cyclic loading. This concept requires a number of anisotropically consolidated tests. Alternatively the stress levels producing maximum tolerable distortion of the laboratory samples can be related to maximum embankment stress. By use of Mohr Circle techniques and equilibrium of each slice it is possible to compute a factor of safety, as shown by Seed (1966).

Clough and Woodward (1967) demonstrate the use of finite element procedures in drained analysis. This was a major advance in slope stability analysis. Seismic analysis finite element methods calculate the static and earthquake induced stresses. Comparison of seismic stresses with the soil strengths determined by cyclic loading tests on samples indicates the slope stability. Lee (1975) expands upon this to estimate permanent deformations. Triaxial test specimens are consolidated

to the appropriate normal and shear stresses corresponding to elements in the field and then subjected to cyclic stresses noting strain as a function of number of cycles. Failure is usually defined in terms of axial strain. Using the calculated stress histories, the number of equivalent uniform applied earthquake cycles is computed for the elements in the soil mass. The ratio of shear strength to applied shear stress is used to determine individual factors of safety or performance for each element of soil. The strain potential of each element can also be evaluated. Judgement is used to relate total soil behavior from element strain potential.

Roth and Lee (1975) demonstrate use of the finite element method. Using finite element analyses and cyclic test data, slip surfaces are examined to determine a minimum overall factor of safety. Thus, this modification allows for a single overall evaluation of the safety by summing the shear strength and the shear loading along the slip surface.

Current research (Prevost and Hughes, 1979; Prevost and Hughes, 1980; and Mroz, Norris, and Zienkiewicz, 1978) is investigating improved soil models with intent to predict effective stresses and pore pressures. These techniques will be another major step in understanding dynamic soil behavior and should prove to be most useful in slope stability analysis.

3.2 REFERENCES

1. Seed, H. B. (1955) "A Method for Earthquake Resistant Design of Earth Dams," ASCE Soil Mechanics and Foundation Division, SM1, Jan 1966.

2. Clough, R. W. and Woodward, R. J. (1967) "Analysis Embankment Stresses and Deformation," ASCE Soil Mechanics and Foundations Division, SM4, Jul 1967.

3. Lee, K. L. (1975) "Seismic Permanent Deformations in Earth Dams," UCLA-ENG-7497, Jan 1975, Los Angeles, Calif.

4. Roth, W. and Lee, K. L. (1975) "A Factor of Safety Approach for Evaluating Seismic Stability of Slopes," National Conference on Earthquake Engineering, University of Michigan, Ann Arbor, Mich., Jun 1975.

5. Prevost, J. and Hughes, T. (1979) "Mathematical Modeling of Cyclic Soil Behavior," Earthquake Engineering and Soil Dynamics, New York, N.Y., American Society of Civil Engineers, Jun 1979.

6. Prevost, J. and Hughes, T. (1980) "Finite Element Solution of Boundary Value Problems in Soil Mechanics," in Proceedings of International Conference on Soils Under Cyclic and Transient Loading, Swansea, United Kingdom, Jan 1980.

7. Mroz, Z., Norris, V., and Zienkiewicz, O. (1978) "An Anisotropic Hardening Model for Soils and Its Application to Cyclic Loading," International Journal for Numerical and Analytical Methods in Geomechanics, vol 2, 1978, pp 203-221.

4.0 PROCEDURES FOR ANALYSIS OF LIQUEFACTION OF SOILS

Earthquake ground motions are capable of causing a loss of shear strength of sand deposits below the water table. Field and laboratory tests have been performed to evaluate the liquefaction potential of soils. This chapter will present field standard penetration test interpretation, a summary of the void ratio concept, Seed's (1976) simplified procedure, a simple computer analysis, a more complex computer analysis, finite element analysis techniques, and some interesting research in progress.

4.1 STANDARD PENETRATION TEST USED FOR LIQUEFACTION PREDICTION

Standard penetration tests can be used directly to give an in-situ evaluation of soil behavior. Seed (1976) presents Figure 6 which is an evaluation of the Niigata, Japan 1964 earthquake. Several lines divide regions of light damage (no liquefaction) from heavy damage (liquefaction). Such a correlation is applicable only to the Niigata soil and earthquake; however, the methodology may be extended. Castro (1975) has compiled earthquake field observations of liquefaction in terms of an effective shear stress ratio

$$\tau_e/\sigma'_v$$

where τ_e is defined* as

$$\tau_e = 0.7 \times A_{max} \times \sigma_v$$

and σ'_v = effective overburden pressure
A_{max} = maximum horizontal acceleration, g's
σ_v = total vertical overburden pressure

*This will be discussed in more detail in the section entitled SIMPLE HAND COMPUTATION.

and a corrected blow count N' defined as

$$N' = \frac{50\ N}{\sigma'_v + 10}$$

where N = standard penetration resistance measured in the field

The relationship is shown in Figure 7.

Christian and Swiger (1975) utilized discriminant analysis techniques to analyze the data from 39 earthquakes. They define a parameter A as

$$A = \frac{a\ \sigma_v}{\sigma'_v}$$

where a = site surface accelerations

The parameter A is a measure of the stress-strength ratio t/s'_v. Relative density is determined by use of the Gibbs and Holtz (1957) relation from standard penetration tests. This value is not used as an absolute but rather as an intermediate correlation. Figure 8 shows the results of their analysis. The probability numbers are the confidence indicators that the line shown is the dividing line separating liquefiable from non-liquefiable cases. Thus, a P = 0.10 means that the location of the line is associated with a 90% confidence that all liquefiable cases are above the line. (Note: It is not to be confused with the probability of occurrence of liquefaction.) These curves give estimates of the standard penetration resistance required at a site to preclude liquefaction for a given confidence level.

Seed (1976) gives the results of a detailed study on penetration resistance in Figure 9a, b, c. To use the information presented in Figure 9, the value of the standard penetration resistance should be corrected to an effective overburden pressure of 1 ton/ft^2 by means of the following expression

$$N_1 = C_N\ N$$

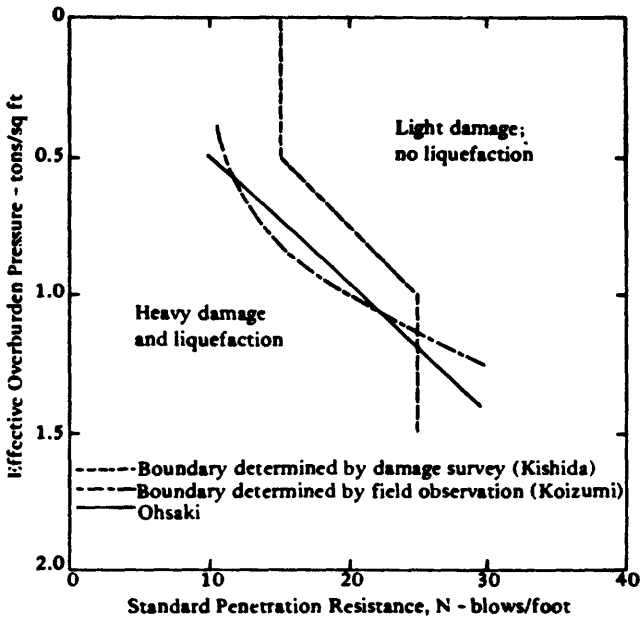

Figure 6. Analysis of liquefaction potential at Niigata for earthquake of June 16, 1964 (from "Liquefaction and Cyclic Mobility of Saturated Sands," by G. Castro in ASCE Geotechnical Journal, GT6, Jun 1975).

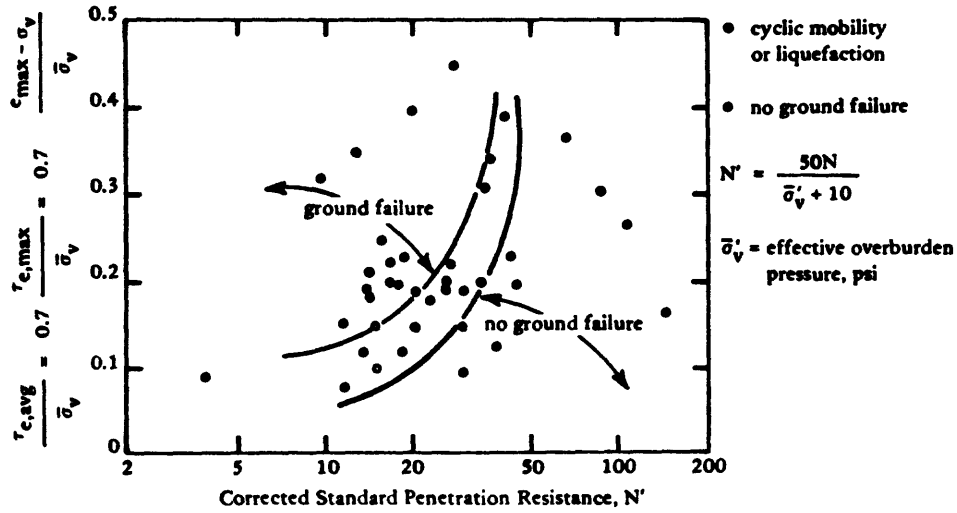

Figure 7. Performance of saturated sands at earthquake sites (from "Liquefaction and Cyclic Mobility of Saturated Sands," by G. Castro in Journal of the Geotechnical Division, ASCE vol. 101, no. GT6, Jun 1975).

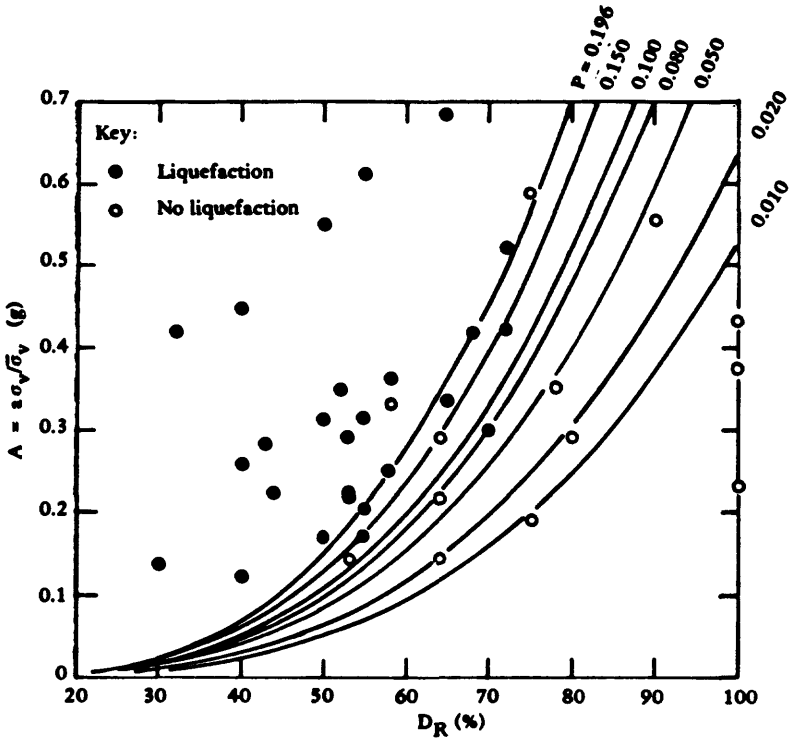

(a) Arithmetic scales.

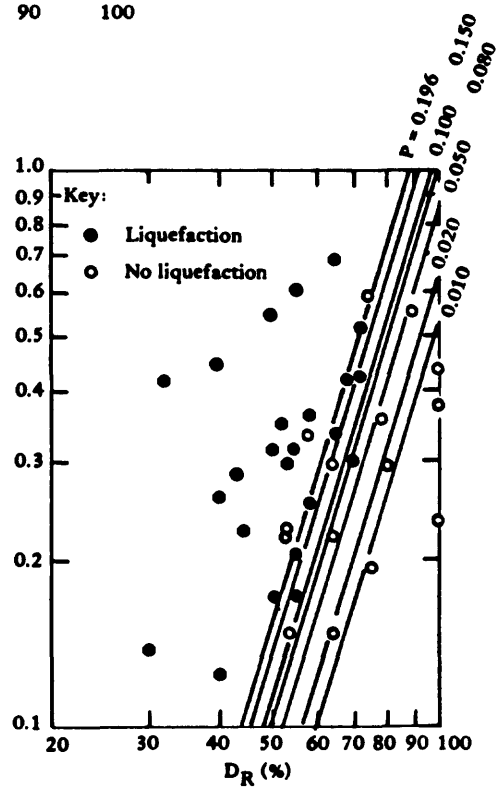

(b) Logarithmic scales.

Figure 8. Historical observations of liquefaction and discriminant curves (from "Statistics of Liquefaction and SPT Results," by J. T. Christian and W. F. Swiger in Journal of the Geotechnical Division, ASCE, vol. 101, no. GT11, Nov 1975 and discussion, vol. 102, no. GT12, Dec 1976).

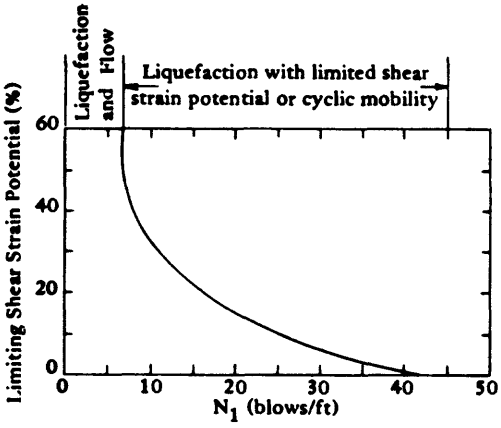

(a) Strain potential.

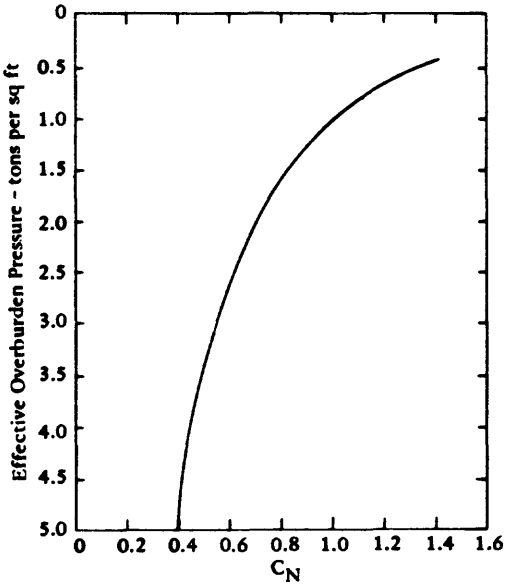

(c) Relationship between C_N and effective overburden pressure.

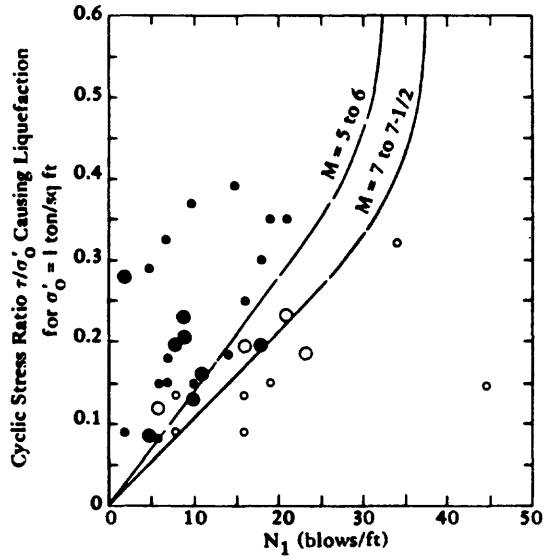

(b) Stress ratio.

Figure 9. Use of standard penetration for liquefaction evaluation (from "Evaluation of Soil liquefaction Effects on Level Ground During Earthquake," by H. B. Seed, in a paper presented at the ASCE Annual Convention, Philadelphia, 27 Sep-1 Oct 1976).

where C_N is taken from Figure 9c and

N_1 = corrected penetration resistance

N = standard penetration resistance as measured at the depth under consideration

σ'_o = effective overburden pressure in ton/ft^2 (where the penetration resistance has the value N)

σ'_1 = 1 ton/ft^2

Liquefaction studies in mainland China conducted independently but along similar lines to those developed in this country have also led to a correlation between earthquake shaking conditions causing liquefaction and the standard penetration resistance of sands. In this correlation, the critical value of the standard penetration resistance, N_{crit}, separating liquefiable from nonliquefiable conditions is determined by the following expression

$$N_{crit} = N[1 + 0.125(d_s - 3) - 0.05(d_w - 20)]$$

where d_s = depth to sand layer under consideration in meters

d_w = depth of water table below ground surface in meters

N = a function of the shaking intensity as follows:

Modified Mercelli Intensity	N (blows/ft)
7	6
8	10
9	16

This correlation was found by Seed (1976) to agree with data in Figure 9.

The data presented in this section can be used to give an approximate estimate of the liquefaction potential at a site. Clearly the number of observations is limited and the scatter in the data large. This method is well-suited for preliminary evaluation of alternative sites when detailed tests are not possible. There are problems with the interpretation of the Standard Penetration Test blowcount, N, such as the number of turns on the cathead, etc. (see Schmertmann, 1977).

4.2 CRITICAL VOID RATIO CONCEPT

Castro (1975) differentiates between liquefaction (occurring as a result of loss of shear resistance under monotonic loading) and cyclic mobility, which he defines as progressive softening of a saturated sand under cyclic load. Castro (1975) questions the belief that cyclic mobility can occur in dilative sands in-situ during earthquakes, at least to the same degree as has been observed in the laboratory. He presents data to suggest that the large strains exhibited in laboratory cyclic tests are due to redistribution of void ratios.

In order to better understand this approach, it is of interest to briefly review typical monotonic triaxial test data for cohesionless material. Figure 10a and b shows drained triaxial test results for a loose sand, a dense sand, and a sand at critical void ratio. Here, critical void ratio is defined as that value of initial void ratio that corresponds to the void ratio that would be reached at the maximum shear stress level for a specific soil under a particular confining stress level. As can be seen at failure, the net volumetric strain of a specimen at critical void ratio is zero at maximum shear loading. Loose and dense may be determined in relation to this. Figure 10c and d shows this more clearly for another series of tests at different initial void ratios and confinements. In Figure 10c volume change at maximum shear stress level is plotted versus initial void ratio for three series of triaxial tests under three different confining stresses. Figure 10d shows volume change versus confining pressure for three series of tests at different initial void ratios.

Information from the foregoing tests may be applied to undrained triaxial tests to predict their behavior. Since drainage is not allowed, volume change - and, thus, void ratio - is essentially unchanged. Figure 10e shows a plot of volume change versus initial confining pressure for drained triaxial tests on sand, similar to Figure 10d. Also shown are state paths for both a dense sand (point A) and a loose sand (point B) undergoing shear under undrained conditions.

Since drainage is not permitted (in test conditions), the dense sand trying to dilate reduces pore pressure, thereby increasing effective confinement under monotonic loading until cavitation takes place, point C is reached, or there is sufficient back pressure to allow negative porewater pressure to develop. The opposite is noted for the loose soil which increases pore pressure as it tends to try to compress. Figure 11 compares drained and undrained triaxial test data for a dense sand. It should be noted that although the dense sand does tend to dilate at failure strains, it initially undergoes compression at lower strain levels. These strain levels, although lower than failure, may be within the strain level noted in some earthquakes. Thus, pore pressure might build up even in dense undrained sands.

Castro (1975) in Figure 12 makes use of a state diagram to explain liquefaction under monotonic or cyclic loading. Under loading, a loose soil responds by an increase in pore pressure (reducing confinement) moving from point C toward point A. At point A, unlimited flow occurs at some small residual stress level.

In order to have a quicksand condition, defined by Castro (1975) as complete loss of strength, the soil would require a void ratio greater than Q. Dense sands may also respond by increase in pore pressure

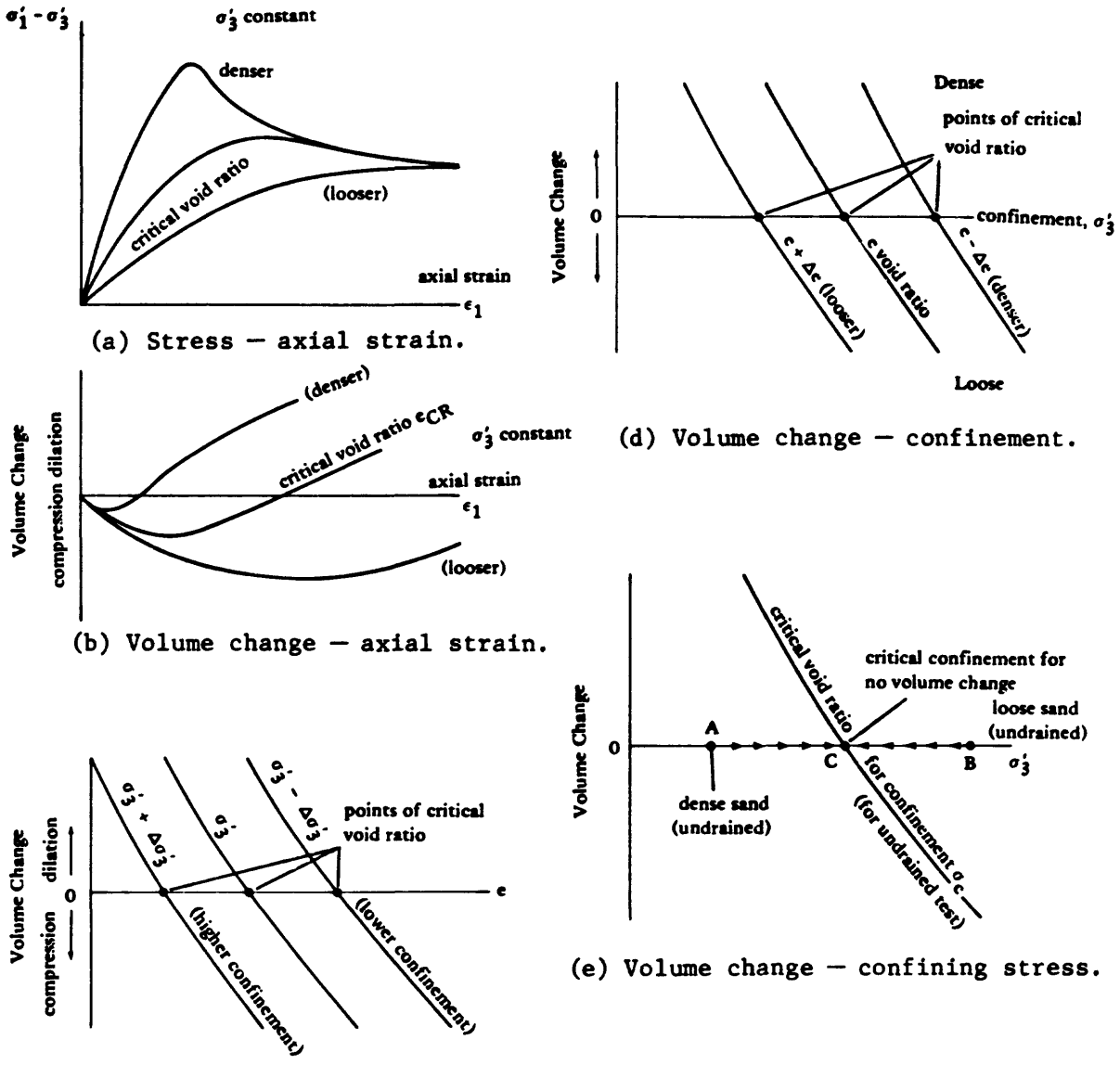

Figure 10. Drained triaxial test data.

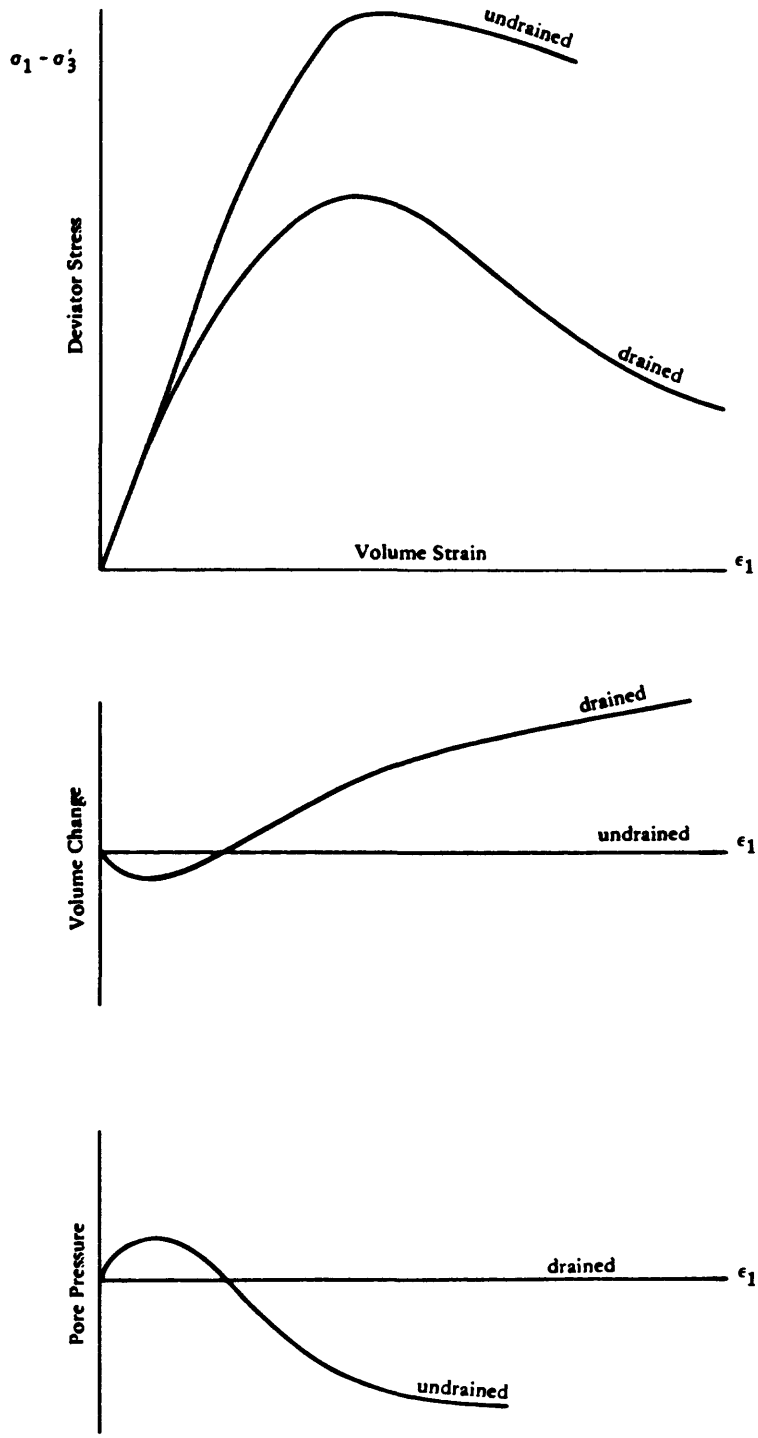

Figure 11. Comparison of drained and undrained triaxial test data for a dense sand.

moving from point D toward point B. Should the cyclic load repetitions be vigorous enough, the sand state reaches point B, where the effective confining stress becomes zero. However, upon shearing, the specimen commences to deform, thereby dilates, and the state of the sand moves toward point D. With further loading the sand state continues to move to the right until, presumably with high enough loading, it meets the steady-state line and commences to deform at constant shear stress level.

This state diagram is used to define a liquefaction potential

$$L_p = \frac{\bar{\sigma}_{3c} - \bar{\sigma}_{3f}}{\bar{\sigma}_{3f}}$$

where $\bar{\sigma}_{3c}$ = the initial effective minor principal stress
$\bar{\sigma}_{3f}$ = the effective minor principal stress at yielding

Since it is assumed that the friction angle of the sand is fully mobilized at steady-state yielding, the liquefaction potential may be defined by using Mohr-Coulomb theory as:

$$L_p = \frac{\bar{\sigma}_{3c} - \bar{\sigma}_{3f}}{\bar{\sigma}_{3f}} = \frac{\Delta u}{\bar{\sigma}_{3f}} = \frac{\Delta u}{\sigma_{df} \frac{1 - \sin \phi}{2 \sin \phi}}$$

where Δu = the pore pressure generated in reaching the critical state line
σ_{df} = the deviator stress existing at this state

The pore pressure Δu can be related to deviator stress σ_{df} by means of Skempton's parameter A_f

$$L_p = A_f \times \frac{2 \sin \phi}{1 - \sin \phi}$$

Although Castro (1975) applies this liquefaction potential value qualitatively (i.e., higher L_p's suggest higher liquefaction tendency), no quantitative criteria are given. Further, a sand classified as dense by this approach would have a negative L_p. Although the implication is that this would not liquefy, no specific statements to this effect are made.

Castro (1975) also shows state diagrams for various sands which show the steady-state lines to be functions of very subtle changes in particle shape, size, and gradation. In some cases these latter parameters are noted to exert an influence on the liquefaction potential as as great as that of relative density, for example.

The foregoing work also states that soils with initial static shear loading may exhibit greater resistance to cyclic mobility. This is explained in terms of the reduced load reversals resulting in reduced void ratio redistribution on laboratory samples.

Castro (1975) points out that tests on undisturbed samples are more realistic than tests on remolded samples; he feels the use of average density specimens to represent stratified sands may introduce large errors. Relative density is not applicable to these types of deposits, and there is no equivalent basis for comparing unit weights of remolded sand with that of the in-situ sand.

4.3 SIMPLE HAND COMPUTATION

Seed and Idriss (1970a) have proposed a simplified hand computation procedure for evaluating liquefaction. They assume that the liquefaction producing shear stresses developed in a soil deposit are caused by upward propagating shear waves. The depth to the soil region under liquefaction investigation is defined as h. The soil column within a depth h is assumed to behave as shown in Figure 13. The maximum shear stress at a depth h is related to the ground acceleration by equilibrium

$$\tau_{max} = \frac{\gamma h}{g} \left(A_{max} \, r_d \right)$$

where γ = total unit weight of soil

h = depth to region where liquefaction is expected

A_{max} = maximum surface acceleration

r_d = acceleration correction factor

The factor r_d is used to reduce the surface acceleration for depth since the soil is a deformable body rather than a rigid one. Figure 14 gives a range of values for r_d with depth. The actual time history of motion will have an irregular form (Figure 15), and an equivalent average stress is taken as 65% of the maximum which corresponds to an equivalent number of uniform cycles. Thus, the average stress τ_{av} is

$$\tau_{av} = 0.65 \left(\frac{\gamma h}{g} \right) A_{max} \, r_d$$

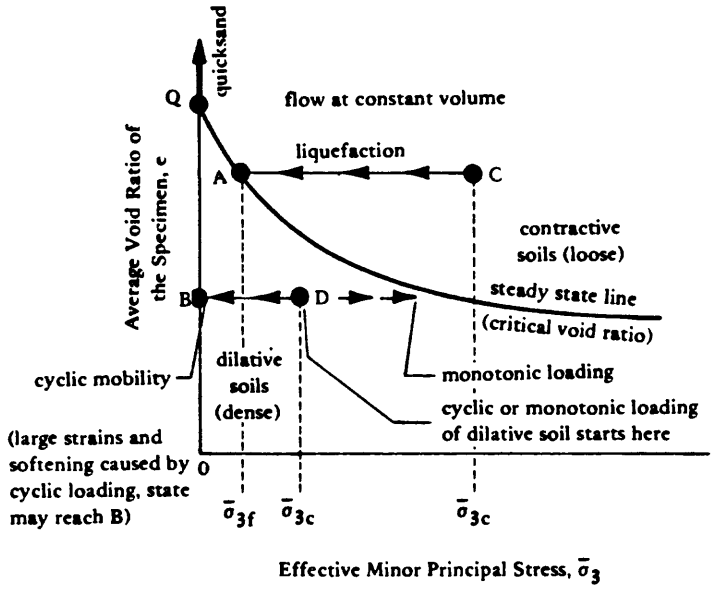

Figure 12. Undrained tests on fully saturated sands depicted on state diagram (from "Liquefaction and Cyclic Mobility of Saturated Sands," by G. Castro in ASCE Journal of the Geotechnical Division, vol. 101, no. GT6, Jun 1975).

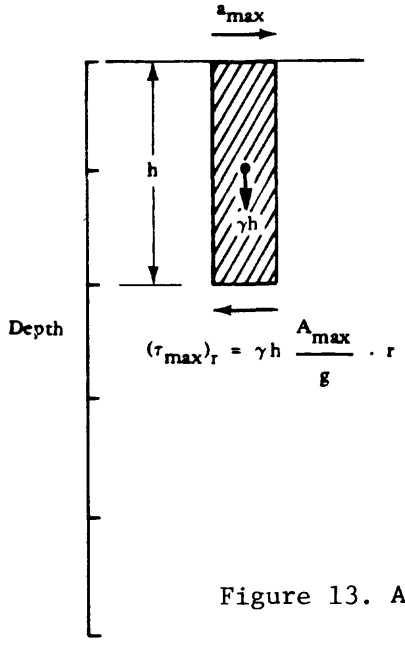

Figure 13. Approximate equilibrium representation.

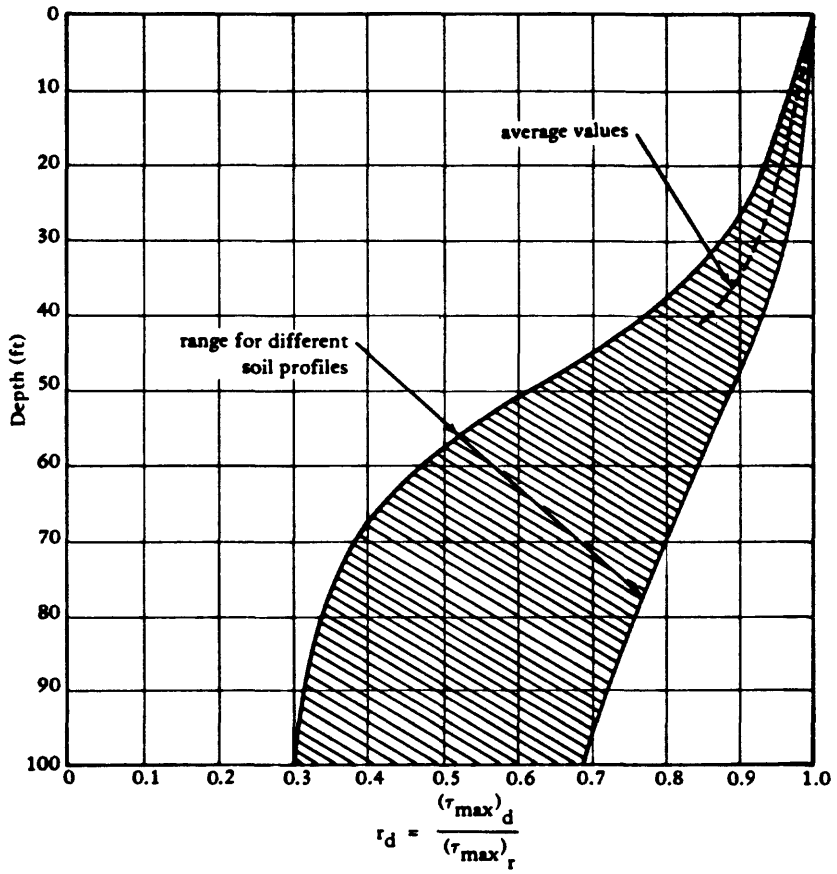

Figure 14. Range of value of r_d for different soil profiles.

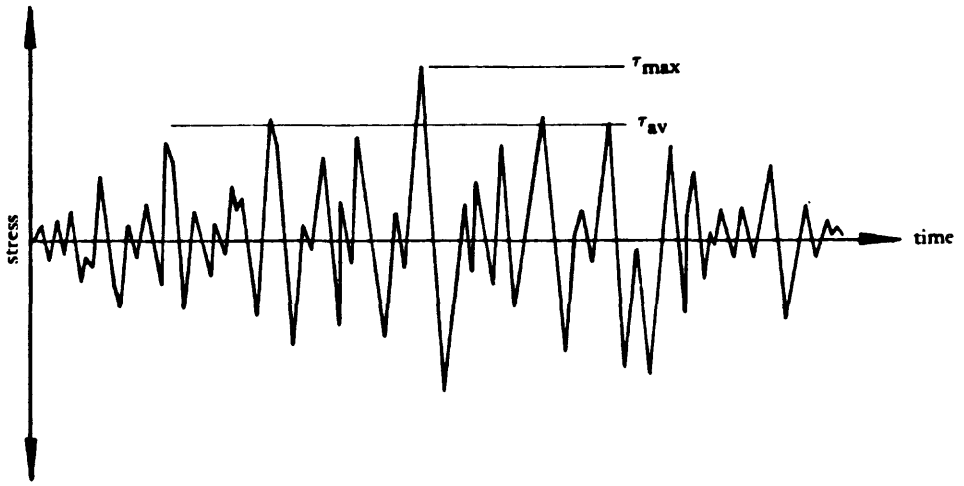

Figure 15. Time history of shear stresses during earthquake.

Evaluation of earthquake data has provided information on the equivalent number of significant stress cycles that can be expected as a function of earthquake magnitude, which will be presented later in this chapter.

Having the number of cycles, the average applied shear stress and the effective confining stress (s'_v, vertical stress), a simple procedure can be used to determine the liquefaction factor of safety. The number of cycles causing liquefaction can be determined by a laboratory test program using cyclic triaxial compression tests. Correction factors have been developed by DeAlba, Chan, and Seed (1975) (Figure 16) to relate triaxial tests to (free-field) field observation. Additional correction factors for multidirectional shaking (Pyke, Chan and Seed, 1974) and soil in-situ overconsolidation (Mulilis, Chan and Seed, 1975) are also given (Figure 16a and b). Laboratory tests on undisturbed (where possible) samples should be performed to determine the number of uniform cycles of shear causing liquefaction as a function of τ_{av}/σ_v. The factor of safety is defined as the ratio of resisting shear stress capacity (determined from corrected triaxial test) to applied shear stress (τ_{av} calculated above) for the number of equivalent uniform earthquake cycles expected.

Figure 17 is a summary of triaxial test data compiled by Donovan (1974). The data is normalized in terms of stress ratio divided by relative density and is limited to D_r less than 75%. The value of σ_3 is used as the effective confining stress. The mean value of the data in Figure 17 appears to be a fairly good representation for uniform sands and could be used when undisturbed samples are not available for testing. Since this curve represents triaxial test results, the stress ratio must be corrected for application to the field.

There are 34 cases of observed liquefaction where data of ground motion and site profile were estimated (Seed and Peacock, 1970). This data was used to plot the points shown in Figure 18 correcting field data to triaxial conditions. As can be seen there are no cases in which liquefaction was observed which extend below the mean minus one standard deviation and no cases in which liquefaction was not observed which extend above the mean plus one standard deviation. Thus additional validity is provided for Figure 17.

4.3.1 Application of Simple Hand Computation in Developing Charts

To evaluate the liquefaction potential of a deposit it is necessary to determine whether the shear stress induced at any depth by the earthquake τ_{av} is large enough to cause liquefaction at that depth as indicated by corrected data from Figure 17 or by laboratory tests. For uniform deposits in which the water table is at a depth of 0 to 10 feet, the critical depth will often appear to be about 20 feet. Thus, the evaluation can often be made simply for a representative element at one of these depths.

Consider for example, a deposit of sand for which the water table is 5 feet below the ground surface and which is subjected to 10 cycles of ground shaking. The average shear stress induced will be:

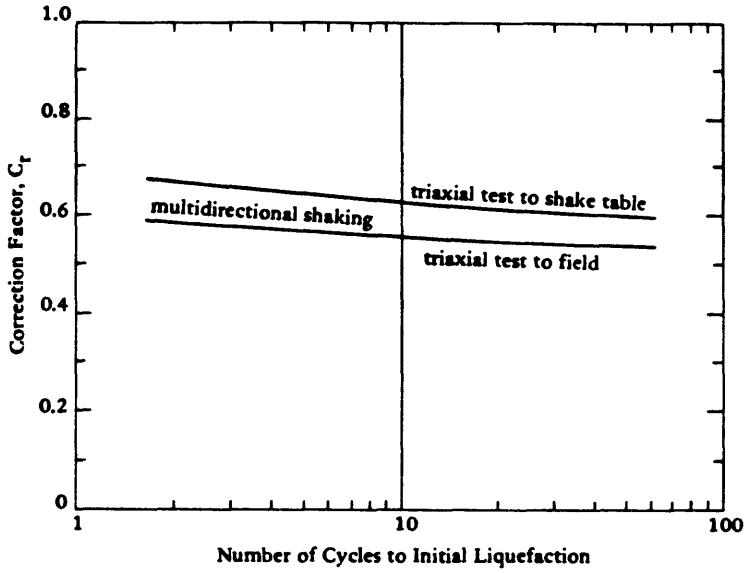

(a) $K_o = 4.$

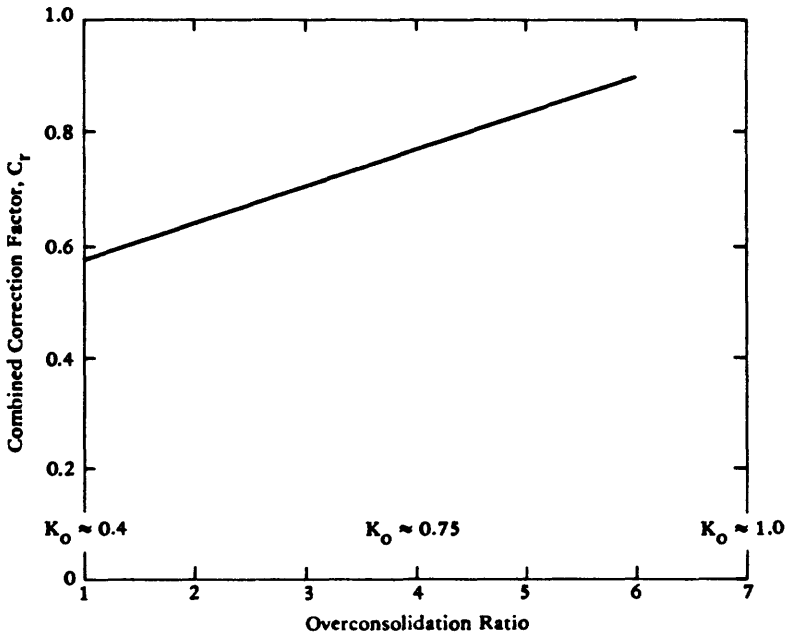

(b) Combined correction factor for cyclic triaxial compression tests accounting for multidirectional shaking and overconsolidation.

Figure 16. Correction factors for triaxial test results (from P. DeAlba, C. K. Chan, and H. B. Seed, 1975).

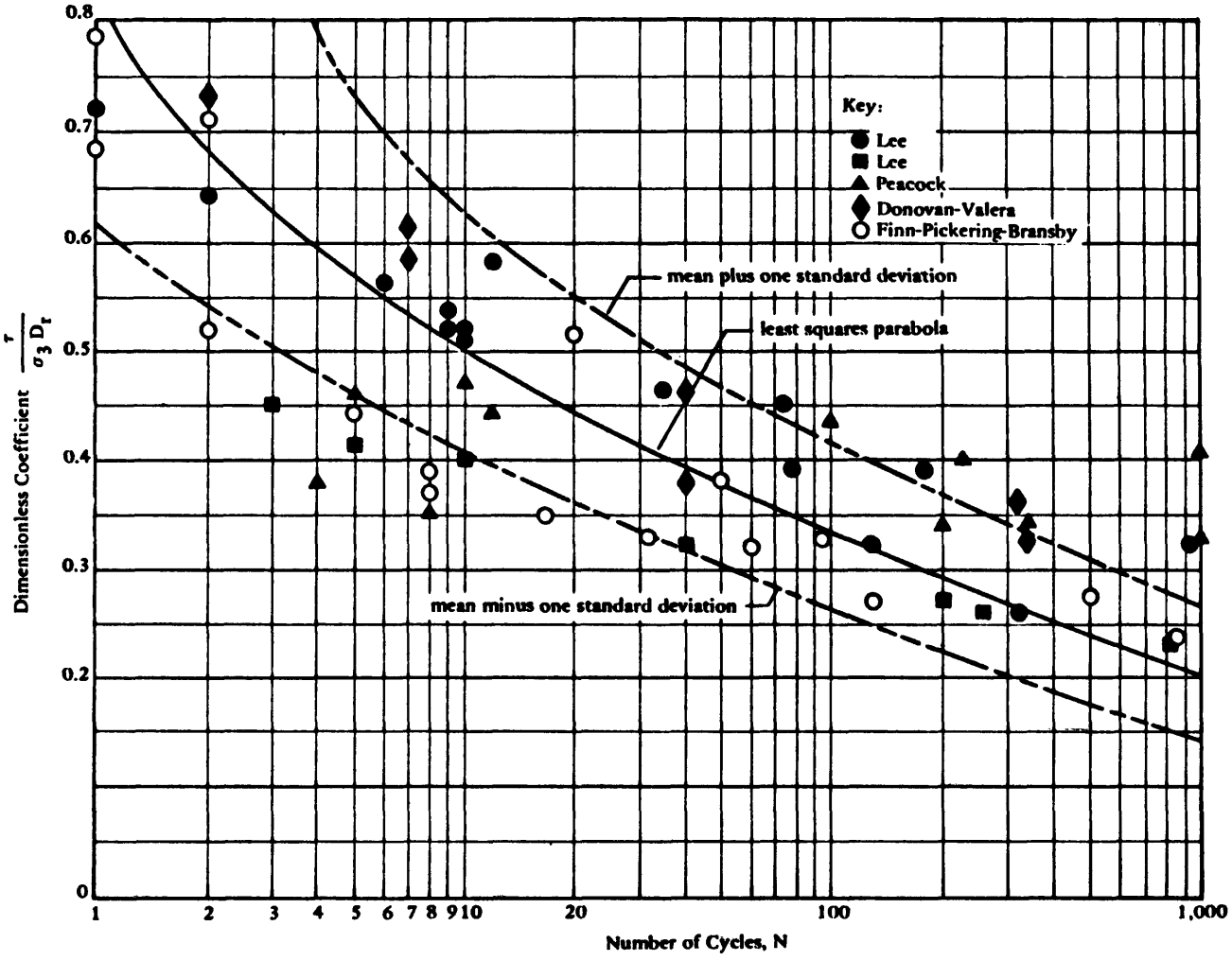

Figure 17. Soil strength for initial liquefaction (triaxial test data) (from Donovan,1974).

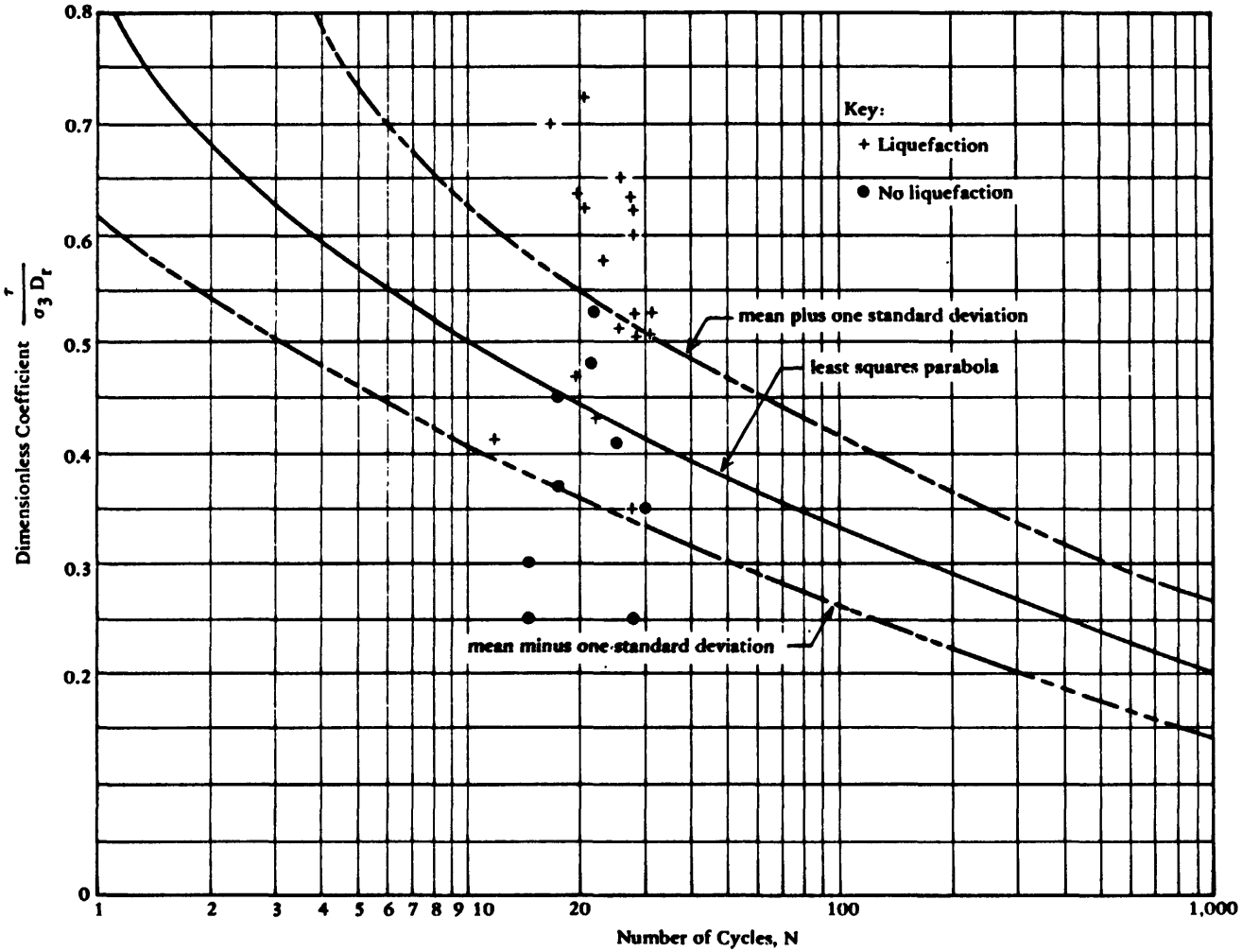

Figure 18. Field observations corrected to triaxial conditions (from Donovan, 1974).

$$\tau_{av} = 0.65 \left(\frac{\sigma_v}{g}\right) A_{max}\, r_d$$

At a depth of 20 feet, $r_d = 0.95$ (see Figure 14) giving

$$\tau_{av} = 0.65 \times 0.95 \times \frac{\sigma_v}{g} A_{max}$$

From Figure 17 the shear stress required to cause initial liquefaction for 10 cycles is

$$\tau/(\sigma_3' D_r) = 0.5$$

and

$$\tau_{av}/\sigma_v' = \frac{\tau C_r}{\sigma_3'}$$

Thus,

$$\tau_{av} = 0.5\, \sigma_v'\, C_r\, D_r$$

where D_r is expressed as a decimal value and C_r is obtained from Figure 16.

Equating the applied τ_{av} with τ_{av} to give initial liquefaction gives

$$0.65 \times 0.95 \left(\frac{\sigma_v}{g}\right) A_{max} = 0.5\, \sigma_v'\, C_r\, D_r$$

$$\frac{A_{max}}{g} = 0.81 \left(\frac{\sigma_v'}{\sigma_v}\right) C_r\, D_r$$

where $\sigma_v = \gamma h$

Assume a total saturated density of 132 lb/ft^3, a total density above the water table of 117 lb/ft^3, and a buoyant density of 69 lb/ft^3. This reduces to

$$\frac{A_{max}}{g} = 0.81 \times \frac{1620}{2565} \times C_r D_r$$

$$\frac{A_{max}}{g} = 0.512 C_r D_r$$

For 10 cycles, $C_r = 0.57$

$$\frac{A_{max}}{g} = 0.29 D_r$$

Thus, the following can be determined:

D_r	A_{max}/g
0.40	0.116
0.50	0.145
0.60	0.174
0.70	0.203

The above values give the acceleration required to cause initial liquefaction at a depth of 20 feet with the water table at 5 feet, subject to 10 cycles of ground shaking.

Observed cases of liquefaction from Seed and Peacock (1970) are summarized in Figure 19 from which the following may be stated:

Maximum Ground Surface Acceleration	Liquefaction Very Likely	Liquefaction Potential Depends on Soil Type and Earthquake Magnitude	Liquefaction Very Unlikely
0.10 g	$D_r < 33$	$33 < D_r < 54$	$D_r > 54$
0.15 g	$D_r < 48$	$48 < D_r < 73$	$D_r > 73$
0.20 g	$D_r < 60$	$60 < D_r < 85$	$D_r > 85$
0.25 g	$D_r < 70$	$70 < D_r < 92$	$D_r > 92$

The data from Seed and Peacock may also be plotted to give Figure 20.

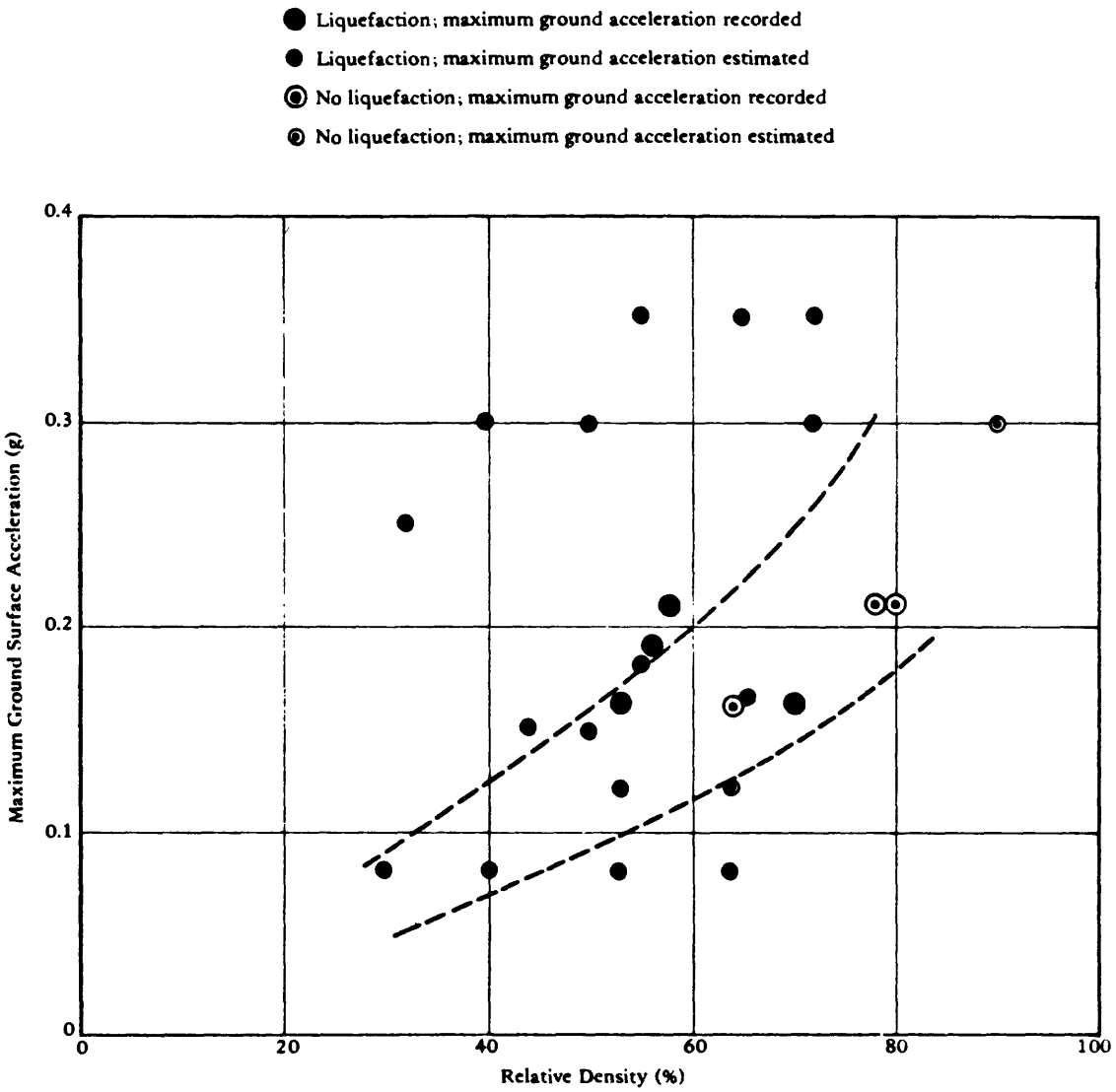

Figure 19. Evaluation of liquefaction potential for sands (water table 5 feet below ground surface) ("Evaluation of Soil Liquefaction Effects on Level Ground During Earthquakes," by H. B. Seed, in ASCE Preprint 2752 of Liquefaction Problems in Geotechnical Engineering, ASCE Annual Convention, Philadelphia, Pa., 27 Sep-1 Oct 1976).

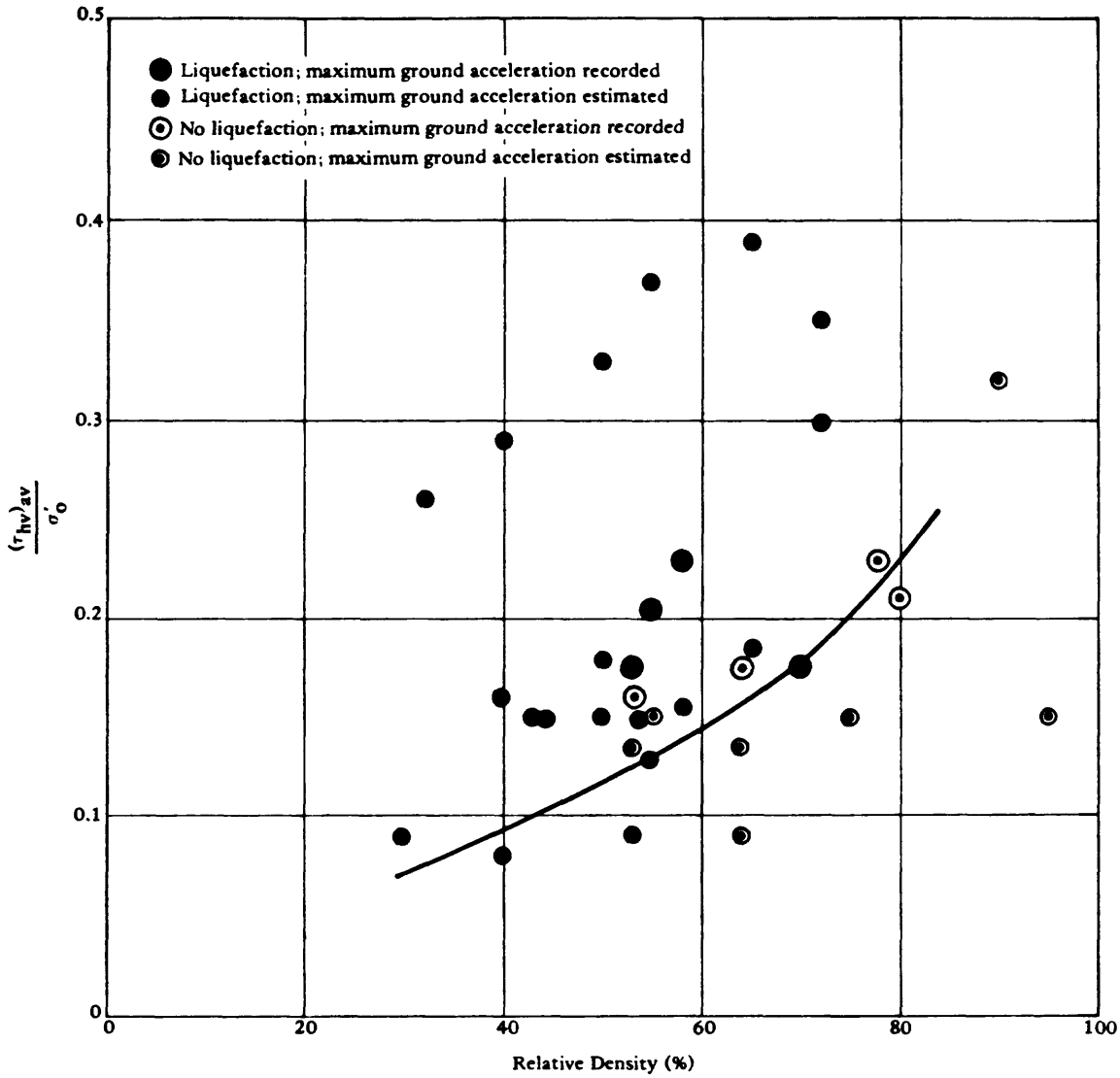

Figure 20. Relationship between $(\tau_{hv})_{av}/\sigma'_o$ and relative density for known cases of liquefaction and nonliquefaction (from Report No. EERC 70-8 by H. B. Seed and W. H. Peacock, Nov 1970).

The values of relative density may be converted to values of standard penetration as a function of depth. Charts have been prepared by Seed and Idriss (1970a) giving the range of penetration resistance values in which liquefaction might be expected, Figures 21a and b.

4.3.2 Simple Computer Analysis

Donovan (1974) has developed a computer program based in part on the simple soil model described in the previous section. The earthquake record is represented in terms of the peak acceleration, duration, and predominant frequency. The number of cycles at various acceleration levels is determined by a Rayleigh distribution. Miner's Linear Damage criteria are used to convert the different stress levels to an average stress for computation of a factor of safety. Donovan (1974) has compiled various triaxial test data, Figure 17. This data is used in the program as a measure of the soil shear strength. The input to the program requires a soil profile, limited knowledge of soil material and limited knowledge of the earthquake. The input to the program is simple and straightforward, consisting of the following:

1. Relative density of the soil layer of interest
2. Depth to center of the layer
3. Correction factor for triaxial test data (Figure 16)
4. Pressure produced by total weight of material above center of layer
5. Effective stress at center of layer
6. Factor relating peak stress to root-mean-square value (3.5 to 4.5 is used) (see Donovan, 1974)
7. Reduction of stress for depth (usually 0.9 to 1.0)
8. Maximum surface acceleration
9. Duration of earthquake
10. Fundamental period of soil deposit
11. Data pairs defining the τ_{av}/σ'_v ratio versus the number of cycles (Figure 17)

The fundamental period of a soil deposit given as item 10 above is equal to the fundamental period of the soil overlying rock-like formations when subject to vertically propagating shear waves. For this usage, a rock-like formation is defined to be any material in which the shear wave velocity at small strains is about 2,500 ft/s or greater. The limit to depth is taken to be 500 feet. Based on this, the natural period will vary from less than 1.0 second to 2.5 seconds. The value 0.5 second is usually used as a minimum natural period. Firm sites, where only dense granular soils overlie bedrock and the depth to bedrock is less than 30 feet or where very dense cemented granular soils overlie bedrock and the depth of bedrock is 70 feet or less, may be considered to have a natural period of 0.5 second. For soils where the shear wave velocity of the soil does not decrease markedly with depth, the characteristic site period may be computed by:

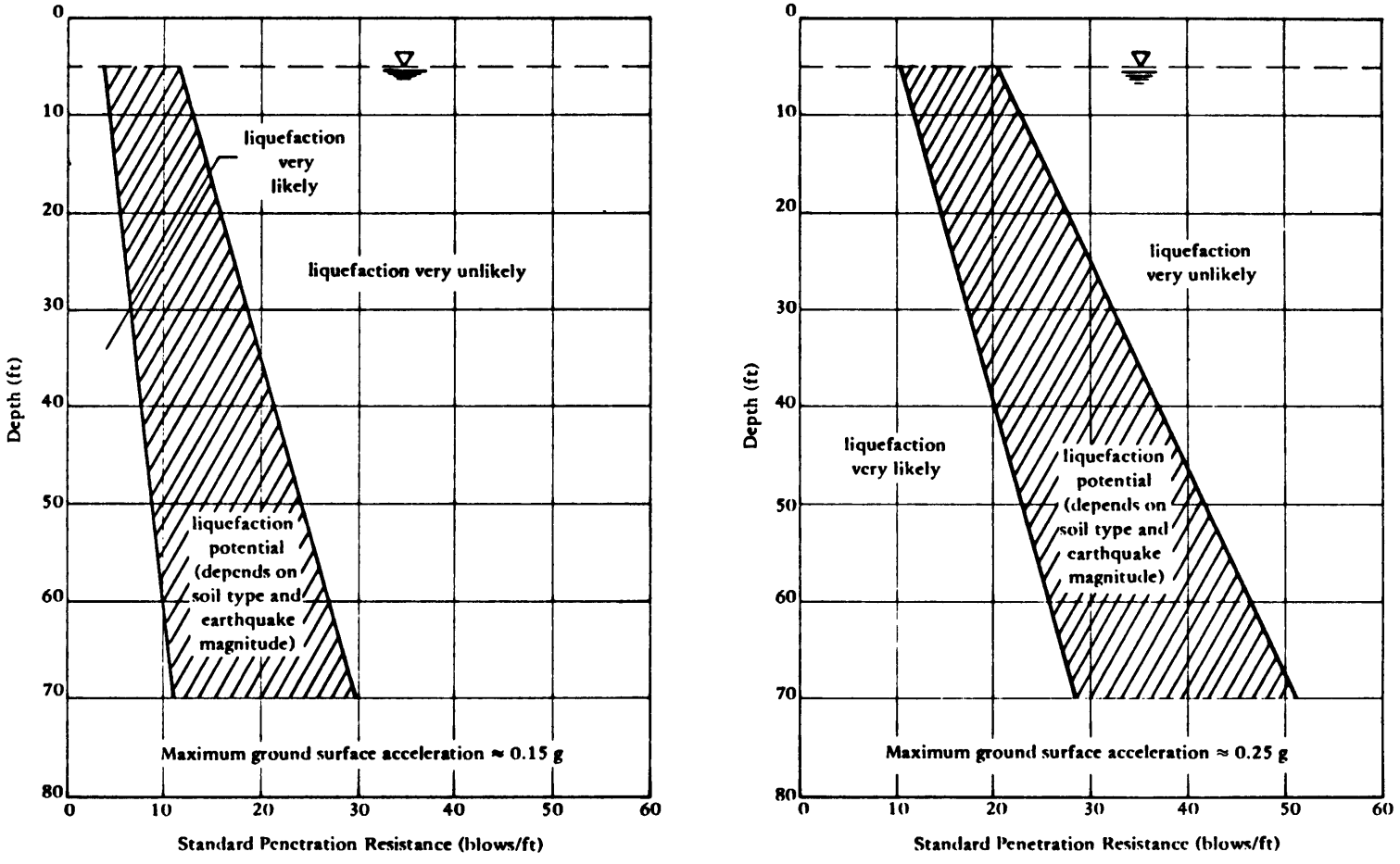

(a) Water table at a depth of about 5 feet.

Figure 21. Liquefaction potential evaluation charts for sands (from Report No. EERC 70-8 by H. B. Seed and W. H. Peacock, Nov 1970).

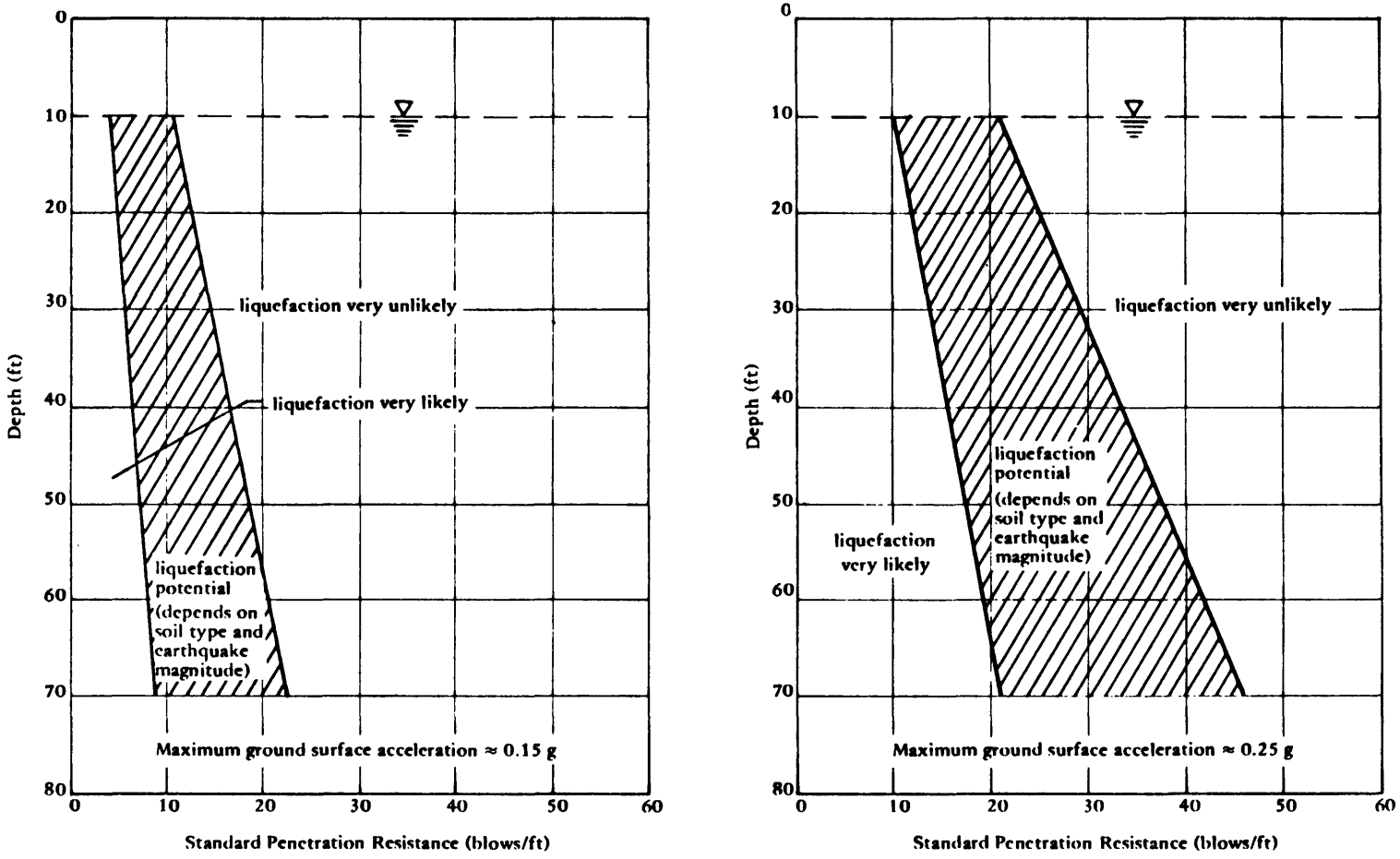

(b) Water table at a depth of about 10 feet.

Figure 21. Continued.

$$T = \frac{4\,H}{R\,V_s}$$

where H = the depth of soil overlying bedrock

V_s = average shear wave velocity of soil as measured in the field

R = correction factor to V_s for higher strain levels as follows:

R	Earthquake Magnitude	Peak Acceleration
0.9	6	0.1 g
0.8	6	0.2 g
0.67	7	0.3 g
0.67	7	0.4 g

The program computes the number of cycles by dividing the duration of the earthquake by the period of the soil deposit.

An example problem is given in Figure 22.

4.4 COMPLEX COMPUTER ANALYSIS, ONE-DIMENSIONAL MODELS

A soil profile may be analyzed as a one-dimensional shear wave problem assuming the stress wave to be only a vertically propagating shear wave. The differential equations of motion can be solved in closed form for linear elastic soil properties. This has been done by Seed and Idriss (1969) and Kanai (1961) to provide a one-dimensional analysis of sites of simple geometry. However, the stress-strain characteristics of a site are highly nonlinear, hysteretic, and strain-dependent.

Streeter, et al (1974) developed a computer program using the method of characteristics for calculating one-dimensional dynamic behavior of soils. A soil profile is divided into layers down to bedrock. Dynamic excitation of the soil is introduced at the rock-soil interface. The response of the soil can be evaluated on the basis of elastic, viscoelastic, or nonlinear (Ramberg-Osgood) soil behavior. The program determines shear, velocity, and displacement information.

An analytical technique for analyzing the response of horizontal soil profiles to earthquake motion is described by Seed and Idriss (1969, 1970b) and Idriss and Seed (1968, 1970). The soil profile is idealized by a series of discrete masses and springs with linear viscous dampers. The nonlinear and hysteretic stress-strain characteristics of the soil are introduced by using an equivalent shear modulus and an equivalent viscous damping factor which can vary with each layer of soil profile and with the strain level within the layer. The equivalent shear modulus for a given strain level is taken as the slope of the diagonal line (average slope) drawn through the hysteresis loop, which is shown in Figure 23 for a cyclically loaded laboratory specimen. The

```
EXAMPLE DATA SET FOR LIQUEFACTION BY STOCHASTIC PROCEDURES:  NCD  6-74
EL CENTRO EARTHQUAKE OF 1940.  LIQUEFACTION IN BRAWLEY, CALIF. (M=7.0)

LIQUEFACTION EVALUATION BY DONOVAN≠S STOCHASTIC PROCESS FOR LAYER
NUMBER 1 AT DEPTH OF 15.0 FEET,    NARROW BANDWIDTH USING ASSUMED
RAYLEIGH DISTRIBUTION

LIQUEFACTION POTENTIAL ESTIMATION BASED ON INTERPOLATION OF A
SERIES OF POINTS ON A (TAU/SIGMA) VS LOG10(NUMBER OF CYCLES)
RELATIONSHIP.  DATA FOR A RELATIVE DENSITY OF  55 PERCENT

       TAU/SIGMA  NUMBER OF CYCLES

  1       .421          1.00
  2       .359          3.00
  3       .332          5.00
  4       .297         10.00
  5       .265         20.00
  6       .225         50.00
  7       .198        100.00
  8       .173        200.00

    AVERAGE MAXIMUM SHEAR STRESS    =    180.0 PSF
    PEAK VALUE SIGMA LEVEL          =      4.0
    SIMPLE SHEAR CORRECTION FACTOR  =      .59
    DEPTH EFFECT REDUCTION FACTOR   =     1.00
    PEAK SURFACE ACCELERATION       =     .100 G
    EFFECTIVE NORMAL STRESS         =   1800.0 PSF
    FUNDAMENTAL PERIOD              =      .50 SECONDS
    DURATION OF STRONG SHAKING      =     30.0 SECONDS
    MOST PROBABLE NUMBER OF CYCLES  =       60
    RELATIVE DENSITY                =    55.000

      ALL STRESS VALUES REPRESENT THE  4.00 TIMES SIGMA LEVEL

      LIQUEFACTION WILL NOT OCCUR AT A RELATIVE DENSITY OF 55.000

    ITERATION NUMBER      =  1
    PEAK SHEARING STRESS  =  180.00 PSF

         STRESS    CUMULATIVE
           PSF       DAMAGE

         180.00   15.154E-03

    ITERATION NUMBER      = 17
    PEAK SHEARING STRESS  =  487.69 PSF
    FACTOR OF SAFETY      =   2.709

         STRESS    CUMULATIVE
           PSF       DAMAGE

         487.69   99.977E-02
```

Figure 22. Example problem using simple computer program.

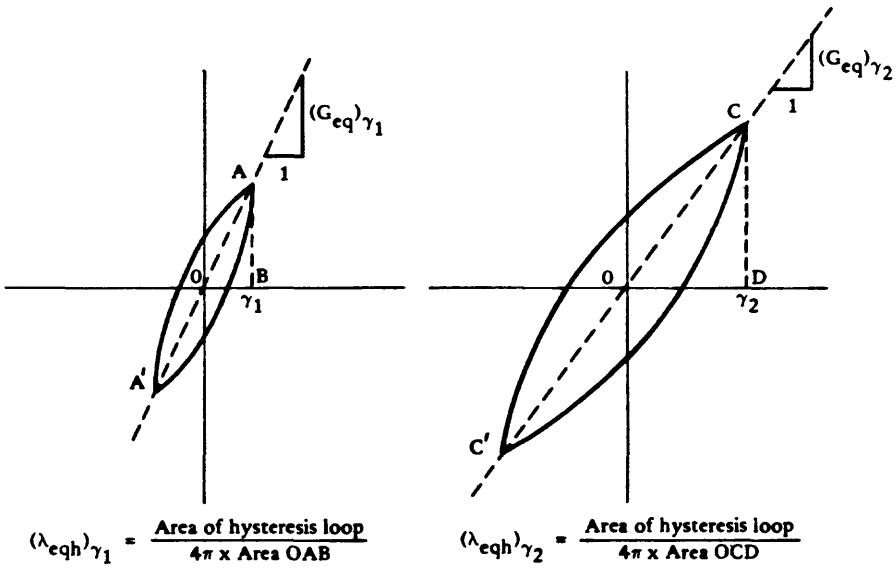

Figure 23. Equivalent linear shear moduli and damping used in discrete mass model (from H. B. Seed and I. M. Idriss, Jan 1969).

average equivalent viscous damping coefficient is proportional to the ratio of area of the hysteretic loop, as shown in the figure, to the maximum stored energy during the cycle.

An iterative procedure is used to obtain strain compatible values of shear modulus and damping. The response of the soil profile modeled as discrete masses is computed, and strains are determined.

Another automated-analysis technique, more widely used today for treating horizontal soil layers, has been develoed by Schnabel, Lysmer, and Seed (1972), based on the one-dimensional wave propagation method. This program, SHAKE, can compute the responses for a given horizontal earthquake acceleration specified anywhere in the system. The analysis incorporates nonlinear soil behavior, the effect of the elasticity of the base rock, and variable damping. It computes the responses in a system of homogeneous viscoelastic layers of infinite horizontal extent, subject to vertically traveling shear waves. The program is based on the continuous solution of the wave-equation adapted for use with transient motions through the Fast Fourier Transform algorithm. Equivalent linear soil properties are obtained by an iterative procedure for values of modulus and damping compatible with the effective strains in each layer. The following assumptions are made:

1. The soil layers extend infinitely in the horizontal direction.
2. The layers are completely defined by shear modulus, critical-damping ratio, density and thickness.
3. The soil values are independent of frequency.
4. Only vertically propagating, horizontal shear waves are considered.

The soil model is similar to that developed by Seed and Idriss (1970c), using data based on Hardin and Drnevich (1970). The absolute range of soil parameter variation may be stipulated by merely in-putting factors whose numerical values may be derived from simple soil strength properties. These strength properties may be the undrained shear strength of a clay or the relative density for sands. The program requires the definition of the soil profile down to bedrock (assumed as seismic velocity 2,500 ft/s) as well as an earthquake time history record in digital form.

The motion used as a basis for the analysis can be given in any layer in the system, and new motions can be computed in any other layer. Maximum stresses and strains, as well as time histories, may be obtained in the middle of each layer. Response spectra may be obtained and amplification spectra determined.

For liquefaction analysis of a soil profile the stress history of the various layers is compared to their susceptibility to liquefaction.

The calculated shear stress history is used to determine a number of equivalent cycles of load at an average stress level from which τ_{av}/σ'_v is determined. The liquefaction susceptibility may be measured directly by cyclic loading test or estimated on the basis of Figure 17.

For laboratory cyclic load tests, soil specimens are prepared to represent the insitu conditions and are subjected to stress cycles of various magnitudes to determine the number of actual cycles necessary to cause liquefaction. The triaxial test information corrected to field conditions is used to estimate the shear stress level to cause liquefaction for the number of cycles determined in the computer analysis. The factor of safety is the ratio of the resisting shear strength from the triaxial test data to the applied shear stress level from the computer analysis.

Lee and Chan (1972) have developed a procedure for computing the equivalent number of cycles. The term equivalent number of significant cycles N_{eq} refers to that number of uniform cycles of stress intensity τ_{av} which, if applied to an element of soil, would have the same effect in terms of the soil strength or deformation as if the actual train of irregular cyclic shear stresses were applied (see Figure 24). The value of τ_{av} is usually taken to be equal to 0.65 τ maximum. To convert the actual stress time history into an equivalent number of uniform cycles, divide the stress range (0 to τ maximum) into a convenient number of levels and note the stress within each level or increment, τ_i as shown in Figure 25 and Table 1. The actual number with peaks in the computed stress history which fall within each of these levels is counted n_{τ_i}. Since the actual time history is not symmetric about the zero stress axis, the number of peaks on both sides are counted, and two peaks are equivalent to one cycle. A shear strength curve from laboratory tests or Figure 17 is corrected to field conditions. This curve represents a factor of safety of 1.0; theoretically the values on the curve should be divided by the estimated factor of safety to correctly show the true relationship for the soil under the specific earthquake.

The number of cycles N_{τ_i} and $N_{\tau_{av}}$ corresponding to the incremental stress levels and τ_{av} level are obtained. The ratio of the number of cycles at the τ_{av} stress level to cause liquefaction $N_{\tau_{av}}$ to the number of cycles at the incremental stress levels to cause liquefaction N_{τ_i} is used to multiply the actual number of counted cycles at that incremental stress level n_{τ_i}. These ratios are summed for all n increments of stress from 0 to τ_{max}

$$N_{eq} = \sum_{i=1}^{n} \left(\frac{N_{\tau_{av}}}{N_{\tau_i}} \text{ from test data or Fig 17} \right) \left(n_{\tau_i} \begin{matrix} \text{actual} \\ \text{SHAKE} \\ \text{data} \end{matrix} \right)$$

If the estimated factor of safety is correct, N_{eq} determined from the summation would equal $N_{\tau_{av}}$ from the laboratory test data or Figure 17 at the average stress level. If it does not, revise the estimate of the factor of safety and repeat. In practice it has been found that it is not necessary to multiply the strength curve by the estimated factor of safety. In this case the factor of safety would then be the ratio of τ at N_{eq} from test data divided by τ_{av}.

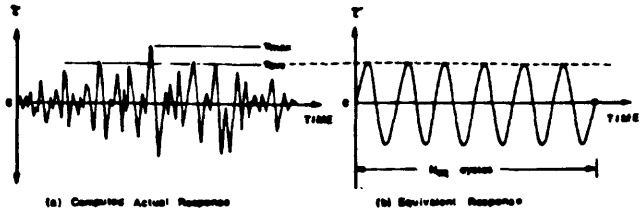

Figure 24. Actual and equivalent earthquake stress history.

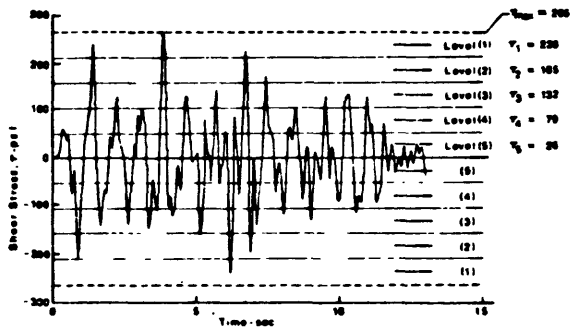

Figure 25. Steps in calculating N_{eq} from seismic stress history.

Table 1. Equivalent Stress Levels

Single Cycle at the Following Stress Levels (τ_{max})	Equivalent Number of Cycles at 0.65 τ_{max}
1.0	3
0.95	2.7
0.9	2.4
0.85	2.05
0.8	1.7
0.75	1.4
0.7	1.2
0.65	1.0
0.6	0.7
0.55	0.4
0.5	0.2
0.45	0.1
0.4	0.04
0.35	0.02

Seed, et al (1975) have proposed Figure 26 as an average shape representation of the relationship between stress ratio and number of cycles to liquefaction. Using Figure 26, Figure 27 is generated; a factor of safety of 1.5 is applied to produce the lower curve. From this curve, Table 1 is obtained which gives conversion factors for equivalent stress levels. An example is given in Figure 28. Seed, et al (1975) have also evaluated the equivalent number of uniform stress cycles based on strong motion data (Figure 29).

4.5 EFFECTS OF SOIL AND SITE PARAMETERS

Frequently, the parameters needed in the response studies are poorly defined at a given location. Often, the values of these parameters must be assumed in order to perform the ground response analyses. Experience has shown that variations in the value of any one of the parameters may affect the solution differently from site to site, and no general rules may be formulated at this time to establish the influence of the variables.

Earthquake motions are produced by a stress wave, which is transmitted more rapidly and with less energy loss through the bedrock than through the overlying soils. When the bedrock has a horizontal surface of great extent and the overlying soil layers are also horizontal, it is frequently assumed that the earthquake motion within the soil is produced essentially by horizontal shear waves which propagate upward through the soil from the bedrock surface. This assumption greatly simplifies the analysis since the problem can be reduced to a one-dimensional shear wave problem. This is a simplification, since vertical components of the earthquake motion are always present and the wave transmission problem may be more complex than can be simulated in a one-dimensional model.

When the bedrock or soil layers are inclined, a one-dimensional shear wave assumption is questionable, and a two-dimensional model may be required to account for the more complex geometry and wave motion.

Lysmer, Seed, and Schnabel (1970) have shown that under identical boundary conditions, the lumped mass solution and the wave propagation solution are basically the same. Arango and Dietrich (1972) have investigated the variation of parameters for the two methods. They note close agreement in peak levels of motion with some differences in computed time histories.

4.6 COMPLEX COMPUTER ANALYSIS, TWO-DIMENSIONAL MODELS

As pointed out earlier, when the ground surface or the soil layers are inclined, one-dimensional wave assumptions may not be valid and a two-dimensional model may be required to represent the more complex geometry. Although two-dimensional liquefaction analyses are not in routine soil practice, the same procedures for evaluation of a stress history can be utilized. Finite element representations have been used to study dams and embankments.

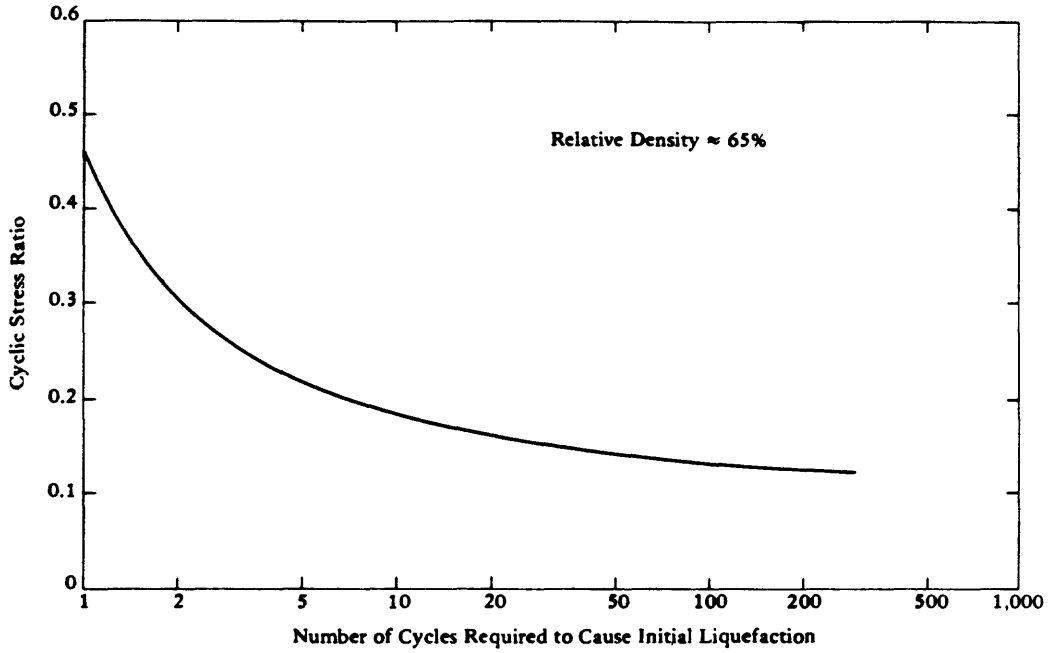

Figure 26. Representative curve for relationship between cyclic stress ratio and number of cycles to liquefaction (from H. B. Seed, 1976).

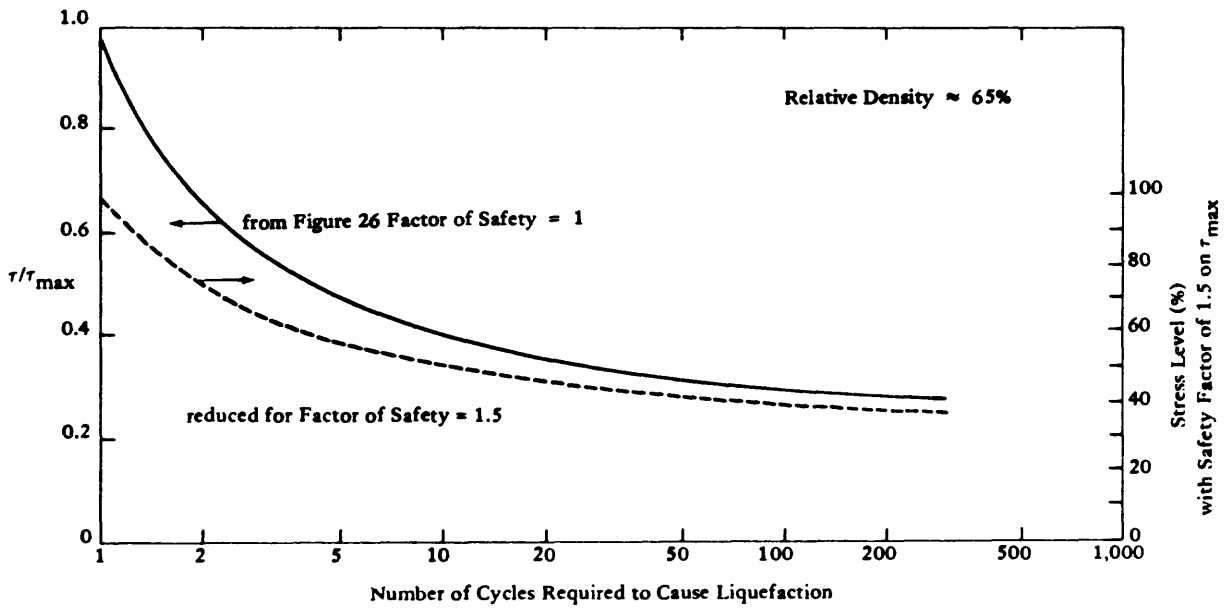

Figure 27. Representative relationship between τ/τ_{max} and number of cycles required to cause liquefaction (from H. B. Seed, 1976).

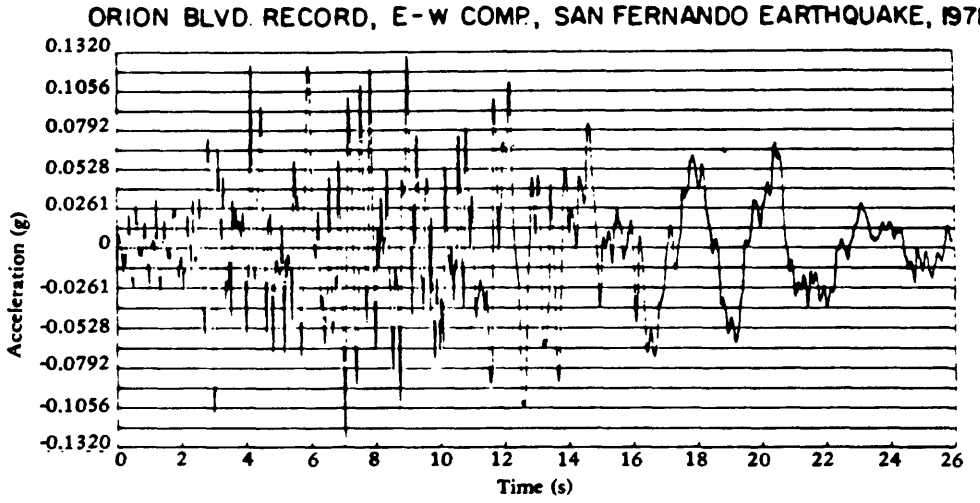

	ABOVE HORIZONTAL AXIS			BELOW HORIZONTAL AXIS		
Stress Level: Fraction of τ_{max}	Number of Stress Cycles	Conversion Factor	Equivalent No. of Cycles at 0.65 τ_{max}	Number of Stress Cycles	Conversion Factor	Equivalent No. of Cycles at 0.65 τ_{max}
τ_{max}	—	—	—	1	3.00	3.00
0.95 "	3	2.70	8.10	—	—	—
0.90 "	1	2.40	2.40	—	—	—
0.85 "	2	2.05	4.10	1	2.05	2.05
0.80 "	—	—	—	2	1.70	3.40
0.75 "	3	1.40	4.20	—	—	—
0.70 "	—	—	—	2	1.20	2.40
0.65 "	1	1.00	1.00	1	1.00	1.00
0.60 "	2	0.70	1.40	1	0.70	0.70
0.55 "	3	0.40	1.20	3	0.40	1.20
0.50 "	1	0.20	0.20	5	0.20	1.00
0.45 "	3	0.10	0.30	5	0.10	0.50
0.40 "	3	0.04	0.12	—	—	—
0.35 "	5	0.02	0.10	7	002	0.14
0.30 "	—	—	—	—	—	—
		Total	23.12		Total	15.39
		Average number of cycles at 0.65 τ_{max} = 19.30				

Figure 28. Evaluation of equivalent uniform cyclic stress series, Orion Boulevard record, east-west component (from H. B. Seed, 1976).

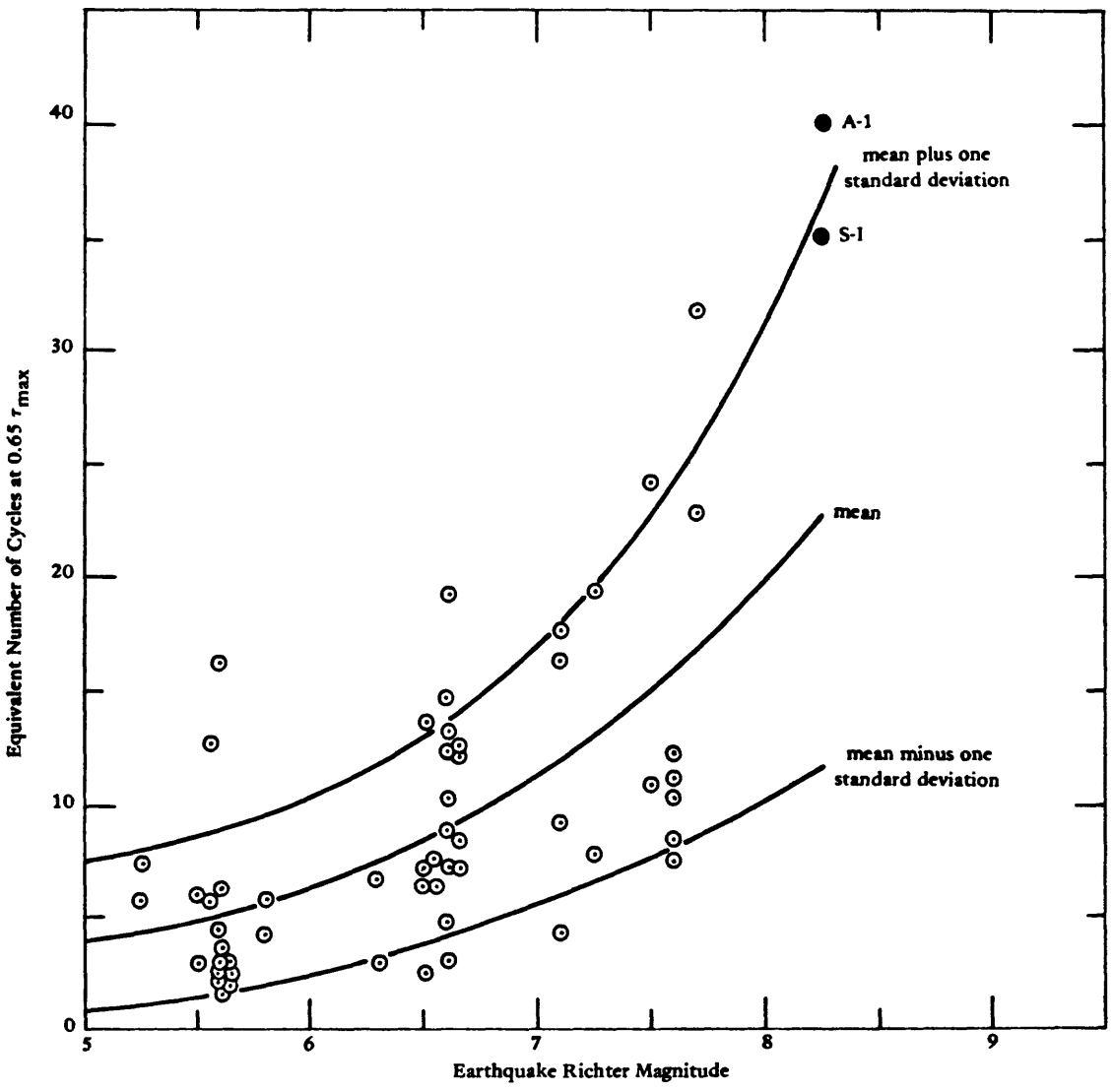

Figure 29. Equivalent numbers of uniform stress cycles based on all components of ground motion (from H. B. Seed, 1976).

Idriss, et al (1973) have developed a two-dimensional finite element program - QUAD-4 - for the evaluation of seismic response of soil deposits. This program allows for variable damping in each element using a Rayleigh damping expression for that element. The damping matrix for the entire assemblage of elements is obtained by appropriate addition of the damping submatrices of all the elements.

The response is evaluated by the solution of the equations of motion using direct numerical integration methods with a time increment small enough to provide stability. The program uses plane strain quadrilateral and triangular elements. An iteration procedure is used to determine the strain-dependent modulus and damping for each element, based on the average strain developed in that element. The relation of modulus and damping is based on Seed and Idriss (1970c). The solution is obtained using the modulus and damping for each element which is compatible with the average strain. The developers of the program report that comparison with one-dimensional methods shows that the finite element solution values of shear stress are about 10% greater. The response spectra of one- and two-dimensional methods are of similar shape. Major differences on response spectra occur only when the input motion has large amounts of high frequency components or when the finite element model is very coarse. The addition of variable damping makes the response calculation results in better agreement with recorded data.

Lysmer, Udaka, Seed, and Hwang (1974) have developed a two-dimensional finite element program, LUSH (revised version called FLUSH), which solves the transient response problem in soil sites by complex frequency response. It can calculate the response of sloping soil layers and can include the soil-structure interaction effect. The program accounts for the nonlinear effects which occur in soil masses by a combination of the equivalent linear method described in the section on one-dimensional analyses (Seed and Idriss, 1969) and the method of complex response with complex moduli allowing for different damping properties in all elements.

The model consists of plane quadrilateral or triangular elements. Three different material types are provided for: nonlinear clays and sands, elastic solids, and rigid solids. Typical relationships between stiffness, damping, and effective shear strains for sand and clay are provided within the program. These are similar to the curves used in SHAKE. Viscous damping is introduced by using complex moduli in the formation of the stiffness matrix which leads to the same amplitude response as nodal analysis with a uniform fraction of critical damping. The initial soil properties are specified at a low strain level ($\gamma = 10^{-4}$% strain) and the program iterates to find material properties at strain levels compatible with the specified motion.

The mesh size of elements in the model should be small compared with the wave length of shear waves propagating through the model. A suggested maximum height element is

$$h = \left(\frac{1}{5}\right)\lambda = \frac{1}{5}\left(\frac{V_s}{\omega}\right)$$

where h = element height

λ = wavelength of shortest shear wave

V_s = velocity of shear wave at strain level of earthquake

ω = highest frequency of the analysis, Hz

The existing methods for liquefaction evaluation discussed above, including finite element programs, do not compute the pore pressure change with loading directly from the material properties and the actual shear strain produced by the actual time-dependent load. The process of liquefaction transforms an element of soil from a saturated granular solid to a viscous fluid. As a result of this change of material state, the soil in a liquefied zone has reduced shear strength and can undergo large displacements. The actual in-situ porewater pressure determination under dynamic field loading conditions is of major interst in the analysis of the liquefaction potential of a soil. The following paragraphs present some current research in progress.

Ghaboussi and Dikmen (1977) have proposed a method for determination of pore pressures and intergranular stresses by considering the soil as a two-phase medium. In the two-phase representation of saturated soils the granular solid skeleton and the fluid are treated as independent materials with individual material properties. The coupling between the volume changes of fluid and solid skeleton is taken into account through an additional material parameter. The flow of fluid with respect to the solid is assumed to be governed by a generalized form of Darcy's flow law, for which the material's parameter is the coefficient of permeability. The bulk modulus of the fluid, the coupling material parameter, and the coefficient of permeability is assumed to remain constant in the present dynamic analysis. The solid granular skeleton, in contrast, is a highly nonlinear material. A realistic constitutive relation for the solid skeleton of saturated granular soils must be capable of simulating the important nonlinear features such as dilatancy, compaction, shear failure and load reversal effects. Stress compaction, a factor in the pore pressure built up, is of special importance in liquefaction analysis.

The onset of liquefaction in an element of saturated soil is to be determined by a "liquefaction criterion" defined as reduction of the mean intergranular pressure. The initiation of liquefaction in any analysis, as determined by satisfying the liquefaction criterion, marks the boundary between two behavior conditions for an element of soil. In the pre-liquefaction state the soil is treated as a two-phase, fluid-saturated, porous solid. The important characteristic of a potentially liquefying soil at this stage is the increase of the pore pressures accompanied by the decrease of the mean intergranular pressure. After the initiation of liquefaction, the behavior of an element of soil changes. A second material model is used to represent the post-failure behavior.

The analysis in the pre-liquefaction stage will lead to determination of the potentiality of liquefaction. If the extent of the development of the liquefaction, and the associated stress and pore pressure distribution are of interest, then the analysis should be carried into the post-liquefaction stage. Doing so requires accounting for the change in behavior from the fluid-saturated granular material to a viscous material in an element of soil which has satisfied the liquefaction criterion.

The key to success for liquefaction analysis of the type proposed by Ghaboussi and Dikmen (1977) lies in the appropriate mathematical modeling of the important features of the constitutive response of the granular solid skeleton of the soil. Loose sands are most susceptible to liquefaction under seismic loading conditions since they tend to compact under shear deformation. This reduction of the volume in loose sands causes the pore pressure buildup and consequent reduction of the mean intergranular pressure, leading to liquefaction. Appropriate representation of the properties of granular soils requires special attention in a liquefaction analysis. Nonlinear material models are required to model the plastic behavior of the soil. This pre-liquefaction condition is under investigation using a soil model developed by Ishihara, et al (1975).

Ishihara et al (1975) have presented a model for liquefaction based upon studies of the cyclic deformation of sands. This model permits assessing pore pressures, shear strains, and the occurrence of liquefaction in undrained horizontal soil layers. This model, originally based on triaxial data, has been revised to fit torsion test results and incorporated into a computer code by Ishihara et al (1976). The applied stress history for the in-situ soil profile may be calculated by some of the foregoing coputer programs, such as SHAKE (Schnabel, Lysmer and Seed, 1972). This stress history is then applied to the soil model to predict pore pressures and shear distortions.

Test data on undrained sands illustrate that for shearing loads below a particular shear stress/effective stress ratio q/p', reloading always retraces the unloading path. Plastic yielding, associated with the original application of shear stress, results in a buildup of residual pore pressure (and thus reduction in effective stress). Thus, it is possible to define for any particular soil density, a so-called virgin state, defined by a relationship such as that of Figure 30, in terms of shear stress, q versus effective mean principal stress p'. A series of such planes form a vector surface in p' - q - e space (where e is void ratio or a measure of density). This "state" surface specifies the route or path in p' - q - e space along which stresses must be changed in order for deformations to be plastic. Plastic yielding occurs only when stresses are changed along paths lying on the state surface, and all other paths away from it are associated merely with elastic deformations. For undrained shearing of saturated sand, the stress paths can be defined for a specific state by a single slice or plane perpendicular to the e axis, such as Figure 31 (for a loose sand). This figure shows yield lines, or "equi-γ lines," which are curves in p' - q space at which yielding occurs whenever stress paths cross them. For stress paths within previously approached yield loci the deformations are assumed to be elastic, and no change in effective stress occurs.

With increase in the q/p' ratio, shear strains are generated with magnitudes equal to those values shown on the equi-γ lines in Figure 31.

Experimental results on saturated sands show that the shear in one direction below some limiting stress ratio does not influence the virgin state response for shearing in the opposite direction. However, beyond a certain q/p' ratio, the pore pressure commences to increase drastically during any unloading (and increases even more dramatically during loading in the opposite direction). This defines a threshold stress value which, if not exceeded, permits elastic response during unloading and provides plastic work-hardening response during any load increase. The angle defined by the threshold stress value is called the angle-of-phase transformation and is slightly flatter than the failure envelope as shown in Figure 31. It is assumed that initial liquefaction occurs where the stress ratio crosses this angle-of-phase transformation.

4.7 REFERENCES

Arango, I. and Dietrich, R. J. (1972) "Soil and earthquake uncertainties on site response studies," in Proceedings of the International Conference on Microzonation for Safer Construction Research and Application, 30 Oct - 3 Nov 1972. Seattle, Wash., National Science Foundation.

Castro, G. (1975) "Liquefaction and cyclic mobility of saturated sands," Journal of the Geotechnical Division, ASCE, vol 101, no. GT6, Jun 1975, p. 551-569.

Christian, J. T. and Swiger, W. F. (1975) "Statistics of liquefaction and SPT results," Journal of the Geotechnical Division, ASCE, vol 101, no. GT11, Nov 1975.

DeAlba, P., Chan, C. K. and Seed, H. B. (1975) Determination of soil liquefaction characteristics by large-scale laboratory tests, University of California, Earthquake Engineering Research Center, EERC Report No. 75-14. Berkeley, Calif., May 1975.

Dezfulian, H. and Seed, H. B. (1969) Seismic response on soil deposits underlain by sloping rock boundaries, University of California, Earthquake Engineering Research Center, EERC Report No. 69-9. Berkeley, Calif., Jul 1969.

Donovan, N. C. (1974) CUMLIQ: Evaluation of potential for liquefaction of a soil deposit using random vibration procedures, University of California, Earthquake Engineering Research Center, National Information Service on Earthquake Engineering. Berkeley, Calif., Jul 1974.

Ghaboussi, I. and Dikmen, S. (1977) LASS II, computer program for analysis of seismic response and liquefaction of horizontally layered sands, University of Illinois, UILU-ENG 77-2010. Urbana, Ill., Jun 1977.

Gibbs, H. J. and Holtz, W. G. (1957) "Research on determining the density of sand by spoon penetration test," in Proceedings of Fourth International Conference on Soil Mechanics and Foundations Engineering, vol 1, London, England, 1957.

Hardin, B. and Drnevich, V. (1970) Shear modulus and damping in soils, University of Kentucky, College of Engineering, Soil Mechanics Series Technical Report UKY 26-70-CE2. Lexington, Ky., Jul 1970.

Idriss, I. M., et al. (1973) QUAD 4: A computer program for evaluating the seismic response of soil structures by variable damping finite element procedures, University of California, Earthquake Engineering Research Center, EERC Report No. 73-16. Berkeley, Calif., Jul 1973.

Idriss, I. M. and Seed, H. B. (1968) "Seismic response of horizontal soil layers," Journal of the Soil Mechanics and Foundations Division, ASCE, vol 96, no. SM2, Mar 1970, pp 631-638.

Ishihara, K., et al. (1975) "Undrained deformation and liquefaction of sand under cyclic stresses," Soils and Foundations (Japan), vol 15, no. 1, Mar 1975.

Ishihara, K., et al. (1976) "Prediction of liquefaction in sand deposits during earthquakes," Soils and Foundations (Japan), vol 16, no. 1, Mar 1976.

Kanai, K. (1961) "An empirical formula for the spectrum of strong earthquake motions," Bulletin, Tokyo University Earthquake Research Institute, vol 39, 1961.

Kiefer, F. W., Seed, H. B. and Idriss, I. M. (1970) "Analysis of earthquake ground motions at Japanese sites," Bulletin of the Seismological Society of America, vol 60, no. 6, Dec 1970, pp 2057-2070.

Lee, K. L. and Chan, K. (1972) "Number of equivalent significant cycles on strong motion earthquakes," in Proceedings of the International Conference on Microzonation for Safer Construction Research and Application, 30 Oct - 3 Nov 1972. Seattle, Wash., National Science Foundation, 1972.

Lysmer, J., et al. (1974) LUSH: A computer program for complex response analysis of soil structure systems, University of California, Earthquake Engineering Research Center, EERC Report No. 74-4. Berkeley, Calif., Apr 1974.

Lysmer, J., Seed, H. B. and Schnabel, P. B. (1970) Influence of base rock characteristics on ground response, University of California, Earthquake Engineering Research Center, EERC Report No. 70-7. Berkeley, Calif., Nov 1970.

Mulilis, J. P., Chan, C. K. and Seed, H. B. (1975) The effects of method of sample preparation on the cyclic stress-strain behavior of sands, University of California, College of Engineering, Earthquake Engineering Research Center, EERC Report No. 75-18. Berkeley, Calif., Jul 1975.

Pyke, R., Chan, C. K. and Seed, H. B. (1974) Settlement and liquefaction of sands under multi-directional shaking, University of California, College of Engineering, Earthquake Engineering Research Center, EERC Report No. 74-2. Berkeley, Calif., Feb 1974.

Schmertmann, J. H. (1977) "Use of the SPT to measure dynamic soil properties - yes but," Dynamic Geotechnical Testing, ASTM STP 654. Philadelphia, Pa., 1977, pp 341-355.

Schnabel, P. B., Lysmer, J. and Seed, H. B. (1972) SHAKE: A computer program for earthquake response analysis of horizontally layered sites, University of California, Earthquake Engineering Research Center, Report No. 72-12. Berkeley, Calif., Dec 1972.

Schnabel, P. B. and Seed, H. B. (1972) Accelerations in rock for earthquakes in the western United States, University of California, College of Engineering, Earthquake Engineering Research Center, EERC Report No. 72-2. Berkeley, Calif., Feb 1972.

Seed, H. B. (1976) "Evaluation of soil liquefaction effects on level ground during earthquakes," ASCE Preprint 2752 (Liquefaction Problems in Geotechnical Engineering), American Society ofr Civil Engineers Annual Convention and Exposition, Philadelphia, Pa., 27 Sep - 1 Oct 1976.

Seed, H. B., et al. (1975) Representation of irregular stress time histories by equivalent uniform stress series in liquefaction analysis, University of California, College of Engineering, Earthquake Engineering Research Center, EERC Report No. 75-29. Berkeley, Calif., Oct 1975.

Seed, H. B. and Idriss, I. M. (1969) "Influence of soil conditions on ground motions during earthquakes," Journal of the Soil Mechanics and Foundations Division, ASCe, vol 95, no. SM1, Jan 1969, pp 99-137.

Seed, H. B. and Idriss, I. M. (1970a) A simplified procedure for evaluating soil liquefaction potential, University of California, Earthquake Engineering Research Center, EERC Report No. 70-9. Berkeley, Calif., Nov 1970.

Seed, H. B. and Idriss, I. M. (1970b) "Analysis of ground motions at Union Bay, Seattle, during earthquakes and distant nuclear blasts," Bulletin of the Seismological Society of America, vol 60, no. 1, Feb 1970, pp 125-136.

Seed, H. B. and Idriss, I. M. (1970c) Soil moduli and damping factors for dynamic response analysis, University of California, Earthquake Engineering Research Center, EERC Report No. 70-10. Berkeley, Calif., Dec 1970.

Seed, H. B. and Peacock, W. H. (1970) Applicability of laboratory test procedures for measuring soil liquefaction characteristics under cyclic loading, University of California, Earthquake Engineering Research Center, EERC Report No. 70-8. Berkeley, Calif., Nov 1970.

Streeter, V. L., Wylie, E. G. and Richart, F. E. (1974) "Soil motion computations by characteristics method," Journal of the Geotechnical Division, ASCE, vol 100, no. GT3, Mar 1974, pp 247-263.

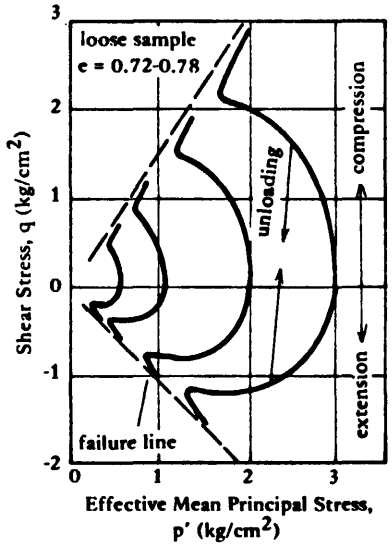

Figure 30. Typical undrained stress paths for loose samples (Fuji River Sand) (from K. Ishihara, 1975).

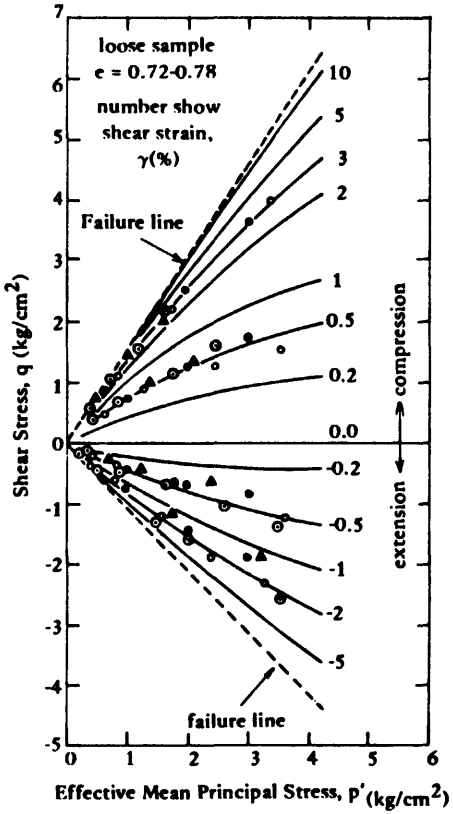

Figure 31. Equi-γ lines for loose samples (Fuji River sand) (from K. Ishihara, 1975).

5.0 CONSEQUENCES OF LIQUEFACTION

The magnitude of the foundation problems associated with liquefaction are directly related to the amount of ground movement or ground failure. Ground failures may be of three basic types: flow landslides, landslides with limited displacement, and bearing capacity failures. Liquefaction of a layer at depth which does not undergo large displacements may actually act as an isolator impeding the transmission of vibration energy from underlying layers to structures at the surface. Seed and Idriss (1967) show an earthquake record at Niigata, Japan, in which the surface motion significantly changes from a predominantly short-period motion to a long-period motion after about 8 seconds of motion. Presumably this indicates the time of the onset of liquefaction (Figure 32).

5.1 LIQUEFACTION FLOW LANDSLIDES

When the in-situ relative density of the soil is low enough (D_r < 45%), unlimited flow may occur. If the soil is unrestrained, sizable masses of earth materials may travel long distances. The principal restraint is only a function of the viscous restraining forces. The flow velocity can be estimated by the following equation for a case where liquefaction propagates to the surface.

$$U = \frac{\gamma_t}{2N}(b^2 - S^2)\sin\theta$$

where U = horizontal flow velocity (ft/s)

N = viscosity (lb-s/ft^2)

γ_t = total unit weight of soil

b = depth to bottom of liquefiable layer

S = depth to top of liquefiable layer

θ = angle of slope with respect to the horizontal

For example, if the depth to the bottom of a liquefiable layer was 20 feet and it propagated to the surface when the ground slope was 2 degrees, the viscosity was 55,000 lb-s/ft^2; and the total unit weight of the soil above the liquefiable layer was 120 lb/ft^2; then,

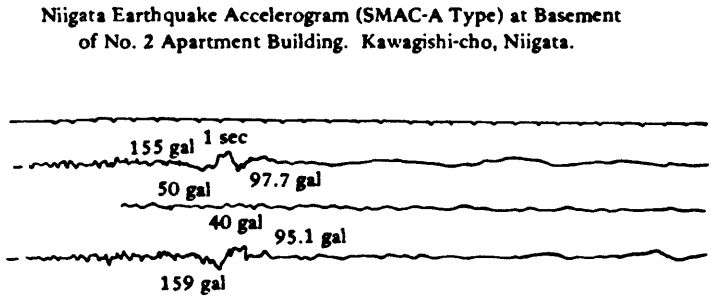

Figure 32. Record of ground accelerations during Niigata earthquake (from "Landslides During Earthquakes due to Soil Liquefaction," by H. B. Seed in Journal of Soil Mechanics and Foundations Division, ASCE, vol. 95, no. SM5, May 1968, Figure 6).

$$U = \frac{120}{2(55{,}000)} (20^2) \sin (2^\circ)$$

$$= 0.0152 \text{ ft/s}$$

$$= 0.18274 \text{ in./s}$$

If the liquefiable condition were to last for 7 minutes, the displacement would be over 6 feet.

The above methodology and example, although highly idealized, can be used to give qualitative evaluations of the amount of flow displacement. One of the problems here is that the viscosity data on real soils is limited. The example shows that very slight slopes are capable of causing large deformations; conversely, horizontal deformation would not be expected on truly flat ground. Flow landslides have occurred under seismic conditions and have been reported in the literature (Crandall, 1908; Seed, 1968). Flow continues as long as pore pressures remain high enough to maintain liquefaction. This condition is a function of the drainage conditions of the site and porosity of the soil and will be discussed later. The duration of liquefaction will also be discussed later.

5.2 LIQUEFACTION WITH LIMITED DISPLACEMENTS

For relative densities greater than about 45%, the data tends to indicate that limited flow rather than unlimited flow might be expected. DeAlba, Chan, and Seed (1975) have conducted shake-table tests, Figures 33 and 34, which suggest limiting horizontal shear strain as a function of relative density. The value of 45% relative density is shown as the approximate division between limited and unlimited flow. Figure 34 could presumably be used to estimate shear strains within the soil layer undergoing liquefaction for use in predicting the horizontal transient displacement for level ground not experiencing flow (note that in Figure 34 shear strain is expressed independent of ground motion level). This fact and the paucity of data at this time make these results preliminary and in need for further verification.

On sloping ground, increments of finite downslope movements could cause dilatancy-induced solidification. Thus, flow could be interrupted by solidification stages which would limit the displacement. There have been numerous cases of limited displacements, also called lateral spreading, reported (Richter, 1958; McCulloch and Bonilla, 1970; Oldham, 1899; Youd, 1973a and b). Observed cases in these references noted movements of several feet on ground sloping from 0.5 to 2%. Youd (1975) deduces several points of interest based on laboratory soil behavior. Episodes of limited flow would be expected to be most prevalent where shear stress reversals occur; thus, limited flow would be expected to occur as long as strong ground shaking exists. The shear stress reversals associated with limited flow are more easily developed beneath mild slopes where static stresses are small, rather than steep slopes. At the conclusion of a series of limited flow cycles, the soil in the failure zone may be

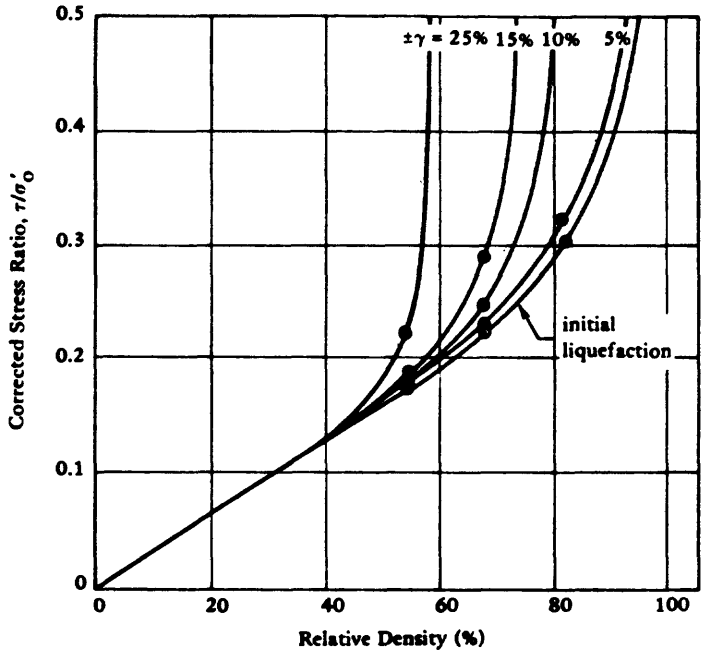

(a) Five stress cycles.

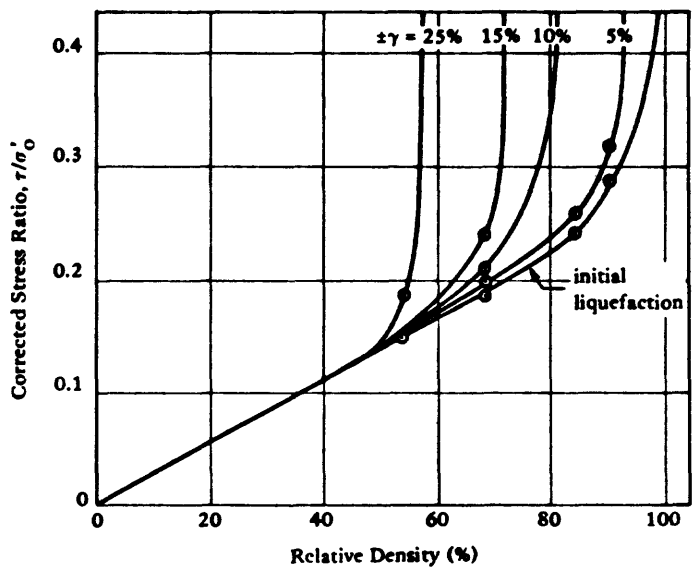

(b) Ten stress cycles.

Figure 33. Limiting shear strains (from H. B. Seed, P. P. Martin, and J. Lysmer, 1975).

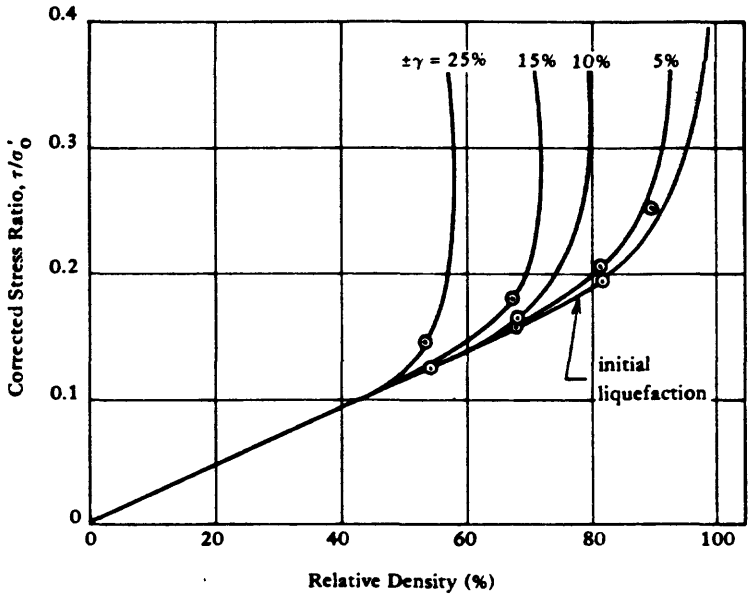

(c) Thirty stress cycles.

Figure 33. Continued

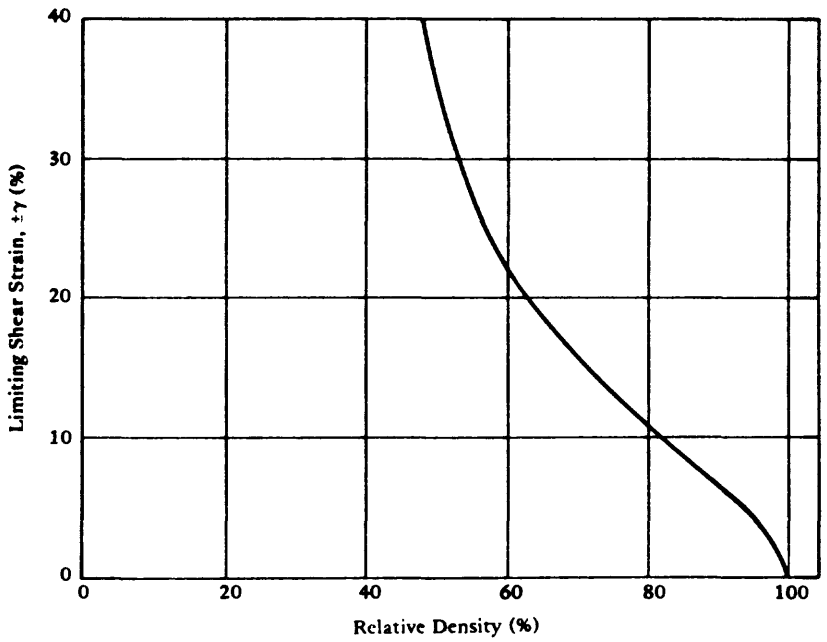

Figure 34. Limiting shear strains independent of loading.

denser or looser or at the same condition as it was before the disturbance, depending on whether pore water migrated into or out of the liquefied soil during shear.

5.3 BEARING CAPACITY FAILURES

When liquefaction occurs in soils beneath structures, flow deformations may develop, allowing vertical motion to occur. Loss of foundation support and buoyant rise of buried tanks are possible types of failures. Several major failures of these types occurred during the 1964 Niigata earthquake, including the spectacular settling and tipping of several high-rise apartment buildings.

DeAlba, Chan, and Seed (1975) conducted model footing tests on a shake table; Figure 35 gives vertical velocity of settlement for a model footing in liquefied sand.

Considering flow, for an equilibrium condition the drag force of the footing must equal the footing weight; therefore

$$C_D \, A \, \rho \frac{V^2}{2} = p \, A$$

where C_D = footing drag coefficient
A = footing plan area
ρ = soil density
V = footing velocity
p = footing contact pressure

Solving for V:

$$V = \sqrt{\frac{2\,p}{C_D\,\rho}}$$

Thus, the footing settlement velocity is proportional to the square root of the footing contact pressure. The data in Figure 35 was obtained for footing pressures of 25 psi. Figure 35 may be used to crudely estimate vertical settlement knowing the duration of liquefaction. Caution must be used since the results are based on a few very small scale model tests of limited scope.

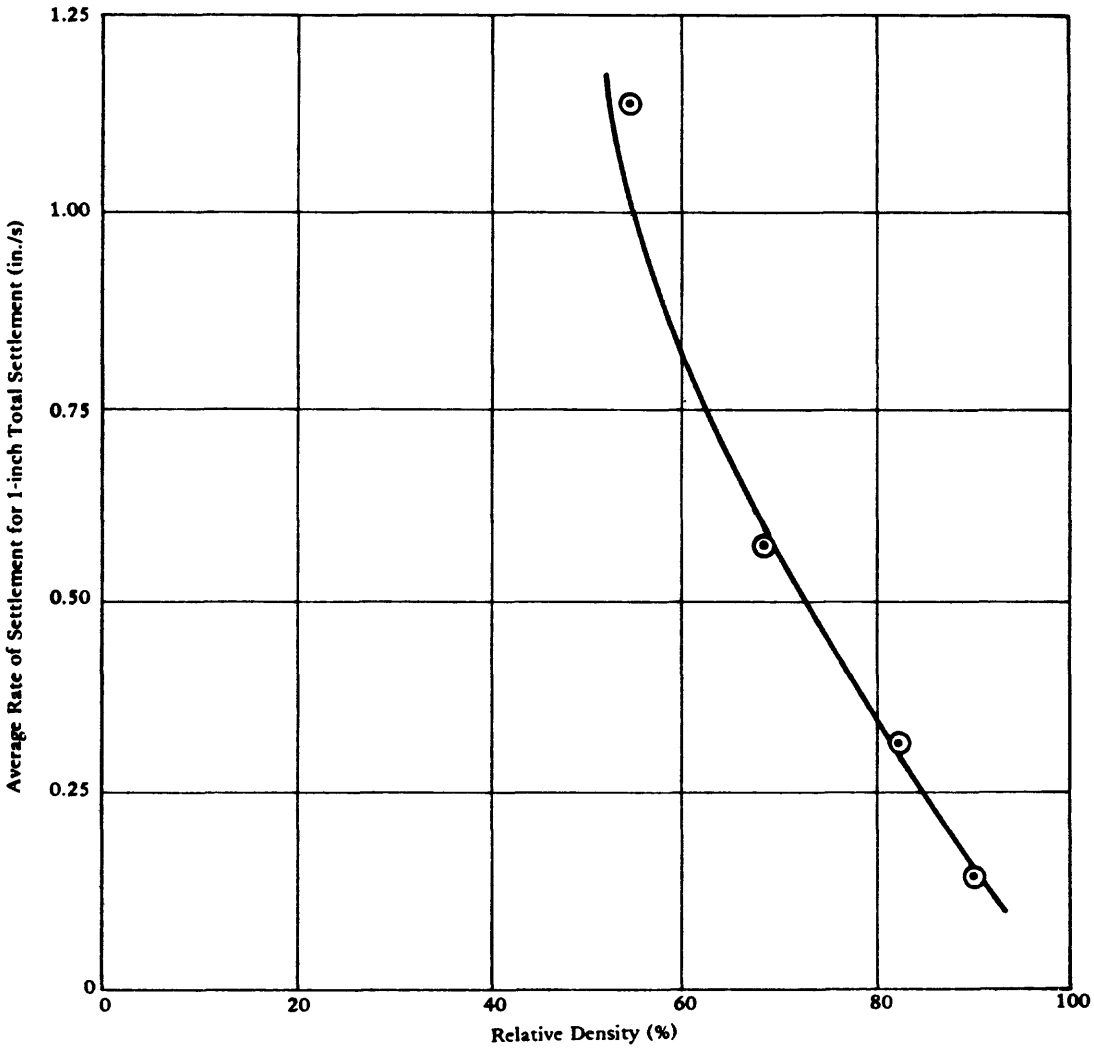

Figure 35. Average rate of footing settlement (from H. B. Seed, P. P. Martin, and J. Lysmer, 1975).

5.4 DURATION OF LIQUEFACTION, PROPAGATION TO SURFACE AND BEARING CAPACITY

The duration and propagation of liquefaction in a subsurface layer is controlled by the drainage path for the build-up of pore pressures, the coefficients of permeability, and the coefficient of consolidation, which dictates the volume change characteristics of the soil layers.

Yoshimi and Kuwabara (1973) have investigated pore pressure dissipation using a finite element analysis, assuming one-dimensional flow (using Darcy's law) and layer II undergoing liquefaction. They assumed that the induced seismic shear stress terminates at the onset of liquefaction, that the soil in layer I undergoes rebound and recompression with a constant coefficient of volume change, and that the soil in layer II undergoes virgin compression with a constant coefficient of volume change.

An example of the results of their analysis is shown in Figure 36 in which the pore pressure buildup in the top layer is given as a function of time for the case where: (1) the coefficient of permeability in both layers are equal and (2) the coefficient of volume change in the bottom layer is 10 times greater than in the top layer. As shown in Figure 36 the pore pressure builds up in the top layer to a value almost equal to the effective vertical stress at a time determined as a function of the thickness of the layer and the coefficient of consolidation (nondimensionalized time factor). The effect of different thicknesses of the soil layers on the peak pore pressure buildup in the top layer is shown in Figure 37 for two compressibility ratios. The effect of different thicknesses of the soil layers on the peak pore pressure buildup in the top layer is shown in Figure 37 for two compressibility ratios. The effect of the relative thickness of layer I on the maximum pore pressure depends on the compressibility ratio (coefficients of volume change). Yoshimi and Kuwabara (1973) have noted that the presence of a permeable layer beneath layer II has a negligible effect on the pore pressures in layer I.

It is possible that an initial excess pore pressure in layer I has been generated by the same seismic action causing liquefaction in layer II. For this case, Figure 38 shows the pore pressure with time for various values of initial pore pressure. It can be seen that the initial pore pressure in layer I has little effect on the peak pore pressure in that layer.

Figure 39 shows the results of variation of permeability and compressibility on pore pressure in the top layer. Also shown is the ratio of shear strength at any time S to initial shear strength S_o defined as

$$\frac{S}{S_o} = 1 - \frac{u}{\sigma'_{vo}}$$

Since the maximum pore pressure varies nearly linearly with depth in layer I, the minimum strength ratio S_{min}/S_o corresponding to the maximum pore pressure may be considered a constant throughout layer I

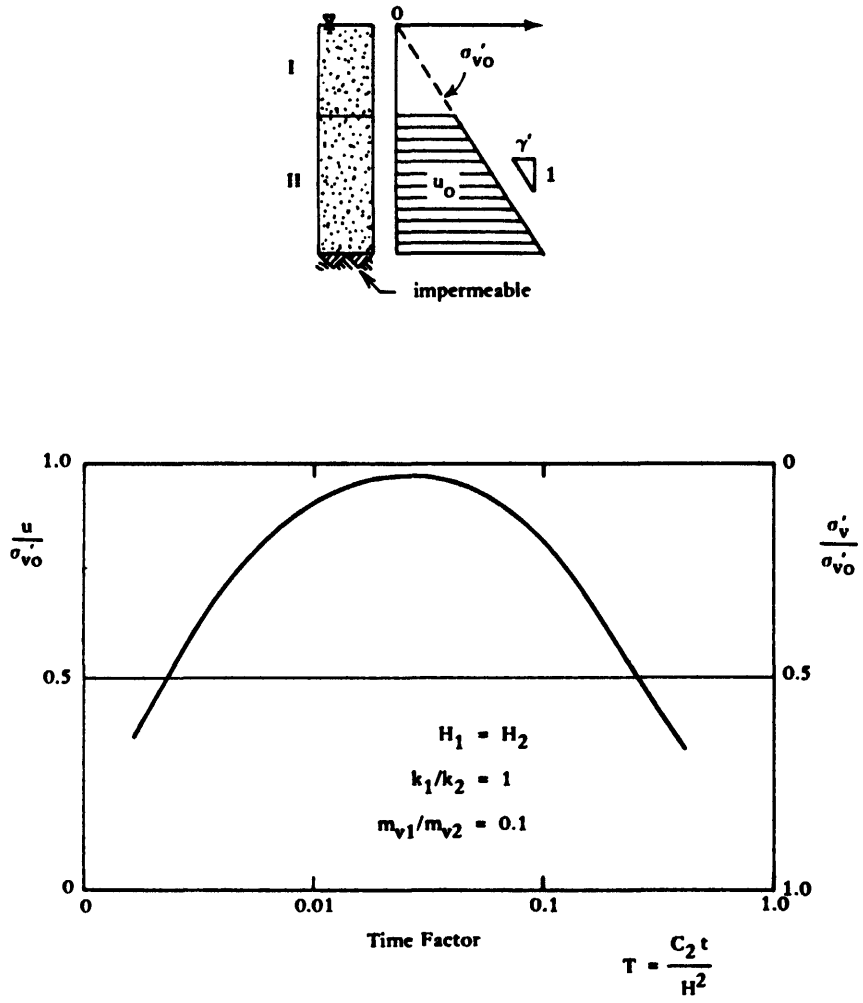

Figure 36. Pore pressure at middepth layer I (from Y. Yoshimi and F. Kuwabara, 1973).

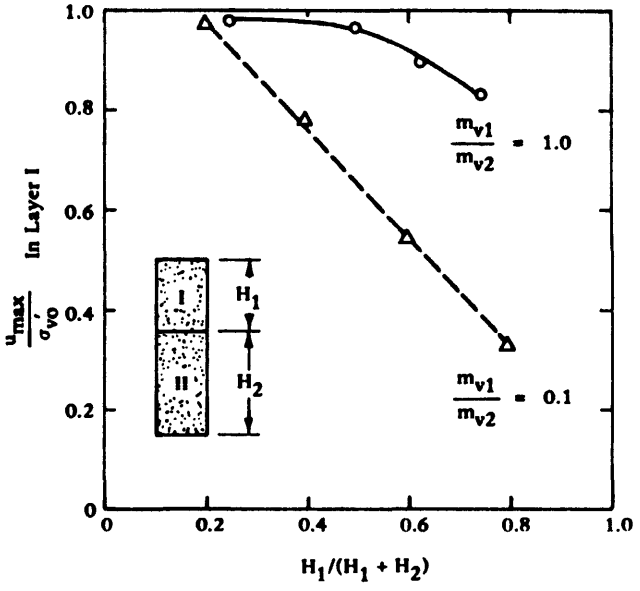

Figure 37. Effect of relative thickness of layer I on maximum pore pressure in layer I (from Y. Yoshimi and F. Kuwabara, 1973).

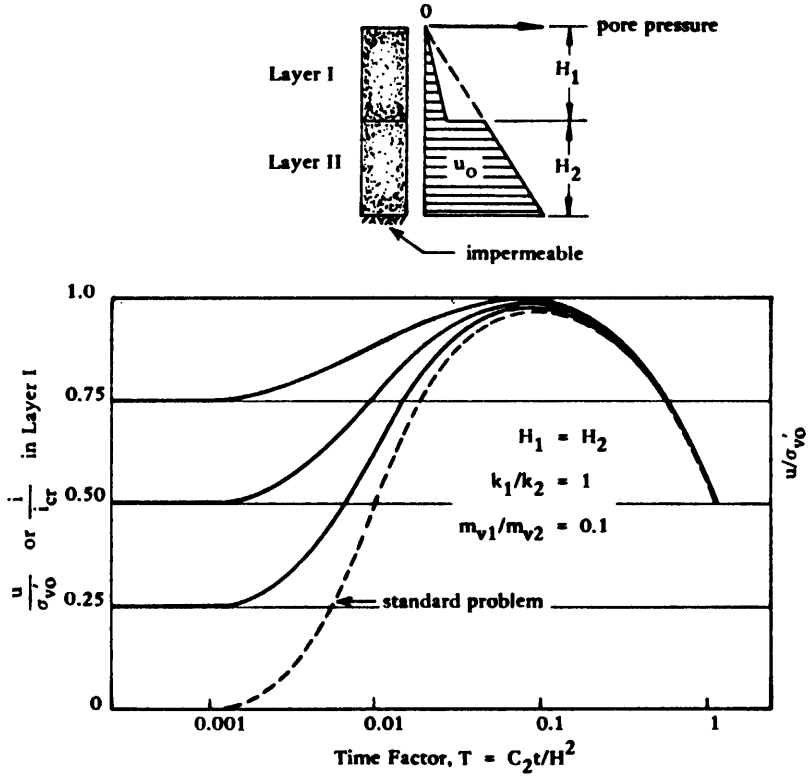

Figure 38. Effect of initial excess pore pressure in layer I (from Y. Yoshimi and F. Kuwabara, 1973).

	a	b	c	d
k_1/k_2	1	1	10	0.1
m_{v1}/m_{v2}	0.1	1	1	0.1
c_1/c_2	10	1	10	1

$H_1 = H_2$
$k_2 = 0.05$ cm/s
$m_{v2} = 0.02$ cm^2/kg

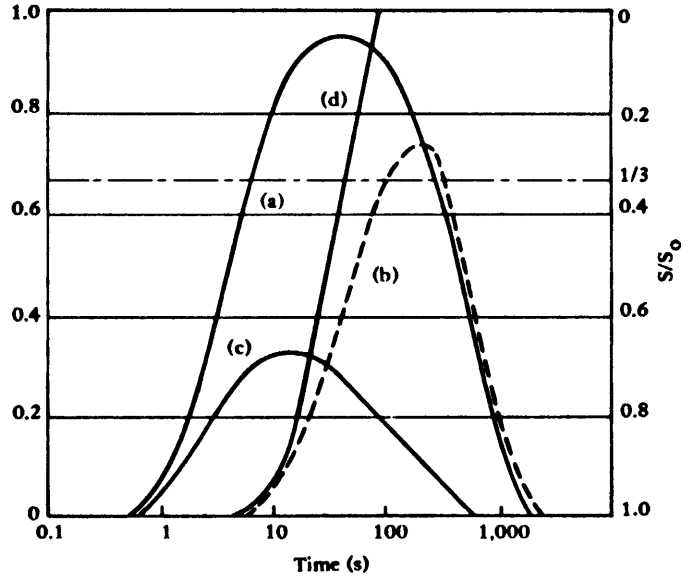

Figure 39. Time histories of excess pore pressure at middepth of layer I (from Y. Yoshimi and F. Kuwabara, 1973).

$$\frac{S_{min}}{S_o} = 1 - \frac{u_{max}}{\sigma'_{vo}} = 1 - \frac{i_{max}}{i'_{cr}}$$

where i_{max} = maximum hydraulic gradient
i_{cr} = critical hydraulic gradient

Figure 40 shows the minimum strength in layer I for use in estimating the liquefaction of that layer. The data are replotted in Figure 41 to show areas where complete liquefaction in layer I occurs. It should be noted that the critical hydraulic gradient corresponding to $u_{max}/\sigma'_{vo} = 1$ in a field situation probably cannot be maintained without causing fissures and local eruption of sand and water. The presence of a foundation will affect the state of stress and seepage conditions; however, the strength ratio S_{min}/S_o may still give a crude indication of the bearing capacity. The time to the minimum strength as noted in Figure 39 depends upon the coefficient of permeability, the compressibility, and the thickness of the soil. These may be in seconds or in minutes, depending on site conditions. Observations during the Niigata earthquake of 1964 noted most of the surface movement occurred minutes after the earthquake strong motion ended. Note that densification causes a reduction in k_1 and m_{v1} of the top layer and a reduction of S/S_o, which is not favorable; however, densification will cause an increase in the initial shear strength S_o, which is beneficial. The net effect of densification of layer I may or may not be advantageous, depending on the initial soil properties and the degree of densification. Increasing the permeability of the top layer markedly increases the stability of the soil. Thus, vibroflotation, sand drains, or using a coarse backfill should be more effective than densification methods in which density alone is increased.

Seed, Martin, and Lysmer (1975) have more recently investigated the distribution of hydrostatic pore pressure in the soil by use of the equation

$$\frac{\partial u}{\partial t} = C_v\left(\frac{\partial^2 u}{\partial z^2}\right) + \frac{\partial u_g}{\partial t}$$

where C_v = coefficient of consolidation of the soil
z = depth within soil
$\partial u_g/\partial t$ = rate of pore pressure generation caused by earthquake

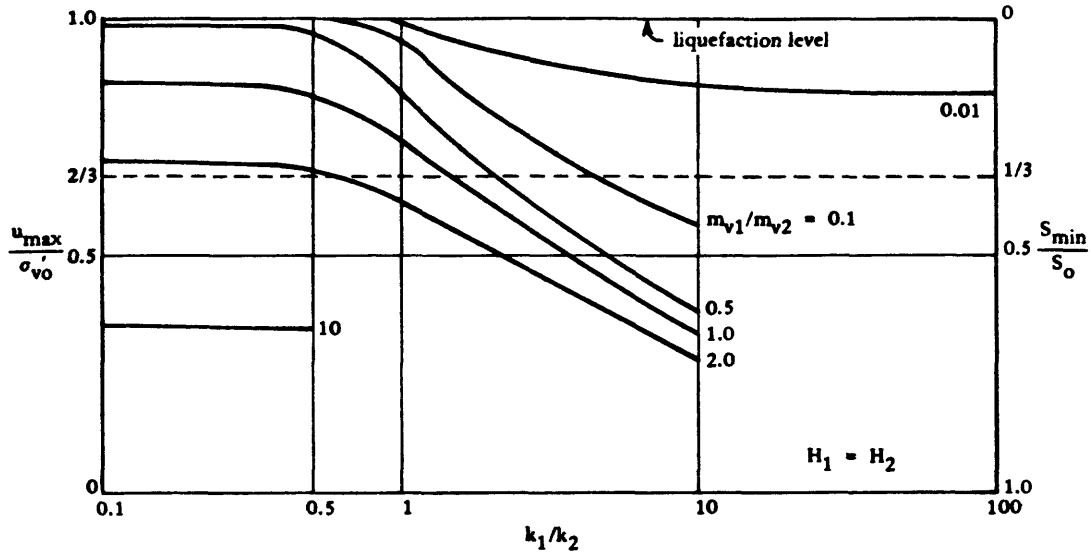

Figure 40. Maximum pore water pressure or minimum strength in layer I (from Y. Yoshimi and F. Kuwabara, 1973).

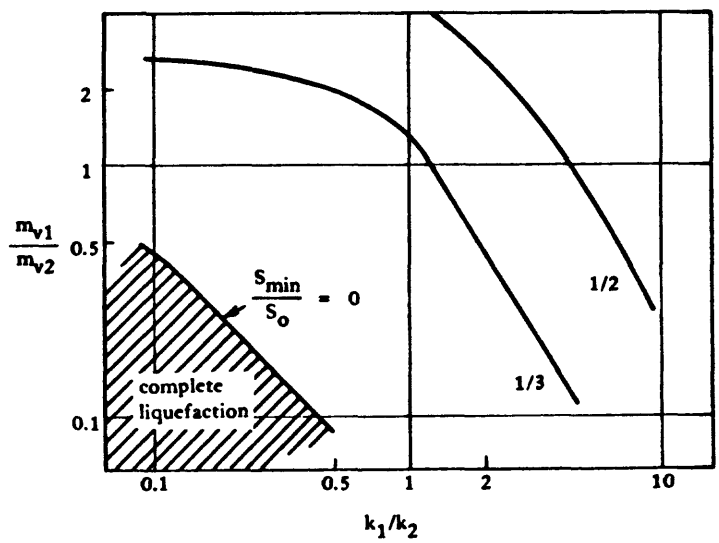

Figure 41. Minimum strength ratio in layer I (from Y. Yoshimi and F. Kuwabara, 1973).

This is the diffusion equation used in Terzaghi's classical consolidation theory, with a pressure-generating term added. The solution of this equation is accomplished by the finite-difference technique using incremental time steps. The pore pressure generation is estimated by Figure 42 as a function of the number of cycles to cause liquefaction.

The coefficient of consolidation C_v, which is defined in terms of the coefficient of volume compressibility m_v and the coefficient of permeability k, may be estimated by means of Figures 43 and 44.

$$C_v = \frac{k}{m_v \gamma_w}$$

The rise in the water table is given by:

$$\Delta H = \frac{-k \left(\frac{\partial u}{\partial z}\right) \Delta t}{n_e}$$

where n_e = the effective porosity

This procedure has been automated in the form of the computer program APOLLO prepared by Martin (1975) and may be used in conjunction with the analysis using the computer program SHAKE described above. SHAKE is used to produce the equivalent uniform cyclic stress (τ_{eq}) and the equivalent number of uniform stress cycles (n_{eq}) for various depths of soil. From strength data the number of cycles to cause liquefaction at each depth is determined. Using this information program APOLLO solves the pore pressure generation-dissipation equation.

The pore pressure generation function is based on undrained test data. This application is deemed sufficiently accurate when small time steps are used to properly account for drainage. The elastic response analysis used to determine the number of cycles to liquefaction can be made to consider the isolation effects of subsurface liquefaction on near surface shaking and the reduction in pore pressure generation when iteration techniques are used.

A typical example from Seed et al (1975) from the Niigata earthquake of 1964 is shown in Figure 45 and Figure 46. The computed variations of pore water pressure with time are given. Figure 46 shows the buildup of pore pressures. It may be seen that the sand layer at a depth of 15 feet liquefies after about 21 seconds of shaking; liquefaction extends to depths of 20, 30, and 40 feet after about 23, 32, and 40 seconds of shaking. Although the layers above 15 feet depth continue to increase in pore pressure as the shaking progresses, the rate of increase is very low after the 15-foot level liquefies. It has been noted in Seed, Martin, and Lysmer (1975) that when the pore pressure ratio in the top

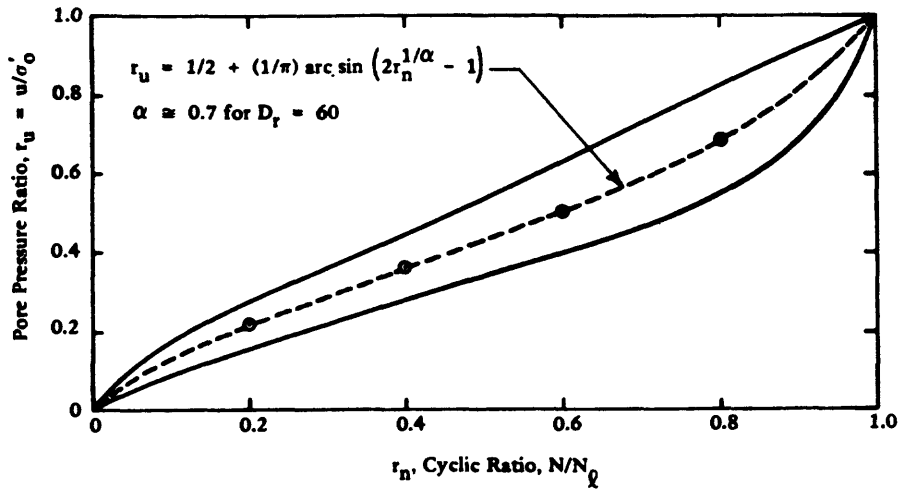

Figure 42. Rate of pore water pressure buildup in cyclic simple shear tests (after P. DeAlba, C. Chan, and H. B. Seed, 1975).

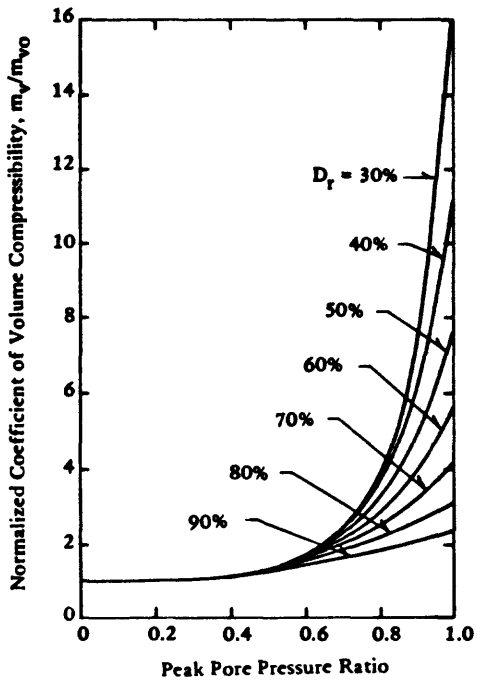

Figure 43. Theoretical relationships between compressibility of sands and pore pressure buildup (from H. B. Seed, P. P. Martin, and J. Lysmer, 1975).

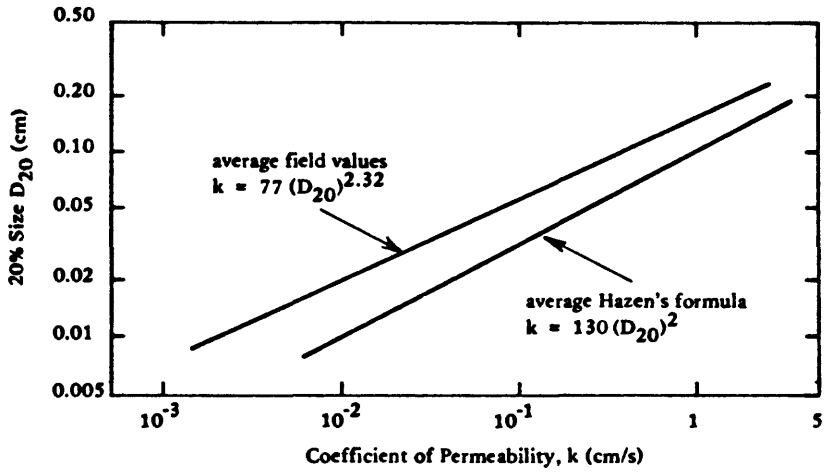

Figure 44. Relationships between grain size and coefficient of permeability for sands (from H. B. Seed, P. P. Martin, and J. Lysmer, 1975).

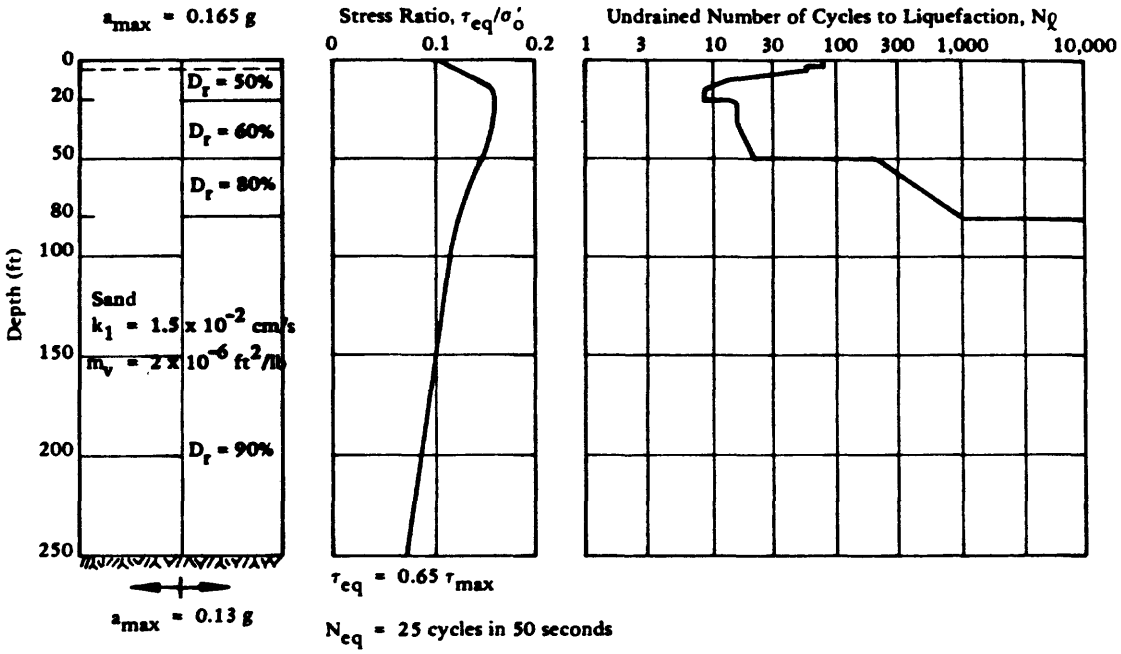

Figure 45. Soil profile and stress conditions used for analysis (from H. B. Seed, P. P. Martin, and J. Lysmer, 1975).

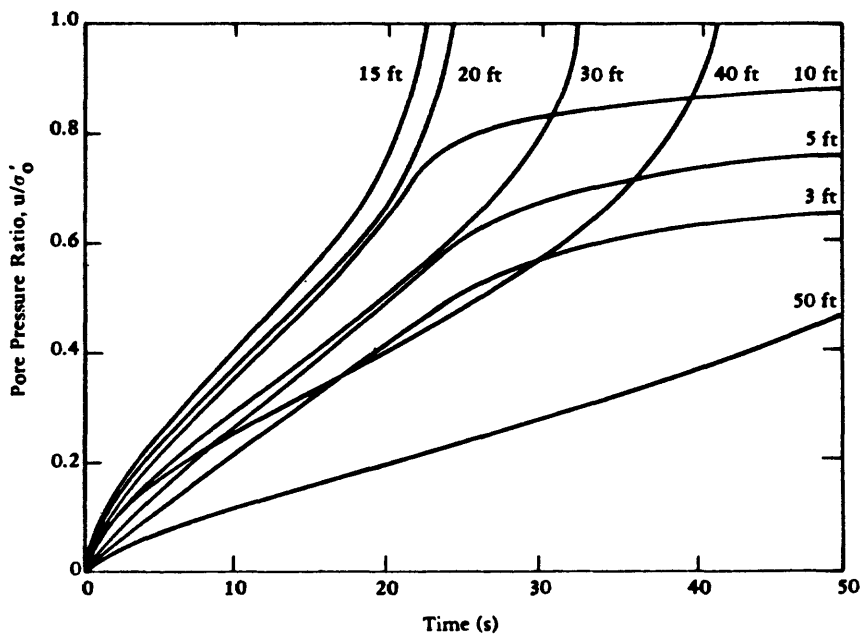

(a) During earthquake shaking.

Figure 46. Computed development and variation of pore water pressures for soil profile shown in Figure 7-8 (from H. B. Seed, P. P. Martin, and J. Lysmer, 1975).

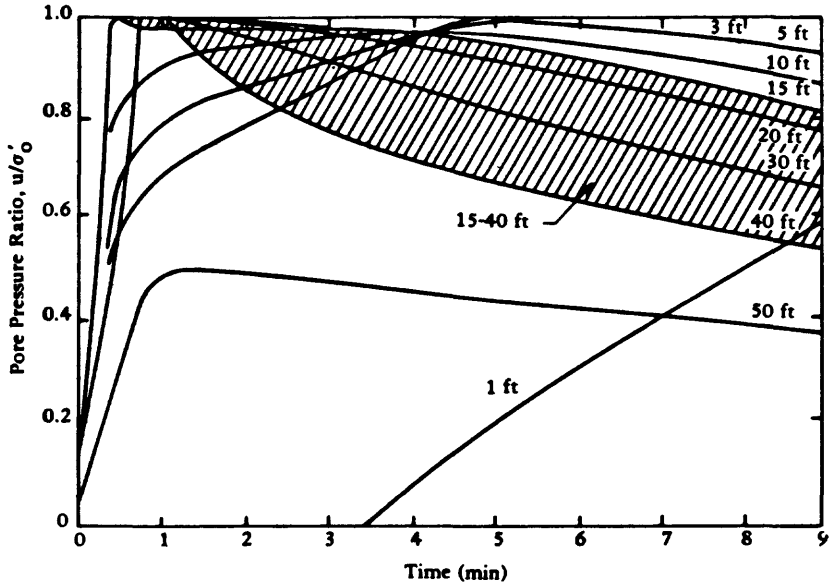

(b) In 8-minute period following earthquake.

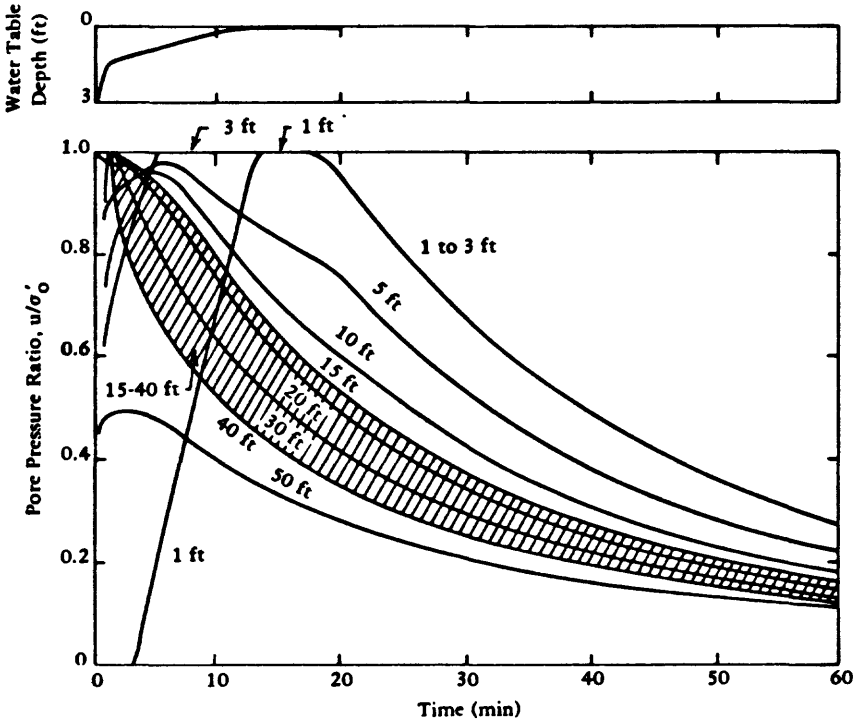

(c) In 60-minute period following earthquake.

Figure 46. Continued

foot of soil reaches 60%, the ground will become soft, and a man will sink. This occurs after about 8.5 minutes in the Niigata analysis. The pore pressure ratio at the ground surface begins to decrease after about 20 minutes but would not support a man until about 40 to 50 minutes after the earthquake. The results of the computer analysis are in general agreement with observed reports.

If the water table were located at a depth of 15 feet, no significant pore pressure increases would occur in the upper 10 feet of soil even though the soil is liquefied between 15 and 40 feet. Thus, in this situation the bearing capacity of small shallow footings near the surface might well be essentially unaffected by the dissipation of pore water pressures in the liquefied zone.

Program APOLLO has been expanded into a two-dimensional computer program called GADFLEA (Booker et al, 1976). The approach is very similar to the one-dimensional analysis requiring as input information the number of cycles cuasing liquefaction by soil element. The number of cycles causing liquefaction is a function of the applied shear stress loading and soil confinement. These may be determined from a conventional two-dimensional elastic or inelastic finite element analysis. Using the input data, Program GADFLEA computes the two-dimensional pore pressure generation and dissipation from the earthquake.

Programs APOLLO and GADFLEA provide a significantly improved picture as to what is occurring in the soil and as such represents very useful tools to an engineer. The programs require values of the coefficient of permeability, coefficient of volume compressibility, and porosity. These values may be obtained for tests but are often assumed based on soil characteristics. The occurrence of liquefaction on near surface regions above the water table was found to be very sensitive to the location of the line of full saturation. Unfortunately, in field conditions a clean demarcation is not always present. As with other one-dimensional representations, the program APOLLO assumes infinite horizontal layers. This may present a problem in areas where discontinuities or slopes are present, since horizontal drainage is usually an order of magnitude greater than vertical drainage. Program GADFLEA should be used in cases requiring a two-dimensional analysis.

5.6 OBSERVATIONS OF LIQUEFACTION

Oldham (1899) reports that during the Assam, India, earthquake of 12 June 1897, a large number of jets of water rose to heights of 2 to 4 feet from fissures on the plains, carrying sand with them. The ejection of water and sand began during the earthquake and continued for 20 to 30 minutes after the shaking of ground had ceased. In many places drainage channels 15 to 20 feet deep had their bottoms forced up until they became level with the tops of their sides. Houses settled until only the roofs remained above ground.

Ambraseys and Sarma (1969) report that after the Kanto earthquake of 1923 in Japan, numerous fissures and mud volcanoes spurted intermittently. In a paddy field near the Sagami River, seven vertical wooden

poles 20 feet in length suddenly emerged, finally reaching a height of about 4.5 feet above ground level. These poles, previously unknown to the local people before the earthquake, were the foundation for an old bridge built in 1182 and abandoned over 600 years earlier. In most cases, little or no damage was done to structures directly as a result of ground shaking, but rather from foundation failures.

Table 2 from Seed and Idriss (1971) summarizes 35 cases where available data was used in evaluation of liquefaction potential. One of the earthquakes that was well-studied occurred at Niigata, Japan in 1964.

5.6.1 Niigata Earthquake of 1964

Seed and Idriss (1967) describe the extensive damage from the Richter magnitude 7.5 earthquake which occurred 35 miles north of the city of Niigata, Japan on 16 June 1964. The acceleration level at the city was about 0.16g. Observed damage may be divided into four groups, as shown in Table 3.

Table 3. Niigata Earthquake

Damage to Foundation	Maximum Settlement (in.)	Angle of Tilt (deg)	Average Relative Density (%)	Range of Relative Density (%)
None	0-8	0-0.3	75	60-90
Slight	8-20	0.3-1	67	50-85
Intermediate	20-40	1-2.3	60	45-75
Heavy	>40	>2.3	45	30-60

The determination of the relative density of the in-situ sands is extremely crude as extrapolated from the data presented by Seed and Idriss (1971).

It was noted that piles driven through loose zones into firm zones experienced significant horizontal displacement. When liquefaction occurs around the upper portion of the pile the pile loses its lateral resistance, producing movement. There were many cases of bending of piles supporting buildings in Niigata.

Kishida (1969) reports that the upper surface of the liquefied soil layer in the most severely damaged area was situated at a depth of less than 25 feet below the ground surface and that soils as deep as 75 feet were liquefied.

Table 2. Site Conditions and Earthquake Data for Known Cases of Liquefaction and Nonliquefaction

Earthquake	Year	Magnitude	Site	Distance From Source of Energy Release (miles)	Soil Type	Depth of Water Table (ft)	Critical Depth (ft)	Average Penetration Resistance at Critical Depth, N	Relative Density (%)	Maximum Ground Surface Acceleration (g)	τ_{av}/σ'_o	Duration of Shaking (s)	Field Behavior
Niigata	1802	6.6	Niigata	24	Sand	3	20	6	53	0.12	0.135	~20	Nonliquefaction
			Niigata	24	Sand	3	20	12	64	0.12	0.135	~20	Nonliquefaction
Niigata	1887	6.1	Niigata	29	Sand	3	20	6	53	0.08	0.09	~12	Nonliquefaction
			Niigata	29	Sand	3	20	12	64	0.08	0.09	~12	Nonliquefaction
Mino Owari	1891	8.4	Ogaki	20	Sand	3	45	17	65	~0.35	0.39	~75	Liquefaction
			Ginan West	20	Sand	6	30	10	55	~0.35	0.37	~75	Liquefaction
			Unuma	20	Sand and Gravel	6	25	19	75	~0.35	0.35	~75	Nonliquefaction
			Ogase Pond	20	Sand	8	20	16	72	~0.35	0.35	~75	Liquefaction
Santa Barbara	1925	6.3	Sheffield Dam	7	Sand	~15	25	—	40	~0.2	0.16	15	Liquefaction
El Centro	1940	7.0	Brawley	5	Sand	~15	~15	—	58	~0.25	0.155	30	Liquefaction
			All-Am. Canal	5	Sand	~20	~25	—	43	~0.25	0.155	30	Liquefaction
			Solfatara Canal	5	Sand	5	~20	—	32	~0.25	0.26	30	Liquefaction
Tohnankai	1944	8.3	Komei	100	Sand	5	13	4	40	~0.08	0.08	~70	Liquefaction
			Meiko St.	100	Silt and Sand	2	8	1	30	~0.08	0.09	~70	Liquefaction
Fukui	1948	7.2	Takaya	4	Sand	11	23	18	72	~0.30	0.30	~30	Liquefaction
			Takaya	4	Sand	3	23	28	90	~0.30	0.32	~30	Nonliquefaction
			Shonenji Temple	4	Sand	4	10	3	40	~0.30	0.29	~30	Liquefaction
			Agr. Union	4	Sand and Silt	3	20	5	50	~0.30	0.33	~30	Liquefaction
San Francisco	1957	5.5	Lake Merced	4	Sand	8	10	7	55	~0.18	0.13	18	Liquefaction
Chile	1960	8.4	Puerto Montt	~70	Sand	12	15	6	50	~0.15	0.15	~75	Liquefaction
			Puerto Montt	~70	Sand	12	15	8	55	~0.15	0.15	~75	Liquefaction
			Puerto Montt	~70	Sand	12	20	18	75	~0.15	0.15	~75	Nonliquefaction
Niigata	1964	7.5	Niigata	32	Sand	3	20	6	53	0.16	0.175	40	Liquefaction
			Niigata	32	Sand	3	25	15	70	0.16	0.175	40	Liquefaction
			Niigata	32	Sand	3	20	12	64	0.16	0.175	40	Nonliquefaction
			Niigata	32	Sand	12	25	6	53	0.16	0.16	40	Nonliquefaction
Alaska	1964	8.3	Snow River	60	Sand	0	20	5	50	~0.15	0.18	180	Liquefaction
			Snow River	60	Sand	8	20	5	44	~0.15	0.15	180	Liquefaction
			Quartz Creek	70	Sandy Gravel	0	~25	40 - 80	100	~0.12	0.145	180	Nonliquefaction
			Scott Glacier	55	Sand	~20	~20	10	65	~0.16	0.185	180	Liquefaction
			Valdez	35	Sand and Gravel	5	~20	13	68	~0.25	0.25	180	Liquefaction
Tokachioki	1968	7.8	Hachinohe	45 to 110	Sand	3	12	14	78	0.21	0.23	45	Nonliquefaction
			Hachinohe	45 to 110	Sand	3	12	6	58	0.21	0.73	45	Liquefaction
			Hachinohe	45 to 110	Sand	5	10	15	80	0.21	0.185	45	Nonliquefaction
			Hakodate	100	Sand	3	15	6	55	0.18	0.205	45	Liquefaction

5.6.2 Mino Owari Earthquake of 1891

The Mino Owari earthquake of 28 October 1891 was a shock of 8.4 magnitude located 18.6 miles from the city of Gifu, Japan. Kishida (1969) has studied the effects of this earthquake and gives profiles of four locations (Figures 47-50) which show various degrees of liquefaction ranging from none to complete. Note that fine sands were most vulnerable.

5.6.3 Tohnankai Earthquake of 1944

The Tohnankai earthquake of 7 December 1944 was a magnitude of 8.3 earthquake located about 100 miles south-southwest of Nagoya City, Japan. Kishida (1969) studied the effects of this earthquake at three locations (Figures 51-53). At the location noted in Figure 51 a Buddhist Temple which was supported on piles did not show any settlement but the ground around the temple subsided about 1-1/3 feet, and water erupted during the earthquake. The tips of the piles were at a depth of about 5 meters below the surface (26.7 feet). Figure 52 shows a soil profile where houses settled as much as 3.3 feet. Fine sand was expelled from the ground. Figure 53 shows a soil profile where differential settlement occurred as a result of partial liquefaction.

5.6.4 Fukui Earthquake of 1948

The Fukui earthquake of 18 June 1948 was a magnitude 7.2 earthquake with its epicenter 3 miles east of Fukui City, Japan. Kishida (1969) studied the effects of this earthquake and gives four profiles (Figures 54-57) where liquefaction was observed in varying degrees. It is interesting to note that although the distance between locations of the soil profiles in Figures 54 and 55 was only about 1,800 feet, one underwent complete liquefaction with sand volcanoes noted on the surface and the other only partial limited liquefaction, the latter being an older area approximately 3.3 feet higher in elevation with more silt. Figure 56 shows a site where water and sand volcanoes were quite prevalent and the main building of a temple settled 1 foot. The distance between the locations shown in Figures 56 and 57 is about 1,800 feet. The site in Figure 57 did not show eruptions of sand and water and only partial liquefaction. This site is again in older ground slightly higher than that of Figure 56.

5.7 REFERENCES

Ambraseys, N. and Sarma, S. (1969) "Liquefaction of soils induced by earthquake," Bulletin of the Seismological Society of America, vol 59, no. 2, Apr 1969, pp 651-664.

Booker, J. R., Rahman, M. S. and Seed, H. B. (1976) GADFLEA: A computer program for the analysis of pore pressure generation and dissipation during cyclic or earthquake loading, University of California, Earthquake Engineering Research Center, EERC Report No. 76-24. Berkeley, Calif., Oct 1976.

Crandall, R. (1908) The San Francisco peninsula in the California earthquake of 1906, vol 1. Washington, D.C., Carnegie Institute, pp 246-254.

DeAlba, P., Chan, C. and Seed, H. B. (1975) Determination of soil liquefaction characteristics by large-scale laboratory tests, University of California, Earthquake Engineering Research Center, EERC Report No. 75-14. Berkeley, Calif., May 1975.

Kishida, H. (1969) "Characteristics of liquefied sands during Mino-Owari, Tohnankai, and Fukui earthquakes," Soils and Foundations (Japan), vol 9, no. 1, Mar 1969.

Kondner, R. L. (1962) "Hyperbolic stress-strain response, cohesive soils," Journal of the Soil Mechanics and Foundations Division, ASCE, vol 89, no. SM1, Feb 1963, pp 115-143.

Lee, K. L. and Albasia, A. (1974) "Earthquake induced settlements in saturated sands," Journal of the Geotechnical Engineering Division, ASCE, no. GT4, Apr 1974.

Martin, P. P. (1975) Non-linear methods for dynamic analysis of ground response, Ph.D. thesis, University of California. Berkeley, Calif., Jun 1975.

McCulloch, D. S. and Bonilla, M. G. (1970) Effects of the earthquake of March 27, 1964, on the Alaska railroad, U.S. Geological Survey, Professional Paper 545-D. Washington, D.C., 1970, 161 pp.

Oldham, R. D. (1899) Report on the great earthquake of June 12, 1897, Memorandum Geological Survey, India, vol 49, 379 pp.

Richter, C. F. (1958) Elementary seismology. San Francisco, Calif., W. H. Freeman, 1958, 786 pp.

Robinson, R., et al. (1975) Structural analysis and retrofitting of existing highway bridges subjected to strong motion seismic loading, Illinois Institute of Technology, Research Institute Report J-6320. Chicago, Ill., May 1975.

Schimming, B. B. (1962) An analytic and experimental study of footings resting on a cohesionless soil, Ph.D. thesis, Northwestern University. Evanston, Ill., 1962

Seed, H. B. (1968) "Landslides during earthquakes due to soil liquefaction," Journal of the Soil Mechanics and Foundations Division, ASCE, vol 93, no. SM5, May 1968, pp 1053-1122.

Seed, H. B. and Idriss, I. M. (1967) "Analysis of soil liquefaction, Niigata earthquake," Journal of the Soil Mechanics and Foundations Divison, ASCE, vol 93, no. SM3, May 1967.

Seed, H. B. and Idriss, I. M. (1971) "A simplified procedure for evaluating soil liquefaction potential," Journal of the Soil Mechanics and Foundation Dvision, vol 97, no. SM6, Sep 1971.

Seed, H. B., Martin, P. P. and Lysmer, J. (1975) The generation and dissipation of pore water pressures during soi liquefaction, University of California, Earthquake Engineering Research Center, EERC Report No. 75-26. Berkeley, CAlif., Aug 1975.

Terzaghi, K. and Peck, R. B. (1967) Soil mechanics in engineering practice. New York, N.Y., John Wiley and Sons, 1967.

Yoshimi, Y. and Kuwabara, F. (1973) "Effect of sub-surface liquefaction on the strength of surface soil," Soils and Foundations (Japan), vol 13, no. 2, Jun 1973.

Yoshimi, Y. and Oh-Oka, H. (1974) "Influence of degree of shear stress reversal on the liquefaction of potential of saturated sand," Soils and Foundations (Japan), vol 15, no. 3, Sep 1974.

Youd, T. L. (1973a) Liquefaction, flow and associated ground failure, U.S. Geological Survey, Circular 688. Reston, Va., 1973, 12 pp.

Youd, T. L. (1973b) Ground movements in the Van Norman Lake vicinity during San Fernando, California, earthquake of February 9, 1971, in San Fernando, California, Department of Commerce, National Oceanic and Atmospheric Administration, vol 3. Washington, D.C., 1973, pp 197-206

Youd, T. L. (1975) "Liquefaction, flow and associated ground failure," in Proceedings of the U.S. National Conference on Earthquake Engineering, Ann Arbor, Mich., Jun 1975. Earthquake Engineering Research Institute, Oakland, Calif., 1975, pp 146-155.

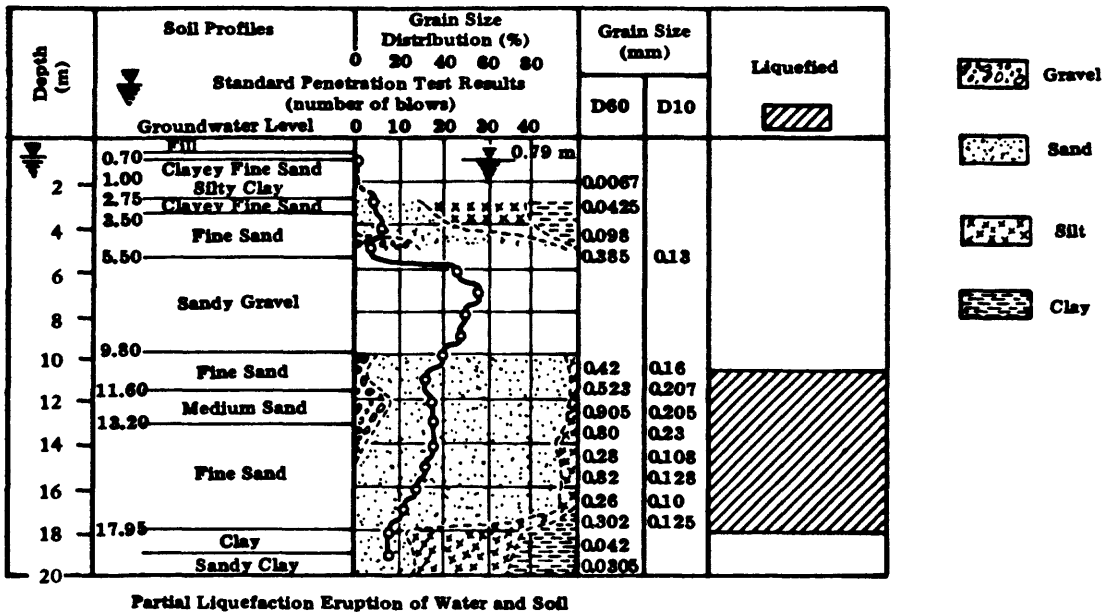

Figure 47. Soil profile, Ogaki City, Bangoku town (from H. Kishida, 1969).

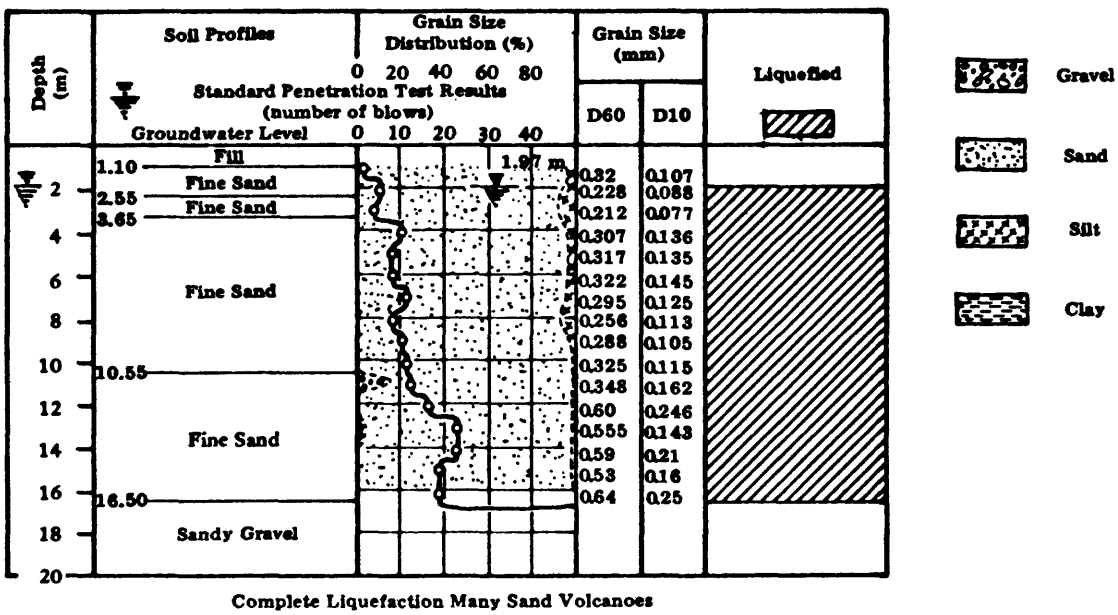

Figure 48. Soil profile, Ginan West Primary School (from H. Kishida, 1969).

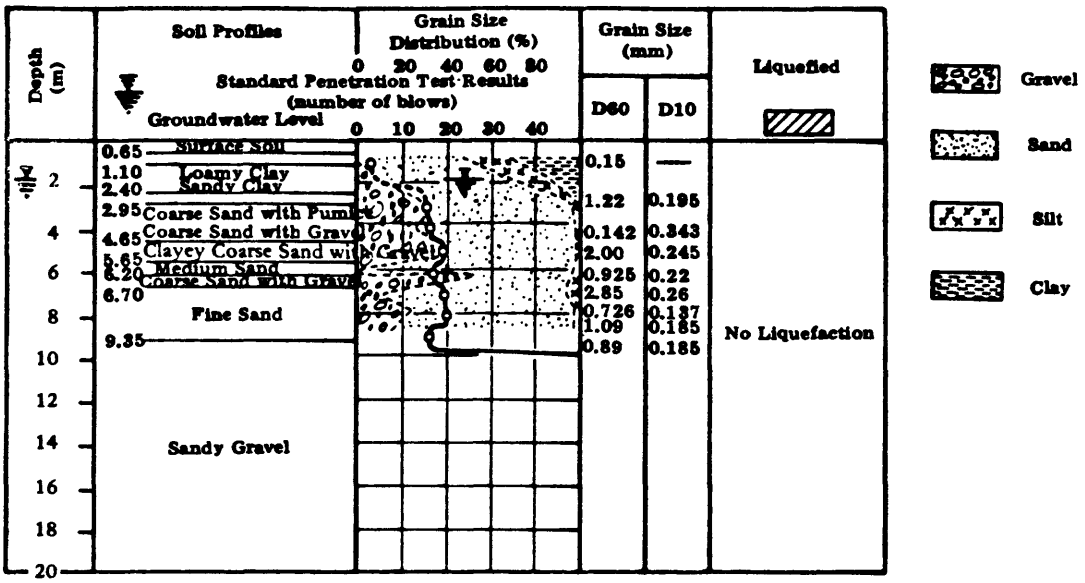

Figure 49. Soil profile, Unuma town (from H. Kishida, 1969).

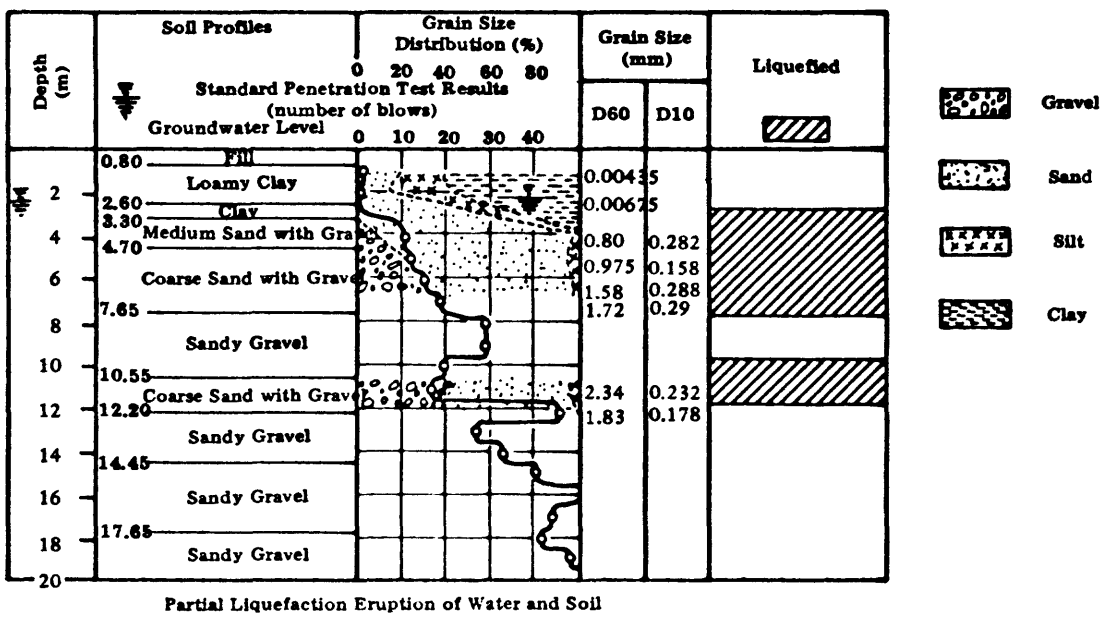

Figure 50. Soil profile, Ogase Pond (from H. Kishida, 1969).

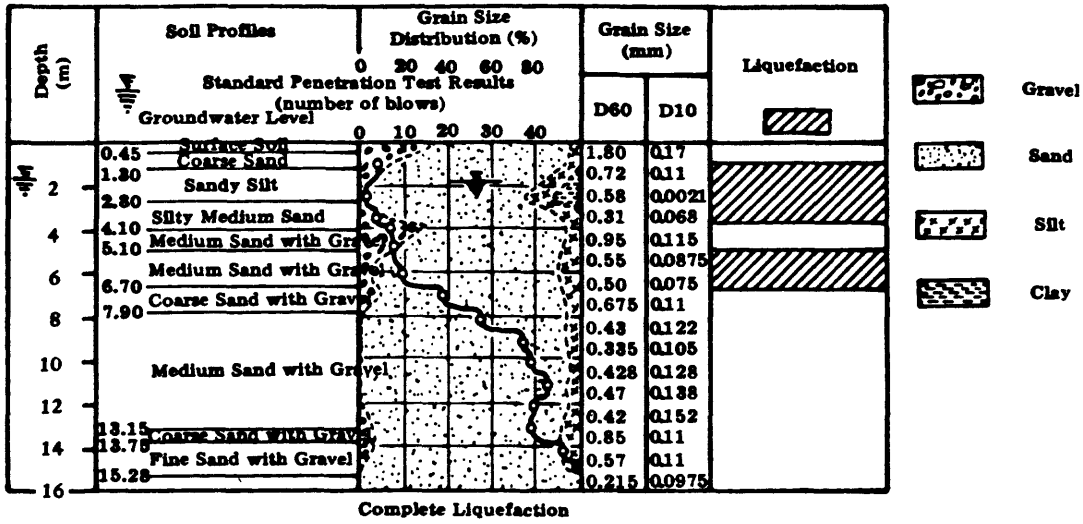

Figure 51. Soil profile, Komei town (from H. Kishida, 1969).

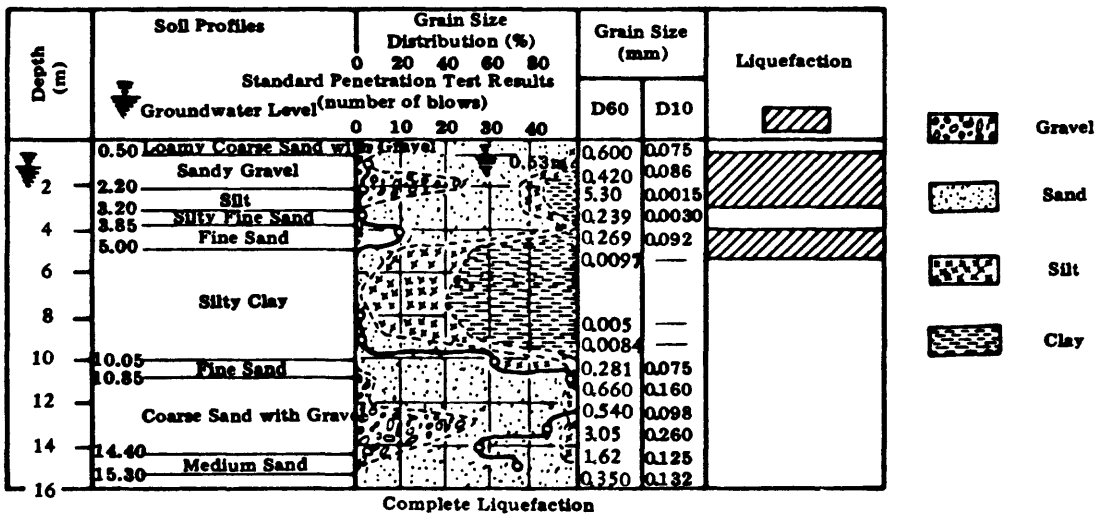

Figure 52. Soil profile, Meiko Street (from H. Kishida, 1969).

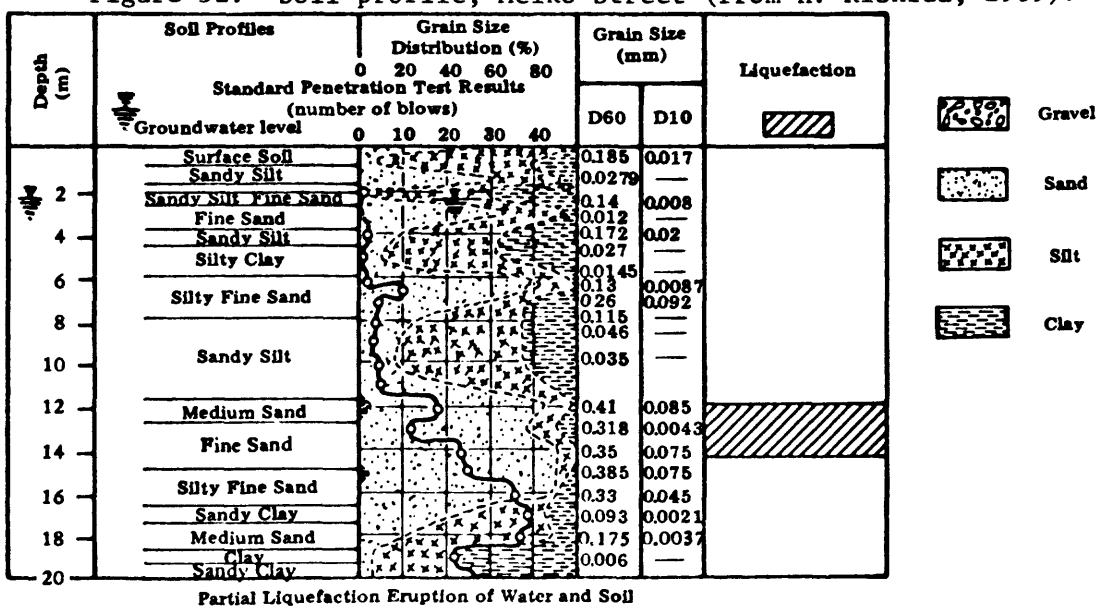

Figure 53. Soil profile, Ienaga Shinden (from H. Kishida, 1969).

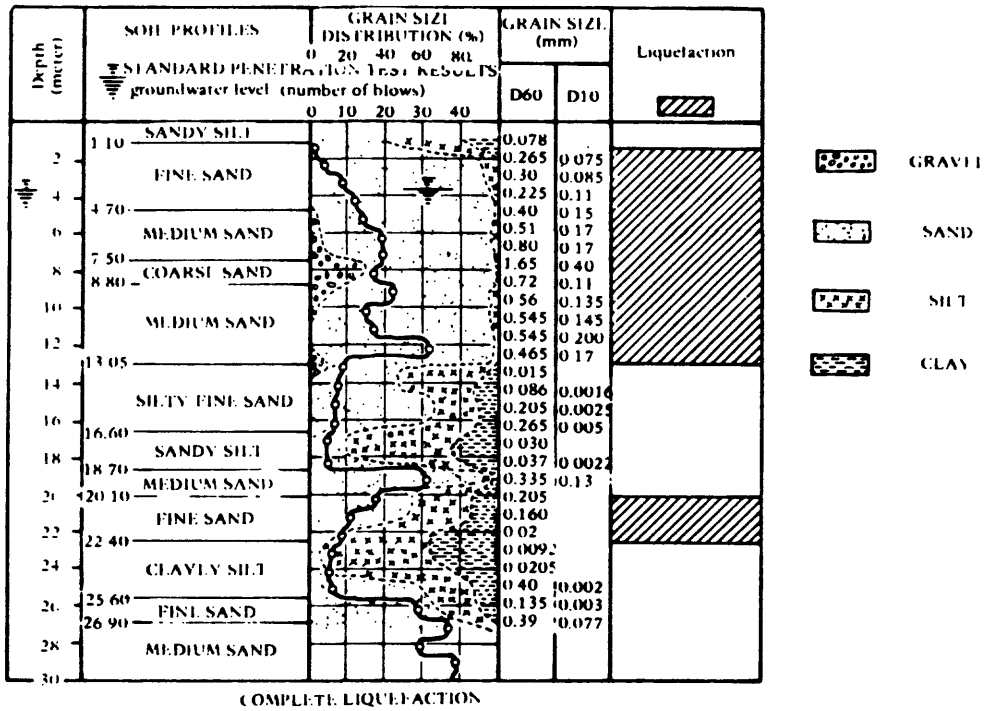

Figure 54. Soil profile, Takaya town 45-35 (from H. Kishida, 1969).

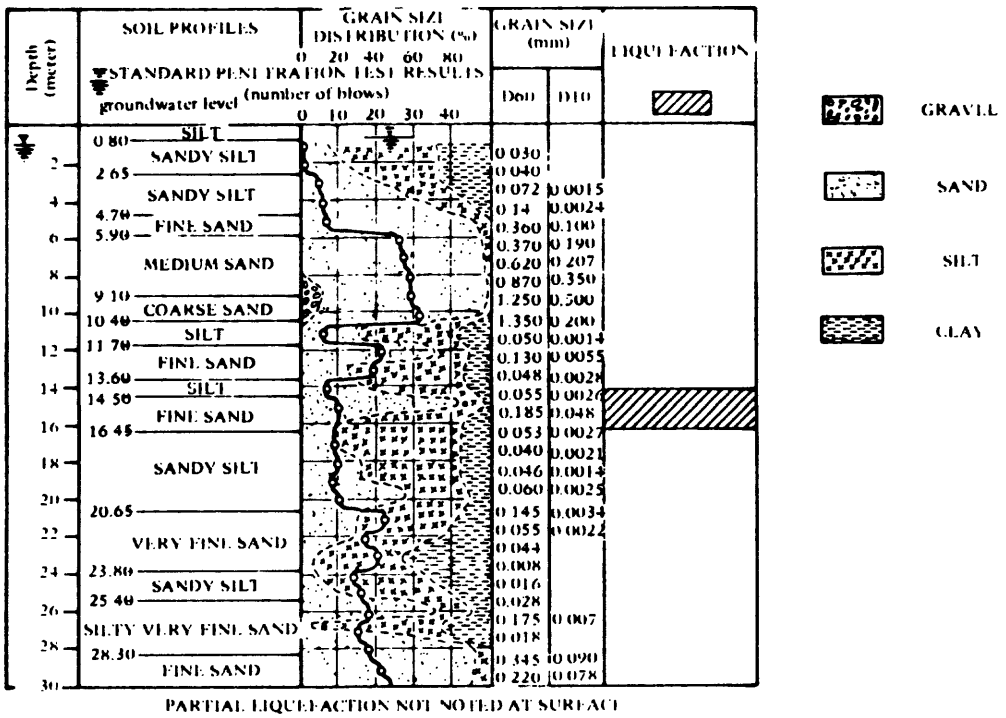

Figure 55. Soil profile, Takaya town 2-168 (from H. Kishida, 1969).

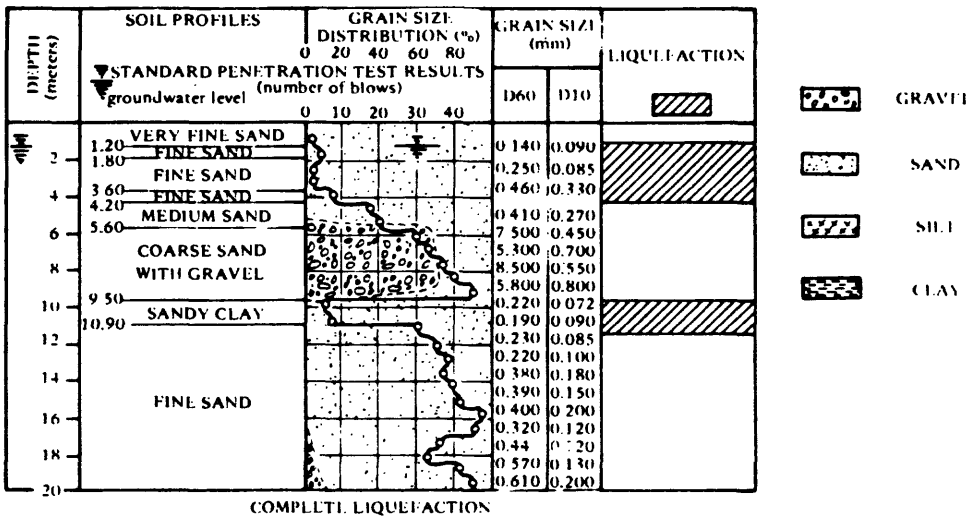

Figure 56. Soil profile, Shonenji Temple (from H. Kishida, 1969).

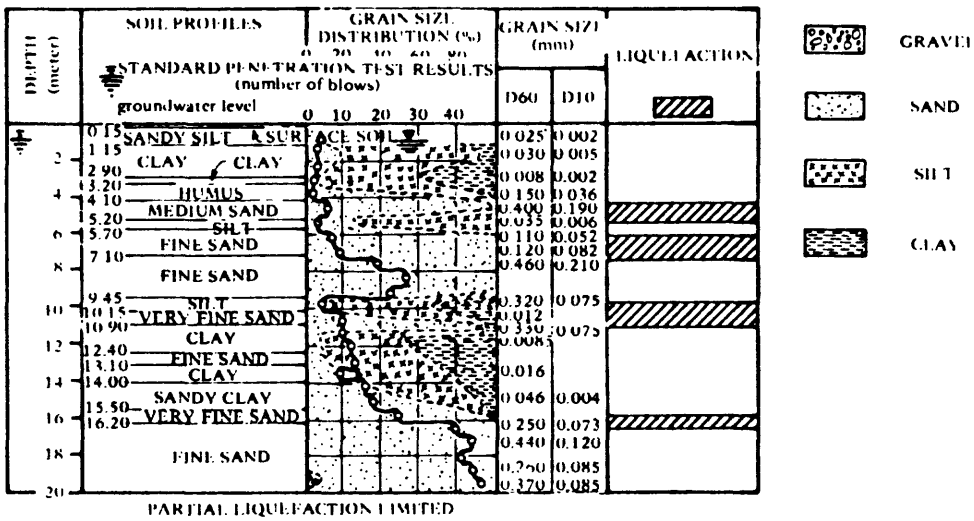

Figure 57. Soil profile, agricultural union (from H. Kishida, 1969).

6.0 LIQUEFACTION RISK ASSESSMENT

A dictionary definition of the term "calculated risk" states: "A hazard or chance of failure whose degree of probability has been estimated before some undertaking is entered upon." Casagrande (1965), in a study of the role of risk in soil mechanics, states that the calculated risk is the type of risk that nobody knows how to calculate, bringing out the ambiguity of the adjective "calculated." He defines the term calculated risk as: the use of imperfect knowledge guided by judgment and experience to estimate the probable ranges for all pertinent quantities that enter into the solution of a problem and to base a decision on an appropriate margin of safety.

The margin of safety that we use should bear a direct relationship to the magnitude of the potential losses and the range of uncertainties at a site. Projects with the potential for catastrophic loss of lives and property should always be planned with an awareness of the responsibility involved. Therefore, the best knowledge and judgment, coupled with the most sophisticated techniques, must be used to ensure the best design. Detailed site investigations should be undertaken to provide all the required information for an analysis. This, along with conservative factors of safety, minimizes the risk. However, when failure of smaller projects involves a tolerable financial loss and no loss of life, the extent or degree of risk must take into consideration economic factors and magnitude of losses that would result from failures. The effort spent in the design is obviously reduced. It is in these routine projects where the calculated risk is greatest. Obviously, the extent of site definition is more limited for smaller projects. It is in these areas that this report attempts to provide most guidance.

Casagrande (1965) divides risk into two groups: engineering risk and human risk. He further divides engineering risk into two groups, unknown risks and calculated risks. Unknown risks are, by definition, those risks which cannot be identified until they reveal themselves by failure. Calculated risks are areas where the state of knowledge is limited, requiring judgment. Significant progress has been made in our understanding of the seismic liquefaction phenomenon. However, uncertainties exist in the determination of site motion, the determination of site soil profile and parameters, and the evaluation of the soil strength. Table 4 summarizes the design philosophy suggested for an average class of structures such as might be designed by the Uniform Building Code seismic methodology.

Table 4. Philosophy of Earthquake-Resistant Design

Structural Criteria	Liquefaction Behavior
1. Prevent nonstructural damage in minor earthquake ground shakings which may frequently occur in the service life of the structure.	1. No liquefacton. Factor of safety >1.3.
2. Prevent structural damage and minimize nonstructural damage in moderate earthquake ground shaking which may occur occasionally.	2. No liquefaction. Factor of safety >1.1.
3. Avoid collapse or serious damage in severe earthquake ground shakings which may rarely occur.	3. Liquefaction limited to confined subsurface layer which does not propagate to surface to cause bearing failure. Horizontal flow potential limited to acceptable level.

6.1 CONSTRUCTION IN AREAS OF POTENTIAL LANDSPREADING

Regional land movement - landspreading - may occur during earthquakes as a result of increased pore pressures and reduced soil strength. Structures which cannot undergo differential settlements of high magnitudes should not be built where landspreading is expected, such as on topographically low areas where the water table is high. The process of site selection should give preference to areas where soils are at higher relative densities and unconsolidated sediments are thinnest. Landspreading may be reduced by elimination of surface depressions. The practice of side borrowing to build embankments increases lateral spreading and should be avoided. Narrow fills, even on well-compacted areas, can settle as a result of ground cracks. Outward flow of soils on the embankment can be expected if the underlying native soils undergo limited flow from liquefaction. When settlements of embankments will occur: the wider the fill, the less chance of damage.

In site selection the toes of alluvial fans and deltas should be avoided. Sites should be limited to older, higher, better drained upper segments of fans and deltas, which are probably more stable. The structural designer must consider measures to mitigate the effects of land spreading, such as limiting the length of structures, articulation, reinforcement, etc.

6.2 PRELIMINARY EVALUATION OF LIQUEFACTION POTENTIAL

A preliminary analysis should be made to determine if a liquefaction problem exists and to what extent a site investigation should be planned. Figure 58 outlines the decision process, and the following information

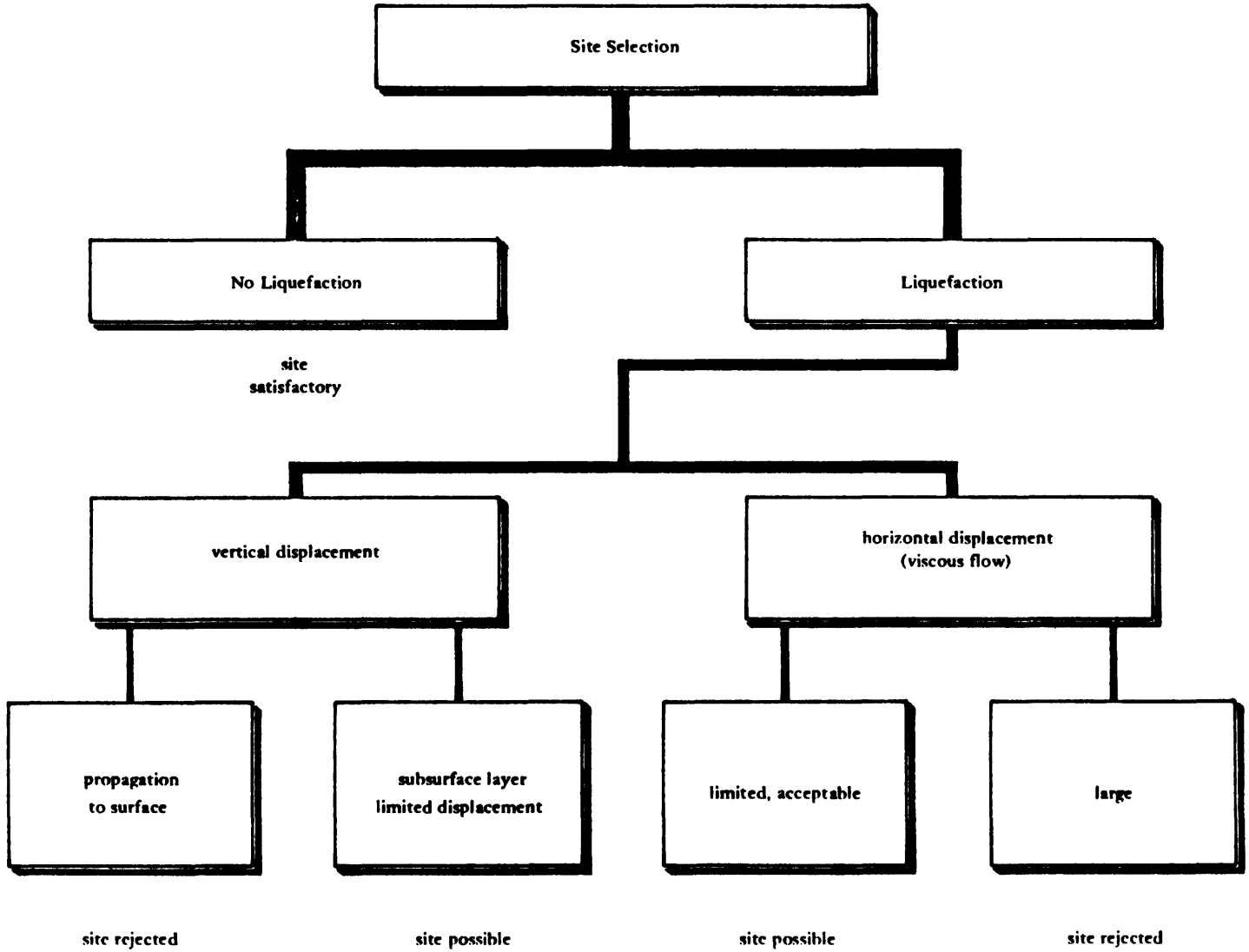

Figure 58. Outline of decisions for site selection.

is required: (1) design earthquakes and (2) a preliminary soil profile and an estimate of in-situ soil conditions.

The site profile may be estimated from standard penetration test results. The simplified hand-computation procedures described in Chapter 3 should be used to define the liquefiable region. For typical soils the soil strength may be estimated from Ferritto and Forrest (1978). The extent of the investigation is controlled by the magnitude of the project; a structure might not justify a large exploration and testing program unless it is of key importance. Generally, a moderate program of standard penetration field tests and cyclic triaxial laboratory tests may cost tens of thousands of dollars by the time the samples are collected and data reduced, evaluated, and presented in a usable form, provided the site is easily accessible to a local soils laboratory.

6.3 DETAILED ANALYSIS OF VULNERABILITY TO LIQUEFACTION

The methods for predicting the occurrence of liquefaction have been described above. By use of either the simplified hand computation or the more complex computer one-dimensional or two-dimensional method, the number of cycles to cause liquefaction at various depths is determined. The soil information required to accomplish this includes a detailed soil profile of the site with estimates of layer density, shear modulus, and strength. Having established a pore pressure generation parameter in terms of the number of cycles to liquefy (N_L), the pore pressure generation/dissipation equation may be solved by the computer programs APOLLO or GADFLEA resulting in a time history of the bearing capacity of the soil, or approximated by Figures 40 and 41. Estimates of soil compressibility and permeability are required. The adequacy of support in bearing may now be estimated. Using consolidation analysis and viscous flow, support motions may be estimated. These support motions may be evaluated by a static structural displacement analysis. The structure should have the design dead weight and live load acting on it in conjunction with the displacements. A static displacement analysis is satisfactory since the occurrence of liquefaction isolates the structure from ground motion and the support displacements are delayed until the liquefaction has time to propagate to the surface.

6.4 MINIMIZATION OF DAMAGE

Three basic ingredients are available to reduce the possible damage from liquefaction: (1) site selection, (2) site improvement, and (3) structure design.

6.4.1 Site Selection

As noted in the Alaskan earthquake, structures located on bedrock suffered least while those on deep fine-grained soils suffered most. The geologic and engineering characteristics of a site should be thoroughly investigated and evaluated. In some cases, geologic and hydrologic factors may dictate a selection that may initially be more expensive than an alternate one on liquefiable soils. However, if repair costs after an earthquake are considered, the overall cost may be less for the

more expensive site. Whenever possible, sites should be selected that avoid areas where thick, unconsolidated, young, water-laid, noncohesive sediments occur. Liquefaction requires a high water table; the probability of occurrence can be reduced by selecting an area with a water table below 10 or 20 feet, if possible. Areas where the ground is sloping offer the possibility of horizontal flow if liquefaction occurs. As noted above, slopes of only a few degrees are capable of creating flows of several feet. Sites with sloping ground and topographically low areas should be avoided as much as possible.

Specifically, the propagation of liquefaction must be evaluated. If the region in which liquefaction occurs propagates to the surface from an earthquake, large motions can be expected and the site should not be considered as satisfactory. If the region in which liquefaction occurs is limited and confined to subsurface layers which do not affect the bearing of the foundation, the site may be considered acceptable if regional subsidence is not large.

Sites where calculations for horizontal and vertical movement must be made using viscosity calculations are probably not well-suited for structures since large deformations would be expected.

As shown above, soils with relative densities less than 45% can undergo unlimited flow and should be avoided. Soils with relative densities of 80% or greater will probably have limited displacements if liquefaction occurs. Structures which are sited on these soils must be designed to withstand the displacements expected. Soils with relative densities between 45% and 80% may or may not be suitable sites; therefore, an extensive analysis should be performed to estimate the potential soil strain which might occur.

Youd and Perkins demonstrate the procedures for constructing maps of liquefaction potential. Although these may be over generalized and lack specific detail they do in principle offer a useful guide to site selection. Table 5 gives the work of Youd and Perkins in relative liquefaction potential to the age of the deposit for various types of the deposit. It is important to note variations in the water table location which might have occurred.

6.4.2 Site Improvement

It has been noted previously that a high groundwater table contributes markedly to liquefaction potential. Lowering the water table has a twofold effect: first, it lowers the region in which liquefaction can be initiated; second, it increases the effective confining stress on the potentially liquefiable soil zone. From a practical point of view, it may not be economical to permanently lower the water table at a site.

Next to lowering the groundwater table, the most important method of reducing the liquefaction potential is by increasing the relative density of the soil. Densification increases the initial shear strength of the soil; however, as pointed out above, densification may cause a reduction in permeability of the top layer of soil resulting in an unfavorable condition. Increasing the permeability of the near surface soil improves it. Vibroflotation or sand compaction piles both densifies the soil and improves drainage when porous material is used. Thus, these methods should be more effective than other densification methods

Table 5. Estimated Susceptibility of Sedimentary Deposits to Liquefaction During Strong Seismic Shaking

Type of Deposit (1)	General Distribution of Cohesionless Sediments in Deposits (2)	Likelihood That Cohesionless Sediments, When Saturated, Would Be Susceptible to Liquefaction (by Age of Deposit)			
		<500 yr (3)	Holocene (4)	Pleistocene (5)	Pre-Pleistocene (6)
(a) Continental Deposits					
River channel	Locally variable	Very high	High	Low	Very low
Flood plain	Locally variable	High	Moderate	Low	Very low
Alluvial fan and plain	Widespread	Moderate	Low	Low	Very low
Marine terraces and plains	Widespread	-	Low	Very low	Very low
Delta and fan-delta	Widespread	High	Moderate	Low	Very low
Lacustrine and playa	Variable	High	Moderate	Low	Very low
Colluvium	Variable	High	Moderate	Low	Very low
Talus	Widespread	Low	Low	Very low	Very low
Dunes	Widespread	High	Moderate	Low	Very low
Loess	Variable	High	High	High	Unknown
Glacial till	Variable	Low	Low	Very low	Very low
Tuff	Rare	Low	Low	Very low	Very low

(continued)

Table 5. Continued

Type of Deposit (1)	General Distribution of Cohesionless Sediments in Deposits (2)	Likelihood That Cohesionless Sediments, When Saturated, Would Be Susceptible to Liquefaction (by Age of Deposit)			
		<500 yr (3)	Holocene (4)	Pleistocene (5)	Pre-Pleistocene (6)
(a) Continental Deposits (cont'd)					
Tephra	Widespread	High	High	?	?
Residual soils	Rare	Low	Low	Very low	Very low
Sebka	Locally variable	High	Moderate	Low	Very low
(b) Coastal Zone					
Delta	Widespread	Very high	High	Low	Very low
Esturine	Locally variable	High	Moderate	Low	Very low
Beach					
• High wave energy	Widespread	Moderate	Low	Very low	Very low
• Low wave energy	Widespread	High	Moderate	Low	Very low
Lagoonal	Locally variable	High	Moderate	Low	Very low
Fore shore	Locally variable	High	Moderate	Low	Very low
(c) Artificial					
Uncompacted fill	Variable	Very high	-	-	-
Compacted fill	Variable	Low	-	-	-

in which density alone is increased. Increased confinement through use of highly porous surcharges such as coarse backfill are also extremely effective in reducing liquefaction potential.

6.4.3 Structure Design

Both structurally indeterminate and determinate structures can be designed to withstand stresses and displacements without failure. However, the more indeterminate a structure is, the more the stresses in the structure are influenced by support displacement. A typically designed indeterminate structure is limited to significantly less displacement than a corresponding determinant structure. However, loss of the support capacity of a column bent for either structure will probably result in damage of the structure. Structures should be designed to be articulated. This is not meant to require expansion joints or other similar devices which have given designers problems in earthquakes; the intent is to make superstructure component stress levels independent of support displacements.

In areas where bedrock is near the surface, caissons to rock provide the most reliable, although probably the most expensive, type of foundation. In regions where liquefaction will occur, vertical piles have been found to have insufficient lateral stability. When the soil becomes liquefied, the horizontal restraint is lost, and the pile may experience large lateral displacements. This is not surprising considering the long unbraced length of the pile and its load. Thus piles, even though driven into competent material below a potentially liquefiable zone and designed not to rely on friction in the liquefiable zone, may still fail because of excessive horizontal motion or from buckling over its unsupported length. Additionally, negative friction can increase the pile load.

In the Alaskan earthquake, heavy objects (automobiles, structures, etc.) gradually settled into the quicksand. In several cases, lightweight buried structures floated to the surface. This may be a problem for Navy drydocks, sewage treatment tanks, and similar structures which displace large amounts of soil but have relatively light weight.

Waterfront bulkheads are especially vulnerable to liquefaction of the backfill since they are often backfilled with loose sand. It is difficult to compact the backfill below the water level. The quay walls and bulkheads in dock areas often suffer major damage during earthquakes from the liquefied backfills which exert higher pressures than those for which the walls are designed.

Shallow, low pressure footings might be suited for liquefaction which does not propagate to the surface and cause bearing failure. The engineer must make foundation choice based on the specifics of the site, the types of structure, and loads. In any case, the structure must be designed such that the combination of dead and live load and liquefaction displacement do not result in overstressing at any point.

6.5 PROBABILITY OF OCCURRENCE

To evaluate the risk of liquefaction at a site, both the damage from liquefaction and the probability of occurrence must be reviewed together. To accomplish this, the designer should prepare a list of

magnitudes of earthquakes from results of liquefaction analyses showing: (1) no liquefaction, (2) liquefaction of subsurface layer without widespread propagation, (3) liquefaction of subsurface layer with propagation to foundation support level, and (4) liquefaction propagating to surface. These levels of liquefaction should then be correlated to the probability that a specific magnitude earthquake occurs. Depending on the method for analysis, uncertainties in acceleration, relative density, and soil strength may be included.

An example of this will be shown. Let us consider a site at a known distance from a fault. The site acceleration and standard deviation may be estimated. The number of earthquake cycles and standard deviation may be estimated from Figure 29. The soil's relative densty and standard deviation may be determined, as discussed above, from laboratory or field tests, and the soil strength and standard deviation, in the absence of actual data, may be estimated. Using the simplified procedure, a factor of safety may be determined directly. However, a Monte Carlo simulation can be performed taking the four variables (soil strength, relative density, site acceleration, and number of earthquake cycles) as random, normally distributed values, shaped by their means and standard deviations.

Consider the following case where the distance to the fault is 40 miles; then the ground motion for various magnitude earthquakes is given in Table 6.

Assume a case where the relative density is 0.60 with standard deviation of 0.06 and the soil strength as indicated in Figure 17; then, by using simple Monte Carlo simulation, the probability of liquefaction may be determined as a function of earthquake magnitude, as shown in Table 7. The probability of an earthquake occurring and causing liquefaction may be estimated by use of recurrence data for a fault (usually expressed as a number of events per year for magnitude greater than or equal to M). The recurrence data are used to determine the number of events expected between a magnitude increment, M_i to $M_i + 1$. The expected number of earthquake events per year is multiplied by the number of years for the life of the structure and by the average probability of liquefaction occurring for the magnitude range M_i to $M_i + 1$ to yield the expected number of earthquakes causing liquefactions for the fault, time period and magnitude increment. The expected number of earthquakes causing liquefaction, λ, is used to compute the probability of an earthquake occurring and causing liquefaction by a Poisson's distribution

$$P_{LE} = 1 - e^{-\lambda}$$

Assuming the fault to be a typical fault system in California with specific recurrence intervals (number of earthquakes per year), the probability of an earthquake occurring and causing liquefaction is shown in Table 8.

For this example the highest probability of liquefaction in the 50-year span is 0.046 from a magnitude 8 earthquake. The most probable earthquake causing liquefaction may occur at any magnitude and is a function of fault activity and site conditions. The consequences and

Table 6. Ground Motion

Earthquake Magnitude	Number of Cycles	Number of Cycles Standard Deviation	Acceleration (g)	Acceleration Standard Deviation (g)
5.0	3.67	3.64	0.005	0.0056
5.5	4.86	3.92	0.0143	0.0146
6.0	6.43	4.11	0.0303	0.0309
6.5	8.51	4.14	0.0516	0.0527
7.0	11.27	5.81	0.0711	0.0725
7.5	14.92	8.19	0.0790	0.0806
8.0	19.76	11.52	0.0790	0.0806

Table 7. Probability of Liquefaction

Earthquake Magnitude, M	Probability of Liquefaction, $P_L(M)$	Median Factor of Safety
5.0	0.000	>10
5.5	0.000	>10
6.0	0.007	5.38
6.5	0.047	3.06
7.0	0.097	2.22
7.5	0.165	1.81
8.0	0.218	1.67

Table 8. Probability of Earthquake Causing Liquefaction

Magnitude	Recurrence Interval, U(M)[a]	Number of Events/Yr, U(M)	Expected Events 50 Years	P_L	Expected Events Causing Liquefaction	P_{LE}
5.0	0.26	0.13	6.5	0	0	0
5.5	0.13	0.063	3.15	0	0	0
6.0	0.067	0.033	1.65	0.007	0.01155	0.011
6.5	0.034	0.017	0.85	0.047	0.03995	0.039
7.0	0.017	0.0076	0.38	0.097	0.03686	0.036
7.5	0.0094	0.0050	0.25	0.165	0.04125	0.040
8.0	0.0044	0.0044	0.22	0.218	0.04796	0.046

[a] Number of events per year $\geq$M and assumed that t = 50 years.

extent of liquefaction for the most probable magnitude earthquake should be determined. (Although the consequences from other magnitude earthquakes will be greater, the probability is lower.) Thus, levels of damage and extent of propagation of liquefaction can be determined as a function of magnitude and probability of occurrence.

The overall risk to a structure may be determined based on the probability of occurrence of liquefaction and the consequences should it occur. It is also obvious that the uncertainty associated with the ability to predict earthquake motion and to determine site properties results in some probability of liquefaction even though the median factor of safety is greater than 1.0. Thus, a degree of conservatism must be exercised until more accurate site definition and earthquake-motion data become available.

6.6 CRITERIA FOR SITES

The criteria for selection of sites shuld be based on earthquakes with the following magnitudes:

M_A = recurrence, once in 10 years

M_B = recurrence, once in 25 years

M_C = recurrence, once in 50 years, or design level earthquake

M_D = recurrence, once in 200 years, or the maximum credible earthquake

Under the proposed criteria the site is considered acceptable if the mean-minus-one-standard-deviation factor of safety $FS_{m-\sigma}$ (84% confidence limit) and the probability of an earthquake causing liquefaction P_{LE} are as shown in Table 9. Note that the probability includes the occurrence of an earthquake and is not simply the probability of liquefaction.

It should be noted that in the proposed criteria liquefaction is allowed to occur for the M_D earthquake (maximum credible earthquake) as long as it remains confined to subsurface layers, does not cause bearing failures, or produce unacceptable horizontal and vertical displacements. Since the displacements would be limited, acceptable levels of damage would be imposed on the structures, and collapse would not occur.

In the proposed siting criteria, the acceptability of a site depends on whether the value of the probability of a design level earthquake causing liquefaction is ≤ 0.10. This value is based solely on engineering judgment. The occurrence of liquefaction does not always result in collapse of the structure. It is very difficult to quantify the dollar value of a functioning structure. The value of human life has always been of highest importance in the United States. Engineers are often faced with problems asking, "How safe is safe enough?" An economic analysis may be of use in comparing alternatives to produce the best return.

In the proposed criteria it should be pointed out that the total probability of liquefaction is the sum of the individual probabilities of liquefaction for a given magnitude earthquake, P_{LE}, taken over all

Table 9. Criteria for Site Selection

Earthquake	Factor of Safety, $FS_{m-\sigma}$	Liquefaction Probability, P_{LE}	Liquefaction Consequences				
			Liquefaction Subsurface Layer	Propagation to Surface	Bearing Failure	Horizontal Flow Failure	Vertical Settlement Failure
M_A	≥ 1.5	≤ 0.1	No	No	No	No	No
M_B	≥ 1.3	≤ 0.1	No	No	No	No	No
M_C	≥ 1.1	≤ 0.1	No	No	No	No	No
M_D	—	—	Yes[a]	No	No	No	No

[a] Upper region pore pressure limited to prevent failure.

the magnitudes. However, this value is misleading since the consequences if liquefaction were to occur would be very different from a brief period of liquefaction caused by a magnitude 5 earthquake than from a prolonged period with a magnitude 8 earthquake. The criterion attempts to limit overall exposure by limiting the function at several selected points representing a design earthquake. Note the dual criteria of factor of safety and probability. Table 9 is intended to present a procedure whose numerical values can only be determined from experience. The numbers used in the table are intended to represent the approximate level of conservatism which is compatible with present engineering practice and should not result in major construction cost increases.

If the earthquake motions are specified at the ground surface, then the stresses developed in, say, the upper 40 feet of a soil deposit can be assessed. The preceding pages have discussed at length the procedures required to make a good assessment of the stresses required to cause initial liquefaction or a given degree of strain. The final acceptable factor of safety will clearly depend on the accuracy with which each of these individual assessments can be made in any given case.

A further consideration which must be taken into account in determining what value constitutes an acceptable factor of safety is the consequences arising, if for some reason the actual factor of safety should be reduced to unity. Clearly, this is very different in the case of a loose sand with a relative density of about 54% as opposed to the same sand in a dense condition, say with a relative density of 82%. Seed (1976) reports in his studies that the limiting strain for Monterey No. 0 sand at 54% relative density is ±30%, while the limiting strain for the same sand at 82% relative density is only ±10%. The stress conditions producing these conditions are shown graphically in Figure 59. Seed (1976) shows that if the stress ratio causing 5% strain at a relative density of 54% is even slightly exceeded, then the sand will undergo strains up to ±30% with almost certain catastrophic consequences. However, if the stress ratio causing 5% strain at a relative density of 82% is slightly exceeded, the only result would be to cause a strain of perhaps 6%, and no more than 10%, even if the factor of safety should drop to 0.5 or even lower.

6.7 REFERENCES

Casagrande, A. (1965) "The role of the calculated risk in earthwork and foundation engineering," Journal of Soil Mechanics and Foundations Division, ASCE, vol 91, no. SM4, Jul 1965.

Ferritto, J. M. (1978) "A Probabilistic Procedure for Estimating Seismic Loading Based on Historic and Geologic Data." Civil Engineering Laboratory, Port Hueneme, Calif. (in publication).

Ferritto, J. M. and Forrest, J. B. (1977) FHWA-RD-77-127, Determination of seismically induced soil liquefaction potential at proposed bridge sites, Department of Transportation. Washington, D.C., Aug 1977.

Seed, H. B. (1976) "Evaluation of soil liquefaction effects on level ground during earthquakes," ASCE Preprint 2752 (Liquefaction Problems in Geotechnical Engineering), American Society of Civil Engineers Annual Convention, Philadelphia, Pa., 27 Sep-1 Oct 1976.

Youd, L. T. and Perkins, D. M. (1978) "Mapping Liquefaction-Induced Ground Failure Potential," ASCE Journal of the Geotechnical Engineering Division, GT4, Vol 104, Apr 1978.

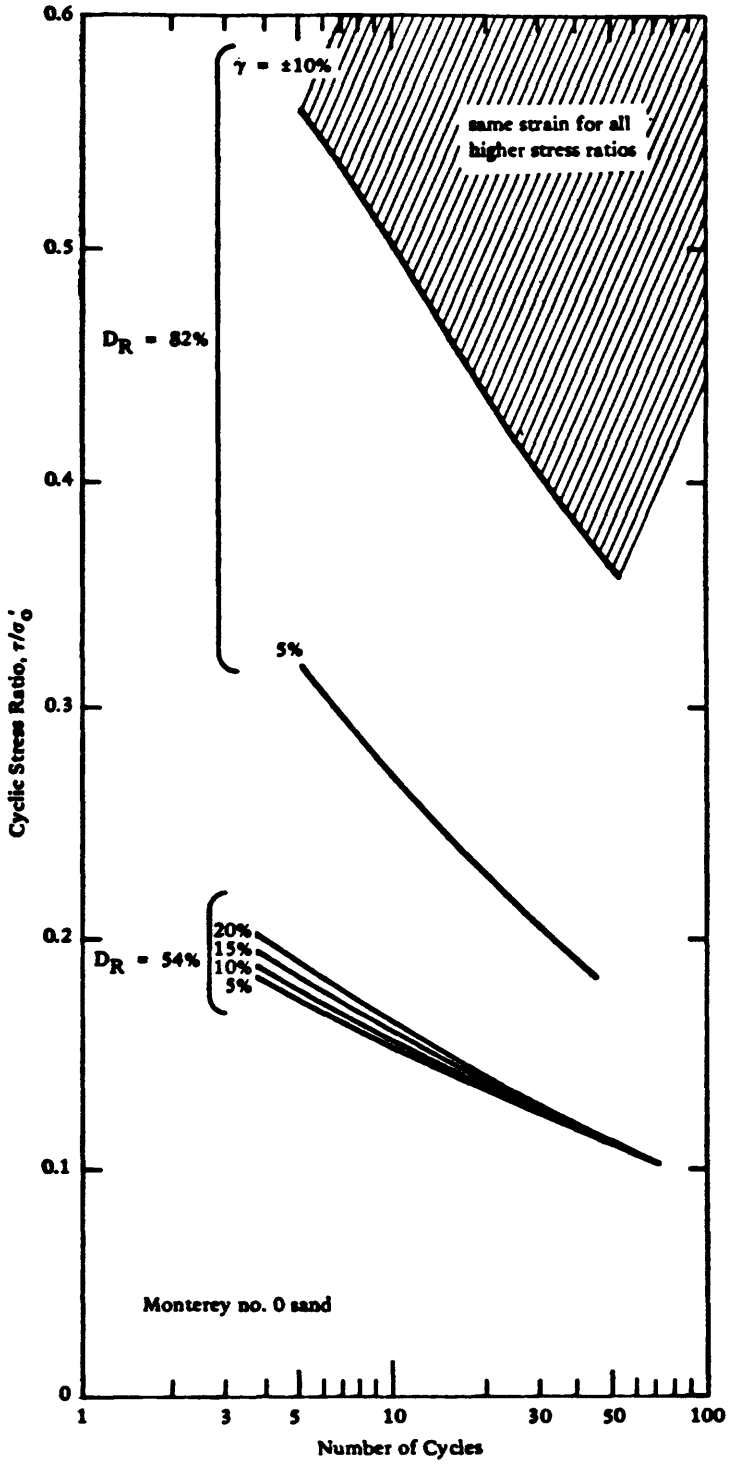

Figure 59. Relationship between τ/σ_o' and number of cycles causing different strain levels (from H. B. Seed, I. Arango, and C. K. Chan, 1975).

7.0 EARTH DAM ANALYSIS

During recent years there has been increased emphasis on insuring dam safety. In the United States Public Law 92-367, enacted in 1972 after several dam failures, authorized the Corps of Engineers to undertake a program of dam inspection. In the United Kingdom the British Reservoirs Act of 1975 also provides for the inspection of dams. A particular problem in seismically active areas is the liquefaction of saturated cohesionless materials. Professor Seed (1979) in an attempt to clarify terminology has adopted the following definitions:

"Liquefaction:" denotes a condition where a soil will undergo continued deformation at a constant low residual stress or with low residual resistance, due to the buildup and maintenance of high pore water pressures, which reduce the effective confining pressure to a very low value; pore pressure buildup leading to liquefaction may be due either to static or cyclic stress applications and the possibility of its occurrence will depend on the void ratio or relative density of a sand and the confining pressure; it may also be caused by a critical hydraulic gradient during an upward flow of water in a sand deposit.

"Peak Cyclic Pore Pressure Ratio of 100%:" denotes a condition where, during the course of cyclic stress applications, the residual pore water pressure on completion of any full stress cycle becomes equal to the applied confining pressure; the development of a peak cyclic pore pressure ratio of 100% has no implications concerning the magnitude of the deformations that the soil might subsequently undergo; however, it defines a condition that is a useful basis for assessing various possible forms of subsequent soil behavior.

"Peak Cyclic Pore Pressure Ratio of 100% with Limited Strain Potential," or "Cyclic Mobility:" denotes a condition in which cyclic stress applications develop a peak cyclic pore pressure ratio of 100% and subsequent cyclic stress applications cause limited strains to develop either because of the remaining resistance of the soil to deformation or because the soil dilates, the pore pressure drops, and the soil stabilizes under the applied loads. Cyclic mobility may also be used in a broader sense to describe the cyclic straining that may occur even with pore pressure ratios less than 100% in which case the actual peak value of pore pressure ratio may simply be stated.

Castro (1976) and Casagrande (1976) use the term liquefaction for situations involving essentially unrecoverable loss of resistance to deformation with attendant gross deformations. Such behavior is common for loose sands. Although accumulation of deformations can occur in a dense sand undergoing cyclic loading, the soil may retain its ability to carry the applied load without unrestrained movement.

Consider the response of a saturated sand under monotonic loading in a standard undrained triaxial compression test. Three different types of material response (such as that presented by Castro (1969) will

be illustrated qualitatively, Figures 60 and 61, to show the behavior of three specimens of sand at low, moderate, and high relative densities. Under increasing vertical (deviator) stress, each of these specimens exhibits a different type of behavior, depending upon its volumetric strain-shear stress coupling which is, in turn, a function of its initial density. The densest sample, test 3, does not undergo liquefaction, but exhibits an initial sharp rise in pore pressure with axial strain (Figure 60b); this corresponds to a decrease in effective stress (Figure 61) and a reduction in stiffness (Figure 60a). The pore pressure rise and loss in stiffness is related to the tendency for the sand to initially compress under applied shear stress. At larger strains, the volumetric strain-shear strain coupling inherent in granular materials causes volume dilation to occur with attendant reduction in pore pressures (Figure 60b), increase in effective stress (Figure 61), and recovery of stiffness (see Figure 60a).

Test 1 is an example of "unlimited flow." The specimen exhibits response behavior similar to that shown in test 3 up to the commencement of yielding (Figure 60a). Beyond this point, the specimen in test 1, because of its loose condition, does not dilate; hence, the pore water pressure approaches the initial confining chamber pressure, and the strength falls off dramatically.

The phenomenon of "limited flow" is demonstrated in test 2. In this test, initial specimen yielding (Figure 60a) did not occur until a considerable amount of strain had occurred. This behavior is attributed to the fact that the density of the specimen was slightly looser than the specimen of test 3. At large axial strain, the test 2 specimen started to dilate, causing a recovery of effective stress (Figure 61) and a re-establishment of some vertical load stiffness (Figure 60a).

According to Castro (1976), any soil whose ultimate undrained residual strength is less than the in situ shear stress is unstable. The undrained shear strength is assumed to be a function of only the initial soil state and therefore independent of the way in which the failure load is applied. This means that the liquefaction (unlimited flow) threat by this definition can be evaluated in terms of only two things: (1) the undrained residual shear strength, and (2) the in situ stress state. Therefore the major difficulty in analyzing cohesionless soils is not with regard to soil liquefaction but rather in prediction of strain accumulations. However cyclic straining should not be as much a threat to most dams as the more easily recognized unrestrained type of liquefaction behavior.

In cyclic triaxial tests with stress reversals (i.e., those incorporating alternating tensile and compressive deviator stress), a type of limited flow, referred to by Castro (1969) as cyclic mobility, may be exhibited. A record from this type of test is shown in Figure 62. In this test the effective confining stresses are incrementally reduced by the increases in residual pore pressure with each load cycle. At some point, generally when the deviator stress is zero, the effective confining stresses approach zero and a period of flow occurs. The specimen deforms rapidly, but then resolidifies from a dilatency-associated decrease in pore pressure upon loading. Upon the ensuing cycle, the specimen again undergoes a period of limited flow, following which the specimen may again regain strength by a dilation-associated increase in effective stress. In this manner cyclic triaxial tests may undergo increasingly larger alternating vertical strain increments with each half-cycle, until the integrity of the specimen is completely destroyed.

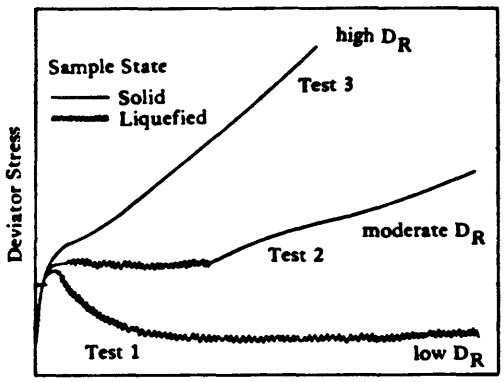

(a) Deviator Stress – Axial Strain.

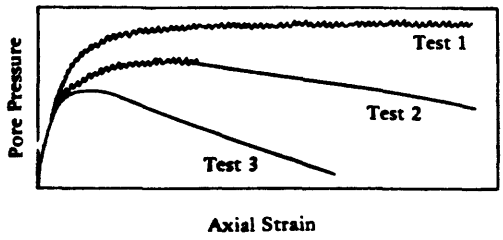

(b) Pore Pressure – Axial Strain.

Figure 60. Stress-strain curves for three monotonically loaded triaxial compression tests on undrained sample of sand (after Castro, 1969).

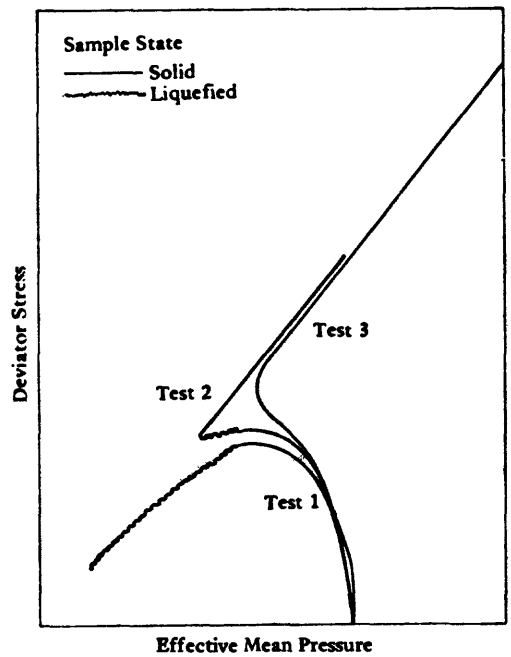

Figure 61. Stress paths for the three triaxial compression tests plotted in Figure 60 (after Castro, 1969).

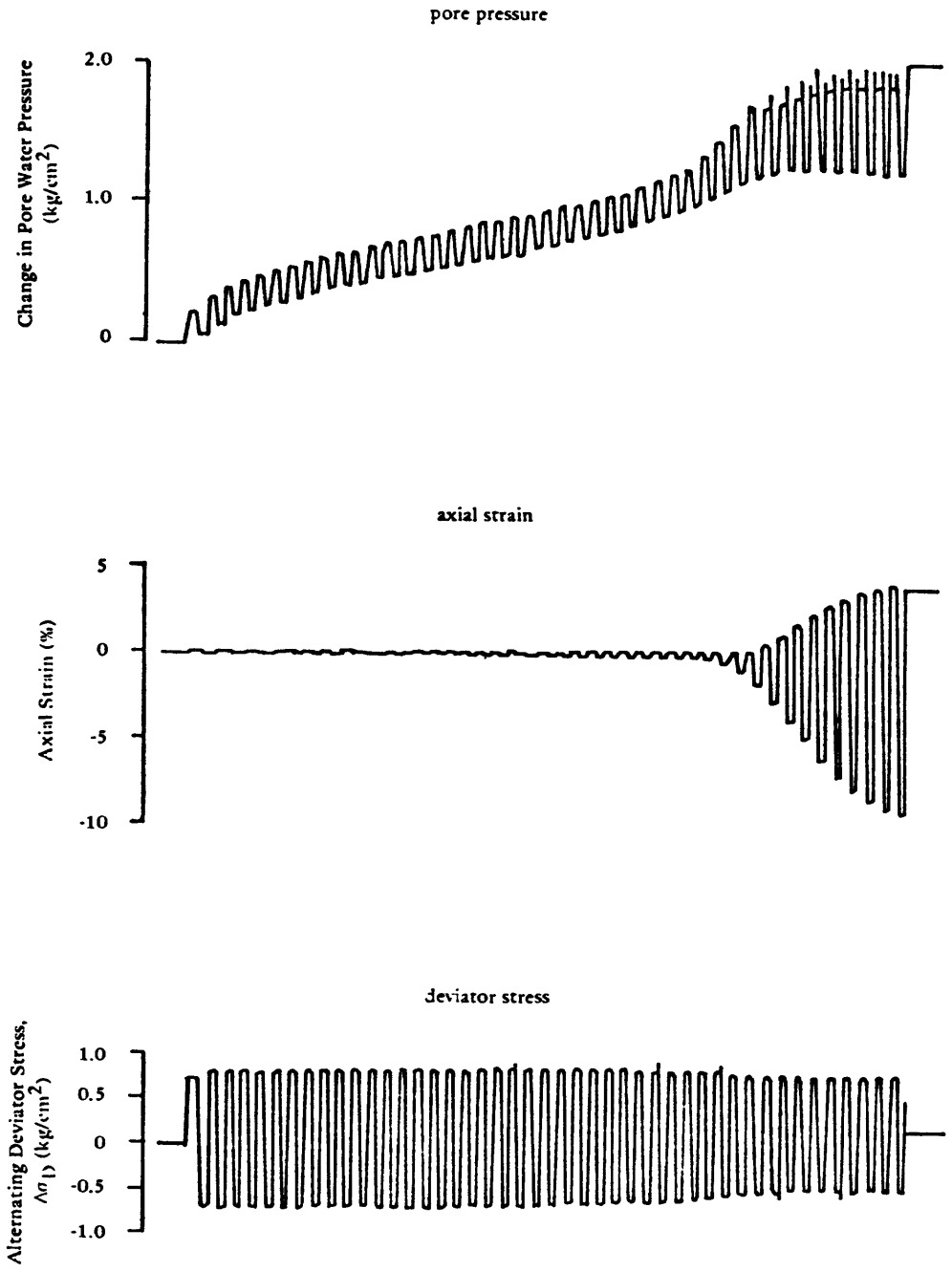

Figure 62. Data from a triaxial test on medium-dense Ottawa sand.

The term initial liquefaction can be misleading in situations involving initial static shear stress as in dams. As noted by Finn (1978), unless stress reversals occur, pore pressures may never rise to the level of confining pressure (effective stresses approaching zero). Nevertheless, a continuous buildup or accumulation of strain may occur.

Liquefaction as defined by Castro and Casagrande can be treated by comparing the in situ stresses with monotonic test data on undisturbed samples.

In an earth dam catastrophic failure can occur by unrestrained soil movement. Obviously the risk of liquefaction with unrestrained movement is an unacceptable condition. However, limited cyclic mobility (limited strain) may not cause high damage levels. Local failure of embedded pipes, however, may be affected. This point is suggested by Seed et al. (1977) when they point out "since there is ample field evidence that well-built dams can withstand moderate shaking [cyclic mobility problem] with peak accelerations up to at least 0.2g with no harmful effects, we should not waste our time and money analyzing this type of problem--rather we should concentrate our efforts on those dams likely to present problems either because of strong shaking or because they incorporate large bodies of cohesionless materials which, if saturated, may lose most of their strength during earthquake shaking and thereby lead to undesirable movements [liquefaction]." Mineiro (1979) notes a danger to be kept in mind in this regard. He points out that "under conventional undrained triaxial cyclic tests, the strains induced are usually not sufficient to mobilize post-peak strengths."

7.1 DAM PERFORMANCE

Seed (1977) has performed a careful review of experience and notes that many hydraulic fill dams have performed well for many years surviving moderate shaking (0.2g) without any major damage. However hydraulic fill dams have been vulnerable to strong shaking. A well built dam of any type can withstand moderate shaking. Dams constructed of clay soils on good foundations have withstood strong shaking (0.35 to 0.84g) from large magnitude events. A primary cause of failure in dams constructed of saturated cohesionless materials is the buildup of pore pressure and corresponding loss of stiffness and strength.

Some typical cases of dam performance will be described:

7.1.1 1906 California Earthquake

At the time of the 1906 San Andreas fault earthquake, magnitude 8-1/4, there were 33 dams ranging in height from 15 to 140 feet located within 37 miles of the fault. Seed et al. (1977) has studied these dams and estimates half of the dams were exposed to bedrock accelerations over 0.6g; the remainder experienced at least 0.25g. Of all these dams only one experienced significant damage, the Lower Howell dam where a breach formed by water escaping from a ruptured outlet pipe. It is remarkable that 32 dams were shaken severely by an 8-1/4 Richter magnitude earthquake without sustaining significant damage. One explanation for such outstanding performance is that all the dams which sustained no

damage were predominantly clayey--such as sandy clays, silty clays, or other lean clays. The dams which suffered minor damage were composed of mixed clays or clayey sands. Two dams composed of sands (one of which suffered minor damage) based on analysis were probably not fully saturated. Thus, the dynamic pore pressure buildup was not a problem.

7.1.2 1939 Ojika, Japan Earthquake

In 1939 a magnitude 6.6 earthquake occurred in the northeast portion of Honshu. Seventy-four embankments were severely damaged, of which 12 failed completely. Nine of the 12 dam embankments were constructed of sand. No complete failure occurred in embankments constructed of clay soils. Of the dams that failed, there were few cases of the dams failing during the earthquake; rather, most failed from a few hours to 24 hours after the earthquake. This suggests a critical re-distribution of pore pressure.

7.1.3 1968 Tokachi-Oki Earthquake

In 1968 a magnitude 7.8 earthquake in northern Honshu caused accelerations in the range of 0.15 to 0.2g damaging numerous earth irrigation dams with heights between 5 to 20 meters. The dam materials were mostly volcanic sand having a low standard penetration resistance. Damage was observed in 93 embankments consisting of sliding upstream and downstream slopes. There was no observed correlation between slopes and performance. The extensive damage can again be attributed to liquefaction.

7.1.4 1971 San Fernando Earthquake

In 1971 a Richter magnitude 6.6 earthquake occurred in California. Within a 25-mile radius there were about 30 operational dams. There was no damage in any of the 25 rolled fill dams. Of the five hydraulic sand fills, two suffered substantial damage. The amplitude (0.5 to 0.6g) and duration of the shaking induced large pore pressures in the saturated sandy soils resulting in liquefaction. One of the dams suffered a major slide on the upstream side, the other had a slide movement of five feet in the downstream side with a corresponding crest settlement of three feet.

7.1.5 1975 Oroville Earthquake

Oroville Dam is the highest earth fill dam in the United States with a height of 235 meters and a span of 2,110 meters. The dam was instrumented with horizontal and vertical movement devices, pore pressure gages, and accelerometers. On August 1, 1975, an earthquake of 5.7 magnitude occurred 7.5 miles southwest of the dam. The main shock was preceeded by numerous foreshocks, the largest of which was magnitude 4.8. Numerous aftershocks followed. The Oroville Dam survived the earthquake with only minor damage. Maximum movement measured was less than 3 cm. The crest of the dam had a maximum settlement of 1 cm and a horizontal upstream movement of 1-1/2 cm. In the main shock the maximum acceleration at the base of the dam was 0.09g in the upstream/downstream

direction and 0.13g in the transverse direction. The vertical acceleration at the base was 0.09g. At the crest of the dam the maximum acceleration was 0.13g in the upstream and downstream direction. Pore pressure increased in the core of the dam and in one area located in the upstream transition zone of the dam. The maximum increase in pressure head was 16.5 meters of water. No change in seepage flow was noted, Stroppini (1976).

7.2 GENERAL METHODS FOR EVALUATING LIQUEFACTION

There are basically two approaches, discussed above, in widespread use by geotechnical engineers for evaluating the liquefaction potential of saturated sands subjected to earthquake shaking (Seed, 1976). The first approach is based on field data on the performance of sand deposits in previous earthquakes. Surveys of areas where liquefaction has or has not occurred have been used to prepare charts, based primarily on the Standard Penetration Resistance of the deposit, for differentiating between liquefiable and nonliquefiable conditions. Empirical comparisons and evaluations of this type do not take account of such significant factors as the duration of shaking or the extent of drainage, and depend upon the reliability of field observations and field tests such as penetration resistance (generally after the fact). Thus, many engineers feel that such correlations provide only preliminary evaluations of liquefaction potential. These, they feel, will often need to be supplemented by detailed studies based on ground stress analyses and soil testing programs. This approach is generally not appliable to dams.

The second approach is based on a comparison of stress conditions in the field and the determination of the stress conditions causing liquefaction. Analytical procedures for evaluating the liquefaction potential of soil deposits involve two independent determinations: (a) an evaluation of the cyclic stress loading induced at different levels in the deposit by the earthquake shaking and (b) an investigation of the cyclic stresses which, for given confining pressures representative of specific depths in the deposit, will cause the soil to liquefy or undergo various degrees of cyclic strain. The evaluation of liquefaction potential is then based on a comparison of the cyclic stresses induced in the field with the stresses required to cause liquefaction, or an acceptable limit of cyclic strain, in representative samples in the laboratory. This approach with respect to dams may be divided into two separate problem areas: (1) the inherently unstable situation where in situ stress exceeds undrained residual shear strength, and (2) the more complex situation where residual strength exceeds in situ stress but where estimation of dynamic strain accumulation is necessary.

The major difficulty involved in analyzing dams with regard to liquefaction is in the prediction of accumulated deformations. Any structure whose residual undrained shear strength does not exceed the initial in situ stress is inherently unstable, and any consideration of dramatic strength loss under cyclic loading (i.e., total liquefaction) need be considered no further. The liquefaction analysis of dams reverts to the one of seismic slope stability. This will be discussed further later.

7.3 INITIAL STATIC SHEAR LOADS

Current laboratory techniques for evaluating the liquefaction resistance of soils to earthquake loading have primarily focused on horizontal planes in level ground where initial static shear stresses on the horizontal plane are minimal (theoretically zero). Studies for evaluating the liquefaction potential of soils in dams must consider the effects of the initial static shear on an element of soil. This shear level varies throughout the dam and is a function of the location within the earth fill. This variation in initial static shear imposes a problem of requiring extensive triaxial testing to define the range of liquefaction potential throughout the earth fill.

It is desirable that a general approach to defining liquefaction criteria be developed that can utilize the available body of triaxial (free field oriented) experimental data, but that can still be applicable to the situation of earth dams where static shear loads are acting. Any parameters selected for defining the liquefaction potential under conditions of initial static shear should, if possible, be general enough to incorporate the bulk of experimental results that are available.

The shear stress levels causing liquefaction in the triaxial test, simple shear and shake-table tests have generally been measured upon planes without any initial static shear stresses (principal planes). Thus, there has been little opportunity to consider initial static shear stresses. For triaxial tests in which cyclic stresses have been superimposed upon an initial static shear stress state, the stresses considered are those exerted on planes subjected to nonsymmetrical stress reversals. The influence of the degree of nonsymmetry of load application does not appear to have been addressed in any general manner, but rather the test data have been applied directly to specific cases.

Where initial static shear loads are acting on the plane of interest, prior to cyclic loading, questions arise such as what are the significant shear stresses to use for liquefaction evaluation (i.e., static plus dynamic, dynamic alone, etc.) and what is the influence of varying degrees of maximum stress reversal. One solution to this is to consider the dynamic shear stress applied on the new major principal plane following application of any static shear stress increments (see Forrest and Ferritto, 1978). Here all the problems dealing with initial static shear load and unsymmetric stress reversals are avoided. Although only dynamic shear stresses are considered, the influence of the initial static shear stress on the dynamic shear stress increment is automatically incorporated. Using this concept all available experimental data are still applicable to areas of initial static shear, such as beneath foundations or in earth dams.

7.4 ANALYSIS PROCEDURES

In the past engineering practice dams and embankments have generally been designed to withstand earthquakes by including the equivalent static inertial forces in the traditional stability analysis checking that the factor of safety is sufficiently above unity. Alternatively, using static procedures, one may compute yield acceleration levels using slip planes in the soil mass.

Seed (1977) concludes that pseudo-static analysis techniques must be used with great caution, and that dynamic analysis techniques provide a more reliable basis for estimating performance and safety.

Evaluation of saturated cohesionless soils can only properly be made when pore pressures and resulting reduced confining stress and stiffness changes are taken into account. Cohesive soils also exhibit complex behavior. Thus, large deformations can occur under prolonged oscillating loads even though maximum applied stresses are less than the static strength of the soil.

The California Water and Power Earthquake Engineering Forum was formed in 1974 by several major local state and federal water and power agencies. One of their subcommittess has reviewed currently available methods for dynamic analysis of embankments and dams. The subcommittee (Anton, 1979) concludes the finite element analysis technique to be the most appropriate technique for analysis of static and dynamic stress and strains. They recommend extensive sampling and testing to fully evaluate the spatial and material property variations of dam fill material. They point out that judgment and experience are essential in the analysis procedure. No specific procedure is recommended; however, some essential steps noted by Anton (1979) are: "(a) describe the nature of the postulated evaluation or design earthquake motion at the particular site; (b) for existing dams, perform field shear wave velocity measurements and undisturbed soil sampling; (c) carefully determine material properties, including cyclic loading laboratory testing to determine the effect of cyclic stresses on samples from embankment; it may be necessary to conduct extensive testing because of material heterogeneity and scatter of results; (d) determine stress conditions in the dam before the postulated earthquake; (e) make a finite element form of dynamic analysis and see how the dam responds to the postulated earthquake; (f) estimate deformation of elements of the dam under applied stresses; and (g) perform a continuity analysis to determine the overall deformation of the dam."

The finite element method has provided a major advance in dynamic total stress slope analysis by permitting calculation of both static and earthquake induced stresses at all locations throughout a dam. Although nonlinear material models are available, their use is generally limited to researchers. Use is limited by the high cost associated with nonlinear dynamic analysis. True nonlinear behavior would afford significant advantage in defining actual deformations and reduce arbitrary procedures for judgmental continuity analysis techniques to relate strain potential.

Total stress equivalent linear techniques have been applied to liquefaction response analysis of several dams (Makdisi and Seed, 1978). Although reasonable success has been achieved in these instances, the current techniques of total stress dam analysis with regard to liquefaction related instability are somewhat arbitrary and lacking from a theoretical aspect. The current procedures generally select the appropriate failure plane as being horizontal, and dynamic horizontal shear stresses are superimposed on the static in situ stresses in a laboratory specimen to investigate strain potential. The treatment of laboratory results is also questionable, since actual bookkeeping of dynamic and static shear strain coupling is not maintained as are factors such as stress reversals, etc. Only loading conditions on an empirically selected

plane are monitored, regardless of the actual stress field at that point. The implication is made that regions of high initial (static) stress ratio are stronger than relatively unstressed (by shear) zones. Obviously, highly stressed zones could be near incipient failure prior to dynamic loading, and require little additional load to result in very large deformations. The present approaches lack generality, also making it difficult to derive any insight for one load case from results on another.

A total stress analysis does not directly yield information on pore pressures and hence strain softening, as the reduction in effective stress reduces shear modulus. Only a nonlinear effective stress model can fully couple pore pressure generation and softening which can significantly affect the dynamic response. Drainage of pore pressure postulated into effective stress models will be required to complete the representation of a soil.

Significant work which is certain to have a major impact on dam analysis is in progress developing effective stress material models for use with finite element codes. The effective stress model will calculate actual dynamically induced pore pressures. Work is in progress by several researchers, Finn, Lee, and Martin (1977), Ghaboussi and Dikmen (1977), Baladi and Rohani (1978), Mroz, Norris, and Zienkiewicz (1978), and Prevost and Hughes (1978).

The nonlinear effective stress material models will require detailed laboratory test data to fit the parameters required. Once an effective stress material model has been implemented in a general finite element code and verified by the engineering community, it will become the most important tool in dam analysis.

7.5 REFERENCES

1. Anton, W. F. CWPEEF's Views on Earthquake-Resistant Design of Earth Dams, American Society of Civil Engineers, Geotechnical Journal, GT1, vol 105, Jan 1979.

2. Baladi, G. Y. and Rohani, B. (1978). Report 5-76-2: Liquefaction Potential of Dams and Foundations Development of Constitutive Relation for Simulating the Response of Saturated Cohesiveless Soil, U.S. Army Corp of Engineers, Waterways Experiment Station. Vicksburg, Miss., Aug 1978.

3. Casagrande, A. Liquefaction and Cyclic Deformation of Sands; A Critical Review, Harvard Soil Mechanics, series no. 88, Jan 1976, Harvard University, Cambridge, Mass.

4. Castro, G. (1969). Liquefaction in Sands, Harvard Soil Mechanics, series no. 81, p. 112.

5. Castro, G. (1976). Comments on Seismic Stability Evaluation of Embankment of Dams, Evaluation of Dam Safety, American Society of Civil Engineers, Dec 1976.

6. Finn, W. D., Leck, W., and Martin, G. R. An Effective Stress Model for Liquefaction, American Society of Civil Engineers, Geotechnical Journal, vol 103, no. GT6, Jun 1977.

7. Finn, et al. (1978). Cyclic Pore Pressures Under Anisotropic Conditions, Earthquake Engineering and Soil Dynamics, American Society of Civil Engineers, Jun 1978.

8. Ghaboussi and Dikmen. UILU-ENG-77-2010: LASS II, Computer Programs for Analysis of Seismic Response and Liquefaction of Horizontally Layered Sands, University of Illinois, Urbana, Ill., Jun 1977.

9. Makdisi, F. I. and Seed, H. B. Simplified Procedure for Estimating Dam and Embankment Earthquake-Induced Deformations, American Society of Civil Engineers, Geotechnical Journal, GT7, vol 104, Jul 1978.

10. Mineiro, A. J. (1979). Discussion, American Society of Civil Engineers, Geotechnical Journal, GT5, May 1979.

11. Mroz, Z., Norris, V. A., and Zienkiewicz, O. C. (1978). An Isotropic Hardening Model for Soil and Its Application to Cyclic Loading, International Journal for Numerical and Analytical Methods in Geomechanics, vol 2, 1978.

12. Prevost, J. H. and Hughes, T. J. R. (1978). Mathematical Modeling of Cyclic Soil Behavior, Earthquake Engineering and Soil Dynamics, vol 11, American Society of Civil Engineers, 1978.

13. Seed, H. B. (1976). Soil Liquefaction and Cyclic Mobility Evaluation for Level Ground During Earthquakes, ASCE, Geotechnical Engineering Division, GT2, Feb 1979, pp 201-255.

14. Seed, H. B., Makdisi, F. I., and Di Alba. EERC 77-20: The Performance of Earth Dams During Earthquakes, University of California, Berkeley, Aug 1977.

15. Stroppini, E. W. (1976). The Oroville Earthquake and the Oroville Dam, The Evaluation of Dam Safety, American Society of Civil Engineers, Dec 1976.

16. Seed, H. B., and Idress, I. M. (1971). "A Simplified Procedure for Evaluating Soil Liquefaction Potential," Journal of the Soil Mechanics and Foundation Division, ASCE, Vol 97, SM6, Sep 1971.

☆ U.S. GOVERNMENT PRINTING OFFICE: 1982—361-614/155